

Charles University in Prague  
Faculty of Mathematics and Physics

## MASTER THESIS



Miroslav Hopjan

# Nerovnovážná supravodivost (Nonequilibrium superconductivity)

Institute of Physics of Charles University

Supervisor of the master thesis: doc. Pavel Lipavský CSc.

Study programme: Theoretical Physics

Specialization: Condensed Matter Physics

Prague 2012

At this point I would like to thank to people who were involved in the creation of this master thesis. First of all, I thank to my supervisor doc. Pavel Lipavský CSc. for leadership, professional advices and technical comments how to write a scientific papers. As an advisor, professor Yuri Galperin helped me with my exchange studies at University of Oslo. He offered me a place for studing at his department and consulted with me my thesis. Thanks to Jakub Zázvorka for critical reading and corrections of the text. Finally, it were my friends and my family who support me during whole my studies, so big thanks to all of them.

I declare that I carried out this master thesis independently, and only with the cited sources, literature and other professional sources.

I understand that my work relates to the rights and obligations under the Act No. 121/2000 Coll., the Copyright Act, as amended, in particular the fact that the Charles University in Prague has the right to conclude a license agreement on the use of this work as a school work pursuant to Section 60 paragraph 1 of the Copyright Act.

In ..... date .....

signature of the author

Název práce: Nerovnovážná supravodivost

Autor: Miroslav Hopjan

Katedra: Fyzikální ústav Univerzity Karlovy

Vedoucí diplomové práce: doc. Pavel Lipavský, CSc., Fyzikální ústav UK

Abstrakt: V předložené diplomové práci studujeme supravodivost v kovových nanotečkách pomocí přiblížení založeného na dvoučásticové T-matici. Po zavedení korekcí známých z mnohanásobného rozptylu do Galitského-Feynmanovy žebříčkové aproximace T-matrice, lze touto metodou popsat i supravodivý stav. Tato sjednocující teorie navíc popisuje supravodivý a normální stav na stejné úrovni přiblížení. Původní teorie pro rovnováhu je v této práci zobecněna na nerovnovážné systémy pomocí zobeněného Kadanoffova-Baymova formalizmu. Tato obecně nerovnovážná verze teorie je určena pro nekonečné systémy, kde moment hybnosti je dobré kvantové číslo. Pro nanosystémy, kde moment hybnosti už není dobré kvantové číslo, byla teorie přeformulována. Modifikace byla zaměřena na nanosféry, u nichž lze využít rozvoj do vlastních stavů momentu rotace. Velká degenerace energetických hladin umožňuje vysoké kritické teploty u nanosfér s magickým počtem elektronů a zlepšuje podmínky pro pozorování jevů za hranicí slabé vazby. Jako vhodnou experimentální techniku diskutujeme tunelovací spektroskopii.

Klíčová slova: supravodivost, teorie mnohačetného rozptylu, tunelovací spektroskopie

Title: Nonequilibrium superconductivity

Author: Miroslav Hopjan

Department: Institute of Physics of Charles University

Supervisor: doc. Pavel Lipavský, CSc., Institute of Physics of Charles University

Abstract: In the present thesis we study superconductivity using approaches based on the two-particle T-matrix. With the multiple scattering corrections the Galitskii-Feynman ladder T-matrix approximation becomes applicable to the superconducting state. This theory describes the superconducting and normal states within the same approximation. In this thesis, the original equilibrium theory is generalized to nonequilibrium systems using the generalized Kadanoff-Baym formalizm. The obtained theory of nonequilibrium superconductors is suitable for bulk systems where the momentum is a good quantum number. We have reformulated the theory for nanosystems, where the momentum is no longer a good quantum number. The modification was aimed at nanospheres, where one can benefit from the expansion in eigenstates of the angular momentum. High degeneracy of energy levels leads to high critical temperatures of sheres with a magical number of electrons, which makes them good candidates for observation of phenomena beyond the weak coupling limit. As a suitable experimental technique we discuss the tunneling spectroscopy.

Keywords: superconductivity, multiple scattering theory, tunneling spectroscopy

# Contents

<b>Introduction</b>	<b>4</b>
0.1 Plan of the thesis . . . . .	5
0.1.1 Review of used methods . . . . .	5
0.1.2 Novel results . . . . .	5
<b>1 Green's functions technique</b>	<b>7</b>
1.1 Introduction . . . . .	7
1.2 Zero Temperature Green functions . . . . .	8
1.3 Equilibrium Matsubara's functions . . . . .	8
1.4 Nonequilibrium Green's function . . . . .	11
1.4.1 History of Green's function approach . . . . .	11
1.4.2 Kadanoff-Baym theory . . . . .	12
1.4.3 Langreth-Wilkins rules . . . . .	13
<b>2 Nambu-Gorkov equations</b>	<b>17</b>
2.1 BCS Hamiltonian . . . . .	17
2.2 Nambu-Gorkov equations . . . . .	18
2.3 Dyson equation . . . . .	21
<b>3 Unified theory of normal and superconducting state</b>	<b>22</b>
3.1 Introduction . . . . .	22
3.2 Galitskii-Feynman $T$ -matrix approximation . . . . .	23
3.3 Kadanoff-Martin $T$ -matrix approximation . . . . .	25
3.4 Multiple scattering corrections to the Galitskii-Feynman approx. . . . .	25
3.5 Limit of Nambu-Gorkov selfenergy . . . . .	27
3.6 Corrections to Kadanoff-Martin approximation . . . . .	28
3.7 Selfconsistent $T$ -matrix theory of superconductivity . . . . .	29
<b>4 Theory of nonequilibrium superconductivity</b>	<b>31</b>
4.1 Introduction . . . . .	31
4.2 Imaginary time formalism . . . . .	31
4.3 Nonequilibrium Green functions . . . . .	32
4.3.1 GKB equation . . . . .	32
4.4 Reduced Green's function . . . . .	33
4.4.1 Selfenergy . . . . .	33
4.5 Two-particle propagator . . . . .	34
4.5.1 $T$ -matrix . . . . .	35
4.5.2 Averaged $T$ -matrix . . . . .	35
<b>5 Spectroscopy of ultrasmall metallic grains</b>	<b>37</b>
5.1 Introduction . . . . .	37
5.2 History of spectroscopy of discrete energy levels . . . . .	37
5.3 SET experiment . . . . .	38
5.4 Coulomb blockade . . . . .	40

<b>6</b>	<b>Superconductivity in metallic grains</b>	<b>42</b>
6.1	Hamiltonian . . . . .	42
6.1.1	Non-interacting electrons in the grain . . . . .	42
6.1.2	Pairing interaction . . . . .	43
6.1.3	Leads . . . . .	44
6.2	Elimination of leads . . . . .	44
6.3	Perturbative expansion . . . . .	46
6.4	Selfenergy . . . . .	46
6.4.1	Multiple scattering theory . . . . .	46
6.4.2	Galitskii-Feynman theory . . . . .	47
6.4.3	Kadanoff-Martin theory . . . . .	47
6.5	Various approximations . . . . .	48
6.5.1	BCS approximation . . . . .	48
6.5.2	Equations for Richardson model . . . . .	49
6.5.3	Approximation of our model . . . . .	50
6.6	Nonequilibrium Green's functions . . . . .	51
6.6.1	Two parallel lines . . . . .	51
6.6.2	Selfenergy . . . . .	51
6.6.3	Matrix products . . . . .	52
6.7	Stationary regime . . . . .	53
6.8	Iteration loop . . . . .	53
6.8.1	Electronic functions in energy domain . . . . .	54
6.8.2	Electronic functions in time domain . . . . .	54
6.8.3	Bosonic functions . . . . .	55
6.8.4	Selfenergy . . . . .	56
6.9	Simplified set . . . . .	56
6.10	Richardson model . . . . .	57
6.11	BCS approximation . . . . .	57
<b>7</b>	<b>Numerics of magic cluster model</b>	<b>59</b>
7.1	Introduction . . . . .	59
7.2	Isolated grain in equilibrium . . . . .	59
7.3	Bardeen formula for current - equilibrium . . . . .	59
7.4	Two-particle propagator . . . . .	61
7.5	BCS theory . . . . .	61
7.6	Characterization of the model for numerics . . . . .	62
7.7	Two-particle propagator with BCS solution . . . . .	62
7.8	Change of origin of energies . . . . .	63
7.9	The single channel approximation . . . . .	64
7.10	Remark of the neglecting of corrections . . . . .	67
7.11	BCS approximation – numerics . . . . .	67
7.12	The single channel approximation– numerics . . . . .	68
7.13	Renormalization of the gap . . . . .	69
	<b>Conclusion</b>	<b>74</b>
	<b>Bibliography</b>	<b>76</b>
	<b>Appendix</b>	<b>77</b>

<b>A</b>	<b>Soven schema</b>	<b>78</b>
A.1	Coherent potential model of substitutional disordered alloys . . .	78
A.2	Renotation of Soven's condition . . . . .	79
A.3	Reformulation of Soven condition . . . . .	80
A.4	Soven schema in superconductivity . . . . .	82
<b>B</b>	<b>Two-particle propagator</b>	<b>83</b>

# Introduction

Superconductivity presents a very complex phenomena. It was discovered by Heike Kamerlingh Onnes on April 8, 1911 in Leiden. Many interesting features like the Meisner effect or the zero resistance (therefore the name superconductors) could not be explained by contemporary theories and in the beginnings the superconductors were described only by phenomenological theories.

It took almost a half of century before a successful microscopic theory has occurred. In 1957 the complete microscopic theory of superconductivity was finally proposed by Bardeen, Cooper and Schrieffer. This BCS theory explained the superconducting current as a superfluid of Cooper pairs, which are pairs of electrons interacting through the exchange of phonons. For this work, the authors were awarded the Nobel Prize in 1972.

More than 50 years after its discovery, the BCS theory still remains the most successful theory. Its modification for realistic retarded interaction put forward by Eliashberg works excellent in conventional superconductors but it works also in areas where it is not expected. In contrast, intensive studies of high-temperature superconductors discovered in 1986 made it obvious that the BCS theory is not a complete theory. Although some properties of high-temperature superconductors were predictable by BCS theory, many were missing.

The high-temperature superconductors represent a challenge for theoretical physicist. It turns out that the properties of the normal state determine how the condensate will look like. The theoretical framework of the BCS theory is not suitable since it describes only the condensate. Any future theory successful in explaining the complex behavior of high-temperature superconductors thus has to cover both the normal and the superconducting states.

One of many attempts to crack this problem is theory suggested by supervisor of author of this thesis. The theory attacks the problem from the second side using the T-matrix approximation, which was originally proposed for the normal state. It was known that the Galitskii-Feynman T-matrix approximation cannot be used for the superconducting state. It turned out that with a slightly corrected schema of the T-matrix approximation based on Soven's idea of the effective medium, this theory describes the superconducting state as well as it does the normal one. The idea of corrections originates from the multiple scattering theory in nuclear reactions, where the problem of repeated collisions was noticed first by Watson. Perhaps the best known implementation of this idea are Fadeev equations, which are suited for a small number of particles, however, and thus inapplicable to the condensed matter.

The problem of repeated collisions in condensed matter appeared in the theory of alloys. Selfconsistent expansion of Green's function brings terms which remind a scattering of electron on the impurity which it just leaves after collision. An elegant solution of this problem was suggested by Soven. He interprets the selfenergy as a priorly unknown coherent potential which one can imagine as an effective medium. Removing this effective potential from the scattering site, where we evaluate the actual collision process, the nonphysical repeated collisions are healed.

The Soven idea was reformulated for the scattering of the pair of electrons



within T-matrix approximation by supervisor of the author of this thesis. This resulting T-matrix approximation with multiple scattering corrections is a desired unified theory of the superconducting and the normal state. Candidate systems where one needs to cover both phases are underdoped high-temperature superconductors with the pseudogap phase in the normal state, ultracold Fermi gases and nanoparticles. Here we focus on metallic nanospheres.

The first theoretical prediction for small particles appeared in 1959 due to Anderson [1]. He claimed that the superconductivity should disappear when the particle has less than  $10^4$  particles. Below this threshold the superconductivity should disappear and the pairing correlations persist only as weak fluctuations. The superconductivity in small metallic grains attracted more researches since middle of 1990's, when the first tunneling experiment with metallic single electron transistor has been performed. Many theoretical approaches were used to study the transition from the bulk system to the fluctuation-dominated regime, the most of them are nonperturbative approaches. The application of the T-matrix approximation to small metallic grains is one of the goals in the thesis.

## **0.1 Plan of the thesis**

### **0.1.1 Review of used methods**

The plan of the thesis is following. In the first chapter we introduce Green's functions and the Kadanoff-Baym technique of analytic continuation. The second chapter is a brief review of the BCS theory in the Nambu-Gorkov formalism. In the third chapter we explain the shortcomings of Galitskii-Feynman T-matrix approximation and the Kadanoff-Martin theory. The Multiple scattering theory is introduced. We show a limit of the Multiple scattering theory and the Kadanoff-Martin theory, by which the Nambu-Gorkov selfenergy is recovered.

### **0.1.2 Novel results**

The fourth chapter is the original contribution of the author. The Kadanoff-Baym formalism is applied to the Multiple scattering theory and the nonequilibrium version of the theory is derived in the full version.

In the fifth chapter we present the single electron transistor for measuring electron states in ultrasmall metallic grains. We suggest how to modify this experiment so that parasitic influences are suppressed and one can measure the properties discussed in this thesis.

The Multiple scattering theory is adapted to ultrasmall metallic grains in the sixth chapter. The nonequilibrium version is also derived. We arrive at a set of equations for nonequilibrium Green functions, that in principle can be directly solved, at least in the steady state, with the help of the fast Fourier transformation. Such solution is highly nontrivial, however, and it was not attempted in this thesis.

In the last chapter we assume nonsymmetric leads for which a strong coupling to one of leads keeps the nanosphere close to the local equilibrium. The local equilibrium simplifies the set of equations which can be then easily solved in part analytically and in part by simple numerical tools. We derive the lowest order

approximation of differences between the BCS theory and the Multiple scattering theory and discuss its expected effects on the superconducting gap and the critical temperature.

In Appendix A we express Soven's idea in the form applicable to the two-particle scattering. Appendix B includes a subsidiary algebra needed to evaluate the two-particle propagator in the lowest order approximation.

# 1. Green's functions technique

## 1.1 Introduction

There is a lot of different many-particle theories like a microscopic mean-field theories (Kohn-Sham and Hartree-Fock), many-body perturbation theory, large-scale diagonalization methods, coupled-cluster theory. These are used in such diverse areas like atomic, molecular, solid-state and nuclear physics, chemistry and material science.

One of the fundamental methods is the Green function approach widely used in relativistic physics. It is the cornerstone of quantum electrodynamics and quantum chromodynamics. This technique of a quantized field is also used in solid state physics. In particular, the theory of Fermi liquids and systems of interacting bosons as well as the theory of superconductivity are based on the Green functions technique.

The perturbation theory based on Green's functions applied to solid states physics is well provided in monograph *Methods of Quantum Field Theory in Statistical Physics* by Abrikosov *et al* [2]. Authors start with a ground state of manybody system where the expectation values are computed within a Fermi vacuum. They introduce the Feynman diagrams technique, Dyson equation and renormalization technique. Analytic properties of Green's function are also shown. After introduction of the Green function technique at zero temperature the theory is extended to a finite temperature. In finite temperature the perturbation theory is developed within a complex segment, where the real time is replaced by an imaginary one. Formally the same rules apply for the Matsubara's function as for the zero temperature Green function. The only difference appears in the evaluation of final diagrams. Despite the success of Matsubara's technique in the thermodynamics, there is no systematic construction of time dependent Green's functions (retarded and advanced) which are suitable for a description of transport properties. The analytic continuation of Green's functions to real time axis is not fully systematic in this approach.

The theory of nonequilibrium quantum phenomena beyond the linear response described in Matsubara's formalism was a difficult task. There are two ways how to make an equation for nonequilibrium Green's function. The first is called Keldysh technique and the second is the generalized Kadanoff-Baym technique. Both techniques are equivalent as they transform the expressions of scattering theory to a set of equations for nonequilibrium Green's functions. We use generalized Kadanoff-Baym technique of analytic continuation. It has an advantage of simpler rules, by which one automatically transforms approximations for Matsubara's function to the approximations for nonequilibrium Green's functions. In the next sections we first introduce basic facts about the Green function technique.

## 1.2 Zero Temperature Green functions

The central target in the zero temperature Green function formalism is to compute an expression called Green function

$$G(1, 2) = -i \frac{\langle 0 | \mathbf{T} \mathcal{S} \psi_1^\dagger \psi_2 | 0 \rangle}{\langle 0 | \mathbf{T} \mathcal{S} | 0 \rangle}, \quad (1.1)$$

where numbers  $1 \equiv (x_1, \alpha)$  and  $2 \equiv (x_2, \beta)$  are cumulative indices for both space-time  $x \equiv (\mathbf{r}, t)$  coordinates and spin index,  $\psi_1^\dagger$  and  $\psi_2$  are creation resp. annihilation operator in Dirac's picture,  $\mathbf{T}$  means Dyson's time ordering, the scattering matrix  $\mathcal{S}$  describes evolution. The Green function is the mean value of fields in distinct points in space and time.

The ground state of interacting particles is computed as the time evolution of initial noninteracting particles to the interacting ones. The interaction is switched on adiabatically from the infinite past to the zero time where reaches its true value and than adiabatically switched off to the noninteracting state in the infinite future. The full Green function (1.1) can be computed by an expansion in the products of noninteracting Green's functions using Wick's theorem and one can derive famous Feynman diagrammatic rules. The ground state is trivial since we start with the ground state of noninteracting particles and end up with the same.

The question is how to compute properties of interacting system if the temperature is finite. There is no specific quantum state of the system in its initial or final state, but one must average over all the set of possible states weighted with Boltzmann factors. We will discuss this problem in the next section.

## 1.3 Equilibrium Matsubara's functions

The next step in building the perturbation theory of Green's function in interacting systems is the extension of formalism to finite temperatures. Matsubara's formalism is commonly applied to different physical systems and there is a lot of appropriate, well established approximations. The equilibrium state is a starting point towards nonequilibrium systems, therefore we want to remind here some basic ideas of Matsubara's function technique. In the next section we extend the theory to a nonequilibrium system.

Formalism for finite temperatures utilize a similarity of grandcanonical and evolution operators. With a help of Wick's rotation of time axis we built the perturbation theory on imaginary segment. Instead of Green's function, the central quantity is called Matsubara's function. Again it can be computed as a series of terms, which consist of noninteracting Matsubara's function. This can be reached with help of so-called generalized Wick's theorem, which can be found in [2].

The particle correlation function is defined by:

$$G^<(1, 2) = G_{\alpha\beta}^<(x_1, x_2) = \mathbf{Tr}(\hat{\rho} \tilde{\psi}_\beta^\dagger(x_2) \tilde{\psi}_\alpha(x_1)), \quad (1.2)$$

where Greek indices denote spin variables and variables in brackets are spacetime coordinates. Here

$$\hat{\rho} = \frac{1}{Z} e^{-\beta(\hat{\mathcal{H}} - \mu\hat{N})} \quad (1.3)$$

is the grandcanonical operator normalized to unity by  $Z = \text{Tr}e^{-\beta(\hat{\mathcal{H}}-\mu\hat{\mathcal{N}})}$ ,  $\hat{\mathcal{H}}$  is the Hamiltonian,  $\hat{\mathcal{N}}$  is the particle number operator,  $\mu$  is the chemical potential and  $\beta$  is the inverse temperature.

In the equilibrium the time dependence of the correlation function follows from the time dependence of creation and annihilation operators

$$G^{<}(1,2) = \frac{1}{Z} \mathbf{Tr}(e^{-\beta(\hat{\mathcal{H}}-\mu\hat{\mathcal{N}})} e^{i(\hat{\mathcal{H}}-\mu\hat{\mathcal{N}})t_2} \psi_{\beta}^{\dagger}(\mathbf{r}_2) e^{-i(\hat{\mathcal{H}}-\mu\hat{\mathcal{N}})t_2} e^{i(\hat{\mathcal{H}}-\mu\hat{\mathcal{N}})t_1} \psi_{\alpha}(\mathbf{r}_1) e^{-i(\hat{\mathcal{H}}-\mu\hat{\mathcal{N}})t_1}). \quad (1.4)$$

For convenience, also for the time evolution the Hamiltonian  $\hat{\mathcal{H}}$  is defined relative to a chemical potential  $\mu\hat{\mathcal{N}}$ .

We should mention a convention mostly used in the Matsubara approach, although we do not follow this formulation. To formally unify the grandcanonical and evolution operators, we extend  $t$  to a pure imaginary time and denote  $it = \tau$  so that the correlation function has a form

$$G^{<}(1,2) = \frac{1}{Z} \mathbf{Tr}(e^{-\beta(\hat{\mathcal{H}}-\mu\hat{\mathcal{N}})} e^{(\hat{\mathcal{H}}-\mu\hat{\mathcal{N}})\tau_2} \psi_{\beta}^{\dagger}(\mathbf{r}_2) e^{-(\hat{\mathcal{H}}-\mu\hat{\mathcal{N}})\tau_2} e^{(\hat{\mathcal{H}}-\mu\hat{\mathcal{N}})\tau_1} \psi_{\alpha}(\mathbf{r}_1) e^{-(\hat{\mathcal{H}}-\mu\hat{\mathcal{N}})\tau_1}), \quad (1.5)$$

where  $1 \equiv (\mathbf{r}_1, \tau_1, \sigma)$ . A definition for the hole correlation function has a similar form

$$G^{<}(1,2) = \frac{1}{Z} \mathbf{Tr}(e^{-\beta(\hat{\mathcal{H}}-\mu\hat{\mathcal{N}})} e^{(\hat{\mathcal{H}}-\mu\hat{\mathcal{N}})\tau_1} \psi_{\alpha}(\mathbf{r}_1) e^{-(\hat{\mathcal{H}}-\mu\hat{\mathcal{N}})\tau_1} e^{(\hat{\mathcal{H}}-\mu\hat{\mathcal{N}})\tau_2} \psi_{\beta}^{\dagger}(\mathbf{r}_2) e^{-(\hat{\mathcal{H}}-\mu\hat{\mathcal{N}})\tau_2}). \quad (1.6)$$

We use convention which uses the time  $t$ .

In the equilibrium, the correlation functions depend only on the difference of times  $t_1 - t_2$ . Particle correlation function  $G^{<}(1,2)$  is defined for  $\beta \geq \tau_2 - \tau_1 \geq 0$  and hole correlation function  $G^{>}(1,2)$  is defined for  $\beta \geq \tau_1 - \tau_2 \geq 0$ . For complex times  $t_1$  and  $t_2$  these conditions read  $\beta \geq \text{Im}(t_1 - t_2) \geq 0$  for  $G^{<}(1,2)$  and  $\beta \geq \text{Im}(t_2 - t_1) \geq 0$  for  $G^{>}(1,2)$ . Both functions are simultaneously defined only for  $\text{Im}(t_1 - t_2) = 0$ . Correlation functions are coupled via the relation

$$G^{<}(t_1, t_2) = G^{>}(t_1, t_2 + i\beta), \quad (1.7)$$

where the times argument  $t_1, t_2$  are complex times discussed above. This relation is the boundary condition for the equilibrium Green functions.

Sometimes it is more convenient to switch from the time representation to the frequency representation. For general case  $t_1 = t + \frac{1}{2}\tau$  and  $t_2 = t - \frac{1}{2}\tau$

$$G^{<}(\omega, t) = \int_{-\infty}^{\infty} d\tau e^{i\omega\tau} G^{<}\left(t + \frac{1}{2}\tau, t - \frac{1}{2}\tau\right). \quad (1.8)$$

In equilibrium,  $G^{<}$  is only the function of time difference and consequently the transformation is function of only  $\omega$  and there is no time dependence on  $t$

$$G^{<}(\omega) = \int_{-\infty}^{\infty} d\tau e^{i\omega\tau} G^{<}\left(t + \frac{1}{2}\tau - (t - \frac{1}{2}\tau)\right) = \int_{-\infty}^{\infty} d\tau e^{i\omega\tau} G^{<}(\tau). \quad (1.9)$$

The boundary condition in the frequency representation became

$$G^{<}(\omega) = e^{-\beta\omega} G^{>}(\omega). \quad (1.10)$$

This condition with a definition of spectral function  $A = G^> + G^<$  allows us to express correlation functions in terms of the spectral function

$$G^<(\omega) = f_{FD}(\omega)A(\omega) = \frac{1}{1 + e^{\beta\omega}}A(\omega), \quad (1.11)$$

$$G^>(\omega) = (1 - f_{FD}(\omega))A(\omega) = \left(1 - \frac{1}{1 + e^{\beta\omega}}\right)A(\omega). \quad (1.12)$$

The decomposition of the correlation function into Fermi-Dirac statistics  $f_{FD} = 1/(1 + e^{\beta\omega})$  and the spectrum  $A$  applies for any interaction.

Matsubara's function is defined via correlations functions. The convergence of the correlation functions is satisfied only for  $\text{Im}t_1 = \text{Im}t_2$ . The natural definition suggested by Matsubara reads

$$G(1, 2) = -i\theta(-\text{Im}(t_1 - t_2))G^>(1, 2) + i\theta(-\text{Im}(t_2 - t_1))G^<(1, 2). \quad (1.13)$$

The complex times are arranged by ordering in a complex segment  $\mathcal{C} = (0, -i\beta)$ , while an older time is more close to zero. A step function within the complex segment takes a form

$$\theta_{\mathcal{C}}(t_1 - t_2) = -i\theta(-\text{Im}(t_1 - t_2)), \quad (1.14)$$

$$\theta_{\mathcal{C}}(t_2 - t_1) = -i\theta(-\text{Im}(t_2 - t_1)). \quad (1.15)$$

The Wick's time ordering operator arranges the creation and annihilation operators

$$\mathbf{T}_{\beta}\psi_1\psi_2^{\dagger} = \begin{array}{ll} \psi_1\psi_2^{\dagger}\dots & \text{Im}t_1 < \text{Im}t_2 \dots \quad t_1 >_{\mathcal{C}} t_2 \\ -\psi_2^{\dagger}\psi_1\dots & \text{Im}t_1 > \text{Im}t_2 \dots \quad t_1 <_{\mathcal{C}} t_2 \end{array} \quad (1.16)$$

The Matsubara's function can be written in a compact form

$$G(1, 2) = -i \frac{\mathbf{Tr}\left(\mathbf{T}_{\beta}e^{-i\int_{\mathcal{C}}d\tau(\hat{\mathcal{H}}-\mu\hat{N})}\psi_1\psi_2^{\dagger}\right)}{\mathbf{Tr}\left(\mathbf{T}_{\beta}e^{-i\int_{\mathcal{C}}d\tau(\hat{\mathcal{H}}-\mu\hat{N})}\right)} = -i \frac{\mathbf{Tr}\left(e^{-\beta(\hat{\mathcal{H}}_0-\mu\hat{N})}\mathbf{T}_{\beta}S(0, -i\beta)\psi_1\psi_2^{\dagger}\right)}{\mathbf{Tr}\left(e^{-\beta(\hat{\mathcal{H}}_0-\mu\hat{N})}\mathbf{T}_{\beta}S(0, -i\beta)\right)} \quad (1.17)$$

and has exactly the same structure as the full Green function in zero temperature (1.1). The only difference is the appearance of a trace instead of the mean value of ground state. Wick's ordering operator and integrations act along the complex time segment. This formal similarity helps us with expansion of full Matsubara's function.

Before we start with the next section, we need to discuss the Wick's theorem in finite temperatures. The problem is that unlike before we have no concept of a normal product, contractions and vacuum. Thus the use of Wick's theorem is not justified. The problem of computing the full Matsubara's function is in the use of a theorem, which in literature is called Wick's theorem for finite temperature. We recall the discussion in the section 12.2 of [2]. Wick's theorem for normal state applies at finite temperature in a sense that the full Matsubara's function can be expanded to the noninteracting Matsubara's functions.

In spite of fundamental character of Wick's theorem, there are some exceptions in its application for systems, which show complex behavior. For example

Bose systems below the transition temperature and superconductors in the superconducting state. For those systems Wick's theorem does not apply. This case is very important in the derivation of Nambu-Gorkov equations for BCS model, where we must incorporate an anomalous function and use decoupling technique instead of expansion. We will see this in the next chapter. For more details about the perturbation Green functions technique in finite temperature, see [2].

## 1.4 Nonequilibrium Green's function

Beside finite temperature and interaction we can also include external fields. After application of external fields the system will be disturbed from equilibrium. If we turn off the external field, the system will relax back to the equilibrium. In this section we explain, how to describe system in nonequilibrium, starting from an initial equilibrium system.

### 1.4.1 History of Green's function approach

After brief review we will describe nonequilibrium systems. The first question one can ask is what actually means nonequilibrium? The natural definition of a nonequilibrium is the opposite of equilibrium system.

The equilibrium state is usually defined by two criteria. The first criterion says that an equilibrium system is characterized by a unique set of extensive and intensive variables, which do not change in time. The second criterion says that after isolation of the system from its environment, all the variables remain unchanged. The latter condition is necessary to distinguish equilibrium from stationary nonequilibrium states [3]. How can one incorporate quantum nonequilibrium phenomena in perturbative theory formalism, which would allow us to study any nonequilibrium system? We can answer this question with the term Nonequilibrium Green function.

The foundations of Green's function theory (Kubo) in nonequilibrium transport phenomena first appeared in 1957 as an alternative approach to quantum generalization of Boltzmann equation (Kohn, Luttinger). At the beginning Green's function technique was used only in linear regime in terms of the Kubo formula. The development of the theory of Nonequilibrium Green's function was due to Bogoliubov and Swinger. Bogoliubov and his successors used a full set of nonequilibrium functions, but this approach was nonsystematic in scheme of approximative selfenergies. Systematic way, how to built selfenergy, was developed by Keldysh. Keldysh theory works with so-called Swinger-Keldysh contour, which is in principle the two-times account of the real axis.

Swinger's original idea was developed by his students Kadanoff and Baym [4]. The idea of their theory was formal link with equilibrium state in some initial time  $t_0$ . From knowledge of Matsubara's functions theory in equilibrium, one can derived a continuation of Green's functions along a general contour. So-called Kadanoff-Baym contour is composed of two-times real segment and an imaginary segment. Further progress in the theory was merit from Langreth and Wilkins. They generalized Kadanoff-Baym formalism adding retarded and advanced Green's functions and formulated simple rules how to prepare equations for real time Green's functions. This makes the generalized Kadanoff-Baym

theory an easy-to-apply formalism [5].

### 1.4.2 Kadanoff-Baym theory

Let us explain Kadanoff-Baym contour approach. We suppose that at some initial time there is a system, which is in thermal equilibrium. The system is described by Hamiltonian  $\hat{\mathcal{H}}$ , which includes free-particle part  $\hat{\mathcal{H}}_0$  and interaction  $\hat{\mathcal{H}}'$ . We assume the density matrix  $\hat{\rho}(t_0) = e^{-\beta(\hat{\mathcal{H}}-\mu\hat{N})}/Z$  at time  $t_0$ . In connection with last chapter we can rewrite this into the form:

$$\frac{e^{-\beta(\hat{\mathcal{H}}_0-\mu\hat{N})}\mathbf{T}_\beta e^{-i\int_C d\tau \hat{\mathcal{H}}'}}{\mathbf{Tr}\left(e^{-\beta(\hat{\mathcal{H}}_0-\mu\hat{N})}\mathbf{T}_\beta e^{-i\int_C d\tau \hat{\mathcal{H}}'}\right)} = \frac{e^{-\beta(\hat{\mathcal{H}}_0-\mu\hat{N})}\mathbf{T}_\beta S(t_0, t_0 - i\beta)}{\mathbf{Tr}\left(e^{-\beta(\hat{\mathcal{H}}_0-\mu\hat{N})}\mathbf{T}_\beta S(t_0, t_0 - i\beta)\right)}. \quad (1.18)$$

Now how can one incorporate external fields? Suppose that the imaginary segment at time  $t_0$  was deformed in the way depicted in figure 1.1. Within the imaginary segment Hamiltonian  $\hat{\mathcal{H}}$  contains only noninteracting part  $\hat{\mathcal{H}}_0$  and interacting part  $\hat{\mathcal{H}}'$ . External forces  $\hat{\mathcal{H}}''(t)$  can be accounted in the part of the complex trajectory, which was created by the deformation of the two-times counting of real axis. Within the top real time axis we switch on external forces  $\hat{\mathcal{H}}''(t)$  and reach the time of measurements  $t_1$  and  $t_2$ . After the top horizontal segment we account bottom horizontal segment which is also a real time axis. We turn off the external forces and end up in time  $t_0$  with the imaginary segment, where Hamiltonian contains only  $\hat{\mathcal{H}}_0$  and interacting part  $\hat{\mathcal{H}}'$ . The imaginary segment is accounted by Matsubara's formalism.

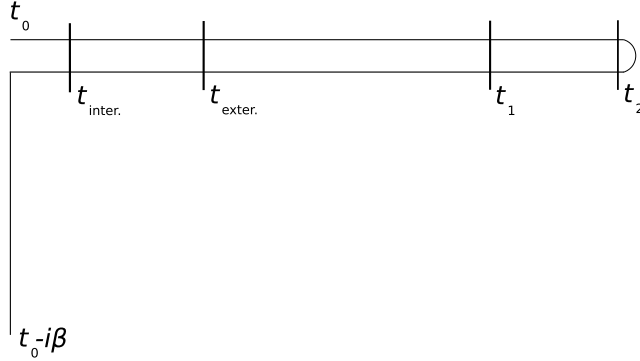


Figure 1.1: The Kadanoff-Baym contour: In the time  $t_{inter.}$  we can adiabatically switch on an interaction. This step is not necessary, because the interaction can be included within the imaginary segment at the beginning, in time  $t_0$ . In time  $t_{exter.}$ , we switch on external fields and the system is driven out of the equilibrium. Times of interest  $t_1$  and  $t_2$  can be infinitely far away from times  $t_{inter.}$  and  $t_{exter.}$

Let us define time ordering within Kadanoff-Baym contour. An earlier event is defined as an event, which we meet earlier than some another event during a way from  $t_0$  to  $t_0 - i\beta$  on the complex contour. With this definition of time ordering  $\mathbf{T}_C$  on the complex contour we can introduce the contour Green function

$$G(1, 2) = -i \frac{\mathbf{Tr}\left(\mathbf{T}_C e^{-i\int_C d\tau (\hat{\mathcal{H}}-\mu\hat{N})} \psi_1 \psi_2^\dagger\right)}{\mathbf{Tr}\left(\mathbf{T}_C e^{-i\int_C d\tau (\hat{\mathcal{H}}-\mu\hat{N})}\right)}. \quad (1.19)$$



The contour Green's function is similar to Matsubara's function. We can apply the same diagrammatic rules as before with the only difference that we operate on the complex contour. This difference appears only in the end of the formal calculation. We can also rearrange the perturbative expansion into Dyson's equation, but now within a complex trajectory. We will see in the next subsection how to prepare equations for functions, which depend only on real times, from equations for general trajectory.

For further discussion it is convenient to rewrite the above definition of contour Green's function

$$G(1, 2) = -i \frac{\text{Tr} \left( e^{-\beta(\hat{\mathcal{H}}_0 - \mu\hat{N})} \mathbf{T}_C \mathcal{S}(t_0, t_0 - i\beta) \mathcal{S}(t_0, t_0) \psi_1 \psi_2^\dagger \right)}{\text{Tr} \left( e^{-\beta(\hat{\mathcal{H}}_0 - \mu\hat{N})} \mathbf{T}_C \mathcal{S}(t_0, t_0 - i\beta) \mathcal{S}(t_0, t_0) \right)}. \quad (1.20)$$

There are two types of S-matrix.  $\mathcal{S}(t_0, t_0 - i\beta)$  describes interactions and  $\mathcal{S}(t_0, t_0)$  describes external fields. The evaluation of the trace with given weight  $e^{-\beta(\hat{\mathcal{H}}_0 - \mu\hat{N})}$  allows Wick's theorem.

The Kadanoff-Baym formalism is adequate for studies of initial correlations for times  $t > t_0$ , without the assumption  $t \gg t_0$ . The price to pay for this general formalism is that the Green's function is defined on a three-branch contour and has a complicated expression in terms of the simultaneous perturbation expansion of two S-matrices. For many practical purposes this is an overkill.

In many cases we can assume that correlations decay in time, so that if we take the limit  $t_0 \rightarrow -\infty$ , at any finite time  $t \gg t_0$ , there is no signature of eventual correlations in the initial density matrix  $\rho(t_0)$ . This is the Bogoliubov principle of weakening of correlations, a general principle in nonequilibrium statistical mechanics. It is however advised to keep in mind that in some cases initial correlations can persist at long times for example due to the presence of metastable states [6].

If we take a limit  $t_0 \rightarrow -\infty$  and neglect initial correlations, which is the same as neglecting the imaginary segment, we end up with expression

$$G(1, 2) = -i \frac{\text{Tr} \left( e^{-\beta(\mathcal{H}_0 - \mu\mathcal{N})} \mathbf{T}_C \mathcal{S}(-\infty, -\infty) \mathcal{S}(-\infty, -\infty) \psi_1 \psi_2^\dagger \right)}{\text{Tr} \left( e^{-\beta(\mathcal{H}_0 - \mu\mathcal{N})} \right)}. \quad (1.21)$$

In the next section we will derive Kadanoff-Baym rules using the same limit.

### 1.4.3 Langreth-Wilkins rules

In this subsection we derive Langreth-Wilkins rules used below to prepare equations for real time Green's functions. In the previous subsection we have introduced the contour Green function. The same diagrammatic expansion holds for the contour Green function as for the zero temperature or Matsubara's function.

The particle correlation functions is defined as

$$G^<(1, 2) = \text{Tr} \left( \mathbf{T}_C \hat{\rho} \psi_1 \psi_2^\dagger \right)_{t_1 < c t_2} = -i G(1, 2)|_{t_1 < c t_2} \quad (1.22)$$

and the hole function reads

$$G^>(1, 2) = \text{Tr} \left( \mathbf{T}_C \hat{\rho} \psi_2^\dagger \psi_1 \right)_{t_1 > ct_2} = iG(1, 2)|_{t_1 > ct_2}. \quad (1.23)$$

Actually the definition above does not restrict times  $t_1$  and  $t_2$  in relation to real axis. We can choose both  $t_1 > t_2$  and  $t_1 < t_2$  and definition above is still valid. One particle Green's function is a fermionic operator. The definitions of the correlation functions are the definitions for fermionic operators. For bosonic function one should slightly change the definition, we will do it later.

Let us suppose that we have some operator  $A$ , which is a product of two operators  $B$  and  $C$ , on a complex segment

$$\begin{aligned} A(1, 2) &= B(1, \bar{3})C(\bar{3}, 2), \\ A &= B \times C, \end{aligned} \quad (1.24)$$

where  $\times$  denotes integration along the complex path. The second equation is a short notation of the first one. We want to know the correlation functions of  $A$ ,

$$\begin{aligned} A^<(1, 2) &= -iA(1, 2)|_{t_1 < ct_2} = \\ &= -i \int_C dt_3 B(1, 3)C(3, 2)|_{t_1 < ct_2} \\ &= -i \int_{t_0}^{t_1} dt_3 B(1, 3)C(3, 2) - i \int_{t_1}^{t_0} dt_3 B(1, 3)C(3, 2) \\ &\quad - i \int_{t_0}^{t_2} dt_3 B(1, 3)C(3, 2) - i \int_{t_2}^{t_0} dt_3 B(1, 3)C(3, 2) \\ &\quad - i \int_{t_0}^{t_0 - i\beta} dt_3 B(1, 3)C(3, 2). \end{aligned} \quad (1.25)$$

The first term is integral from time  $t_0$  to time  $t_1$ , the second part from  $t_1$  to  $t_2$  is contained in the second and third integral. The fourth integral relates to part between times  $t_2$  and time  $t_0$ . The fifth integral is part from imaginary segment. We are interested in the limit  $t_0 \rightarrow -\infty$ . If we apply the Bogoliubov principle of weakening correlations, the last integral diminished because the times of measurements are infinitely far away from the initial time,

$$\begin{aligned} A^<(1, 2) &= -i \int_{-\infty}^{t_1} dt_3 B^>(1, 3)C^<(3, 2) + i \int_{t_1}^{-\infty} dt_3 B^<(1, 3)C^<(3, 2) \\ &\quad + i \int_{-\infty}^{t_2} dt_3 B^<(1, 3)C^<(3, 2) - i \int_{t_2}^{-\infty} dt_3 B^<(1, 3)C^>(3, 2), \end{aligned} \quad (1.26)$$

where we used definitions of correlations functions. We reverse integration in the second and fourth term and group terms together

$$\begin{aligned} A^<(1, 2) &= \int_{-\infty}^{t_1} dt_3 (-i)(B^>(1, 3) + B^<(1, 3))C^<(3, 2) \\ &\quad + \int_{-\infty}^{t_2} dt_3 B^<(1, 3)i(C^<(3, 2) + C^>(3, 2)) \\ &= \int_{-\infty}^{\infty} dt_3 (-i)\theta(t_1 - t_3)(B^>(1, 3) + B^<(1, 3))C^<(3, 2) \\ &\quad + \int_{-\infty}^{\infty} dt_3 B^<(1, 3)i\theta(t_3 - t_2)(C^<(3, 2) + C^>(3, 2)). \end{aligned} \quad (1.27)$$

With definitions of retarded and advanced Green's function

$$\begin{aligned} B^R(1, 2) &= -i\theta(t_1 - t_2)(B^>(1, 2) + B^<(1, 2)) \\ B^A(1, 2) &= i\theta(t_2 - t_1)(B^>(1, 2) + B^<(1, 2)) \end{aligned} \quad (1.28)$$

we can rewrite these equations to

$$A^<(1, 2) = \int_{-\infty}^{\infty} dt_3 (B^R(1, 3)C^<(3, 2) + B^<(1, 3)C^A(3, 2)). \quad (1.29)$$

We have obtained the Langreth-Wilkins rule, which in the short notation reads

$$A^< = B^R \cdot C^< + B^< \cdot C^A, \quad (1.30)$$

where  $\cdot$  denotes the time integration along the real time axis. In a very similar manner one finds

$$A^> = B^R \cdot C^> + B^> \cdot C^A. \quad (1.31)$$

Since the formalism has particle-hole symmetry, so that all relations hold after interchange  $>\longleftrightarrow<$ , we take these two relation as a single rule.

We can employ spectral identity to derive a rule for retarded and advanced functions,

$$\begin{aligned} i(A^R - A^A) &= A^> + A^< \\ &= B^R \cdot (C^< + C^>) + (B^< + B^>) \cdot C^A \\ &= B^R i \cdot (C^R - C^A) + i(B^R - B^A) \cdot C^A \\ &= i(B^R \cdot C^R - B^A \cdot C^A). \end{aligned} \quad (1.32)$$

Integration in term  $B^R(1, 3)C^R(3, 2)$  is restricted to time domain  $t_1 > t_3 > t_2$  and for  $t_1 < t_2$  the term  $B^R(1, 3)C^R(3, 2)$  is zero. Similarly the term  $B^A(1, 3)C^A(3, 2)$  is restricted to time domain  $t_1 > t_2$ . The last line can be decomposed to retarded and advanced part

$$\begin{aligned} A^A &= B^A \cdot C^A, \\ A^R &= B^R \cdot C^R. \end{aligned} \quad (1.33)$$

This is the second Langreth-Wilkins rule. These rules are equivalent to Keldysh technique except they are easier to learn and more convenient to apply [7, 8].

We will often need a correlation function of the general expression

$$C = \frac{A}{(1 + A \times B)}. \quad (1.34)$$

Applying the analytical continuation for expression

$$A^< = (C + C \times B \times A)^<, \quad (1.35)$$

and the Langreth-Wilkins rules we get

$$A^< = C^< + C^R \cdot B^R \cdot A^< + C^R \cdot B^< \cdot A^A + C^< \cdot B^A \cdot A^A. \quad (1.36)$$

Our aim is to evaluate the correlation function  $C^<$ ,

$$C^< = (1 - C^R \cdot B^R) \cdot A^< \cdot \frac{1}{(1 + B^A \cdot A^A)} - C^R \cdot B^< \cdot \frac{A^A}{(1 + B^A \cdot A^A)}. \quad (1.37)$$

By rearrangement

$$C^< = \left( 1 - \frac{A^R}{(1 + A^R \cdot B^R)} \cdot B^R \right) \cdot A^< \cdot \frac{1}{(1 + B^A \cdot A^A)} - C^R \cdot B^< \cdot C^A \quad (1.38)$$

the final equation is

$$C^< = \frac{1}{(1 + A^R \cdot B^R)} \cdot A^< \cdot \frac{1}{(1 + B^A \cdot A^A)} - C^R \cdot B^< \cdot C^A. \quad (1.39)$$

Beside time integrals we will also need analytical continuation of direct products. This component we will discuss directly on physical quantities.

# 2. Nambu-Gorkov equations

## 2.1 BCS Hamiltonian

The first microscopic theory of superconductivity is the theory of Bardeen, Cooper and Schrieffer (1957) – the BCS theory. We start from the BCS Hamiltonian, which includes an attractive interaction between two electrons. This attraction is needed for electrons to form Cooper pairs. The Cooper pairs then condense into a superconducting state.

The BCS interaction is separable, therefore the interaction among electrons with parallel spins drops out by antisymmetry with respect to exchange of two operators. This restricts applicability of this model to a spin-singlet superconducting states. However, all real superconductors belong to this type. So far, the only triplet pairing was found in He-III. The Fermi statistic of electrons requires a spin-singlet state to have an even parity with respect to the transposition of the particle coordinates or with respect to inversion of the relative momentum of the particles. This means that the superconducting state should have either *s*-wave or *d*-wave symmetry. We start our consideration with *s*-wave superconducting state.

There are various physical mechanisms of attraction between electrons. In phonon model, for example, the attraction is mediated by an exchange of phonons. The pairing interaction usually works in a restricted energy range and vanishes for energy transfer larger than some cut-off value  $\Omega_{BCS}$ . For phonons this cut-off is crudely the Debye frequency  $\Omega_D$ . If the interaction is relatively weak, the characteristic energies of the particles participating in superconducting phenomena are much smaller than Fermi energy and the cut-off energy also. For these cases we approximate interaction by a point-like interaction

$$U(\mathbf{r}_1 - \mathbf{r}_2) = \frac{g}{2} \delta(\mathbf{r}_1 - \mathbf{r}_2) \quad (2.1)$$

with the option that cut-offs will be included into certain momentum integrals. The potential is attractive for  $g < 0$ . The limit of small interaction corresponds to  $|g\nu| \ll 1$  where  $\nu$  is the density of states at the Fermi level in a normal state. It is called weak-coupling approximation [9].

Now we will derive equations for Green's function for BCS model following monographs [2] and [9]. We start with the BCS Hamiltonian

$$\hat{\mathcal{H}}_{BCS} = \sum_{\alpha=\uparrow\downarrow} \int \left[ -\psi_{\alpha}^{\dagger} \frac{\nabla^2}{2m} \psi_{\alpha} + \frac{g}{2} \psi_{\bar{\alpha}}^{\dagger} \psi_{\alpha}^{\dagger} \psi_{\alpha} \psi_{\bar{\alpha}} \right] d^3r, \quad (2.2)$$

where  $\bar{\alpha}$  is flipped spin  $\alpha$ . The particle number operator has a form

$$\hat{\mathcal{N}} = \sum_{\alpha=\uparrow\downarrow} \int \psi_{\alpha}^{\dagger} \psi_{\alpha} d^3r. \quad (2.3)$$

We want to apply the Heisenberg picture in the complex time representation, where the field operators depend on the imaginary time

$$\begin{aligned} \tilde{\psi}_{\alpha}(\mathbf{r}, \tau) &= e^{(\hat{\mathcal{H}} - \mu \hat{\mathcal{N}})\tau} \psi_{\alpha}(\mathbf{r}) e^{-(\hat{\mathcal{H}} - \mu \hat{\mathcal{N}})\tau}, \\ \tilde{\psi}_{\alpha}^{\dagger}(\mathbf{r}, \tau) &= e^{(\hat{\mathcal{H}} - \mu \hat{\mathcal{N}})\tau} \psi_{\alpha}^{\dagger}(\mathbf{r}) e^{-(\hat{\mathcal{H}} - \mu \hat{\mathcal{N}})\tau}. \end{aligned} \quad (2.4)$$

The Heisenberg operators satisfy the Heisenberg-like equations

$$\begin{aligned}\frac{\partial \tilde{\psi}_\alpha}{\partial \tau} &= \left( \hat{\mathcal{H}} - \mu \hat{\mathcal{N}} \right) \tilde{\psi}_\alpha + \tilde{\psi}_\alpha \left( \hat{\mathcal{H}} - \mu \hat{\mathcal{N}} \right), \\ \frac{\partial \tilde{\psi}_\alpha^\dagger}{\partial \tau} &= \left( \hat{\mathcal{H}} - \mu \hat{\mathcal{N}} \right) \tilde{\psi}_\alpha^\dagger + \tilde{\psi}_\alpha^\dagger \left( \hat{\mathcal{H}} - \mu \hat{\mathcal{N}} \right).\end{aligned}\tag{2.5}$$

Using these equations we can calculate the time derivative of the Heisenberg operators  $\tilde{\psi}$

$$\begin{aligned}\frac{\partial \tilde{\psi}_\alpha}{\partial \tau} &= \left( \frac{\nabla^2}{2m} + \mu \right) \tilde{\psi}_\alpha(x) - g \tilde{\psi}_\gamma^\dagger(x) \tilde{\psi}_\gamma(x) \tilde{\psi}_\alpha(x), \\ \frac{\partial \tilde{\psi}_\alpha^\dagger}{\partial \tau} &= - \left( \frac{\nabla^2}{2m} + \mu \right) \tilde{\psi}_\alpha^\dagger(x) + g \tilde{\psi}_\alpha^\dagger(x) \tilde{\psi}_\gamma^\dagger(x) \tilde{\psi}_\gamma(x),\end{aligned}\tag{2.6}$$

where  $x = (\tau, \mathbf{r})$ . We remind that time  $\tau$  is real and is defined via complex time  $\tau = it$ .

## 2.2 Nambu-Gorkov equations

Our aim is to derive equations for Matsubara's functions. To this end we take the derivative of Matsubara's function,

$$\begin{aligned}\frac{\partial G_{\alpha\beta}(x_1, x_2)}{\partial \tau_1} &= \frac{\partial}{\partial \tau_1} [\delta_{\alpha\beta} \delta(\mathbf{r}_1 - \mathbf{r}_2) \theta(\tau_1 - \tau_2) \\ &+ \left\langle \mathbf{T}_\beta \left( \frac{\nabla^2}{2m} + \mu \right) \tilde{\psi}_\alpha(x_1) \tilde{\psi}_\beta^\dagger(x_2) - g \tilde{\psi}_\gamma^\dagger(x_1) \tilde{\psi}_\gamma(x_1) \tilde{\psi}_\alpha(x_1) \tilde{\psi}_\beta^\dagger(x_2) \right\rangle \\ &= \delta_{\alpha\beta} \delta(\mathbf{r}_1 - \mathbf{r}_2) \delta(\tau_1 - \tau_2) + \left( \frac{\nabla^2}{2m} + \mu \right) G_{\alpha\beta}(x_1, x_2) \\ &- g \left\langle \mathbf{T}_\beta \tilde{\psi}_\gamma^\dagger(x_1) \tilde{\psi}_\gamma(x_1) \tilde{\psi}_\alpha(x_1) \tilde{\psi}_\beta^\dagger(x_2) \right\rangle.\end{aligned}\tag{2.7}$$

We have used equations (2.5) and (2.6) and denoted the trace by angular brackets,  $\mathbf{Tr}(\dots) = \langle \dots \rangle$ . This is the exact equation of motion for Matsubara's function.

Let us focus on the last term. According to Wick's theorem

$$\begin{aligned}\left\langle \mathbf{T}_\beta \tilde{\psi}_\gamma^\dagger(x_1) \tilde{\psi}_\gamma(x_1) \tilde{\psi}_\alpha(x_1) \tilde{\psi}_\beta^\dagger(x_2) \right\rangle &\approx - \left\langle \mathbf{T}_\beta \tilde{\psi}_\gamma(x_1) \tilde{\psi}_\gamma^\dagger(x_1) \right\rangle \left\langle \mathbf{T}_\beta \tilde{\psi}_\alpha(x_1) \tilde{\psi}_\beta^\dagger(x_2) \right\rangle \\ &+ \left\langle \mathbf{T}_\beta \tilde{\psi}_\alpha(x_1) \tilde{\psi}_\gamma^\dagger(x_1) \right\rangle \left\langle \mathbf{T}_\beta \tilde{\psi}_\gamma(x_1) \tilde{\psi}_\beta^\dagger(x_2) \right\rangle.\end{aligned}\tag{2.8}$$

The Wick's theorem applies for noninteracting particles, here we are using the same relation for the interacting system. This schema is not the traditional finite temperature perturbation theory and Wick's theorem. This schema is called decoupling.

According to Wick's theorem, the two-particle Green function decouples to the products of two one-particle Green's functions. In the theory of supercon-

ductivity, however, we need to introduce an additional term

$$\begin{aligned}
\left\langle \mathbf{T}_\beta \tilde{\psi}_\gamma^\dagger(x_1) \tilde{\psi}_\gamma(x_1) \tilde{\psi}_\alpha(x_1) \tilde{\psi}_\beta^\dagger(x_2) \right\rangle &= - \left\langle \mathbf{T}_\beta \tilde{\psi}_\gamma(x_1) \tilde{\psi}_\gamma^\dagger(x_1) \right\rangle \left\langle \mathbf{T}_\beta \tilde{\psi}_\alpha(x_1) \tilde{\psi}_\beta^\dagger(x_2) \right\rangle \\
&+ \left\langle \mathbf{T}_\beta \tilde{\psi}_\alpha(x_1) \tilde{\psi}_\gamma^\dagger(x_1) \right\rangle \left\langle \mathbf{T}_\beta \tilde{\psi}_\gamma(x_1) \tilde{\psi}_\beta^\dagger(x_2) \right\rangle \\
&- \left\langle \mathbf{T}_\beta \tilde{\psi}_\alpha(x_1) \tilde{\psi}_\gamma(x_1) \right\rangle \left\langle \mathbf{T}_\beta \tilde{\psi}_\gamma^\dagger(x_1) \tilde{\psi}_\beta^\dagger(x_2) \right\rangle.
\end{aligned} \tag{2.9}$$

It turned out that traditional perturbative expansions failed for superconductivity. Bardeen, Cooper and Schrieffer have introduced a wave function, which is not sharp in the number of particles. Such wave function is not an eigen-state of the particle number operator, which commutes with the Hamiltonian. Therefore its use is in conflict with the particle conservation law. Nevertheless, this variational wave function gave a very low ground state energy and helped to explain many features of superconductors. Provided that the system is described by such function, the last term results non-zero. This term is called anomalous Green's function.

We can write

$$\begin{aligned}
&\left\langle \mathbf{T}_\beta \tilde{\psi}_\gamma^\dagger(x_1) \tilde{\psi}_\gamma(x_1) \tilde{\psi}_\alpha(x_1) \tilde{\psi}_\beta^\dagger(x_2) \right\rangle \\
&= -\Sigma_{\gamma\gamma}(x_1) G_{\alpha\beta}(x_1, x_2) + \Sigma_{\alpha\gamma}(x_1) G_{\gamma\beta}(x_1, x_2) - \frac{\Delta_{\alpha\gamma}(x_1)}{|g|} F_{\gamma\beta}^\dagger(x_1, x_2),
\end{aligned} \tag{2.10}$$

where we used some of following definitions

$$\begin{aligned}
G_{\alpha\beta}(x_1, x_2) &= \left\langle \mathbf{T}_\beta \tilde{\psi}_\alpha(x_1) \tilde{\psi}_\beta^\dagger(x_2) \right\rangle, \\
\bar{G}_{\alpha\beta}(x_1, x_2) &= - \left\langle \mathbf{T}_\beta \tilde{\psi}_\alpha^\dagger(x_1) \tilde{\psi}_\beta(x_2) \right\rangle, \\
F_{\gamma\beta}^\dagger(x_1, x_2) &= \left\langle \mathbf{T}_\beta \tilde{\psi}_\gamma^\dagger(x_1) \tilde{\psi}_\beta^\dagger(x_2) \right\rangle, \\
F_{\gamma\beta}(x_1, x_2) &= \left\langle \mathbf{T}_\gamma \tilde{\psi}_\gamma(x_1) \tilde{\psi}_\beta(x_2) \right\rangle.
\end{aligned} \tag{2.11}$$

And defined selfenergy in terms of the Matsubara's function

$$\begin{aligned}
\Sigma_{\gamma\beta}(x_1) &= |g| \left\langle \mathbf{T}_\beta \tilde{\psi}_\gamma(x_1) \tilde{\psi}_\beta^\dagger(x_1) \right\rangle, \\
\Delta_{\alpha\beta}(x) &= |g| F_{\alpha\beta}(x, x), \\
\Delta_{\alpha\beta}^*(x) &= |g| F_{\alpha\beta}^\dagger(x, x).
\end{aligned} \tag{2.12}$$

The function  $\Delta$  is the superconducting gap. As one can see, it relates to the anomalous function. Since the anomalous functions are non-zero only for an attractive interaction, we assume  $g < 0$ .

The selfenergy  $\Sigma_{\gamma\bar{\gamma}}$  is zero for our model, because there is no spin-flipping term in the Hamiltonian. The selfenergy  $\Sigma_{\gamma\gamma}$  is nonzero, but it is usually neglected, because in the BCS model the selfenergies leads only to renormalization of the chemical potential.

The equation of motion for Matsubara's function

$$\begin{aligned}
&\left( \frac{\partial}{\partial \tau_1} - \frac{\nabla_1^2}{2m} - \mu \right) G_{\alpha\beta}(x_1, x_2) + |g| \left\langle \mathbf{T}_\beta \tilde{\psi}_\alpha(x_1) \tilde{\psi}_\gamma(x_1) \right\rangle \left\langle \mathbf{T}_\beta \tilde{\psi}_\gamma^\dagger(x_1) \tilde{\psi}_\beta^\dagger(x_2) \right\rangle \\
&= \delta_{\alpha\beta} \delta(x_1 - x_2)
\end{aligned} \tag{2.13}$$

can be written as

$$\left(\frac{\partial}{\partial\tau_1} - \frac{\nabla_1^2}{2m} - \mu\right)G_{\alpha\beta}(x_1, x_2) + \Delta_{\alpha\gamma}(x_1)F_{\gamma\beta}^\dagger(x_1, x_2) = \delta_{\alpha\beta}\delta(x_1 - x_2). \quad (2.14)$$

The function  $F_{\gamma\beta}^\dagger(x_1, x_2)$  is odd in transposition of the particle coordinates and spin indices because of the statistics of electrons. For a pairing interaction which has an even parity in the orbital space such as  $s$ -wave or  $d$ -wave interaction, the Cooper pairing can occur between the electrons with opposite spin projections into a singlet state. Therefore the pair wave function is antisymmetric in spin indices  $\Delta_{\alpha\gamma}(x) = -\Delta_{\gamma\alpha}(x)$ . With this we can write

$$\begin{aligned} \Delta_{\alpha\gamma}(x) &= i\sigma_{\alpha\beta}^{(2)}\Delta(x) \\ \Delta_{\alpha\gamma}^\dagger(x) &= i\sigma_{\alpha\beta}^{(2)}\Delta^*(x) \end{aligned}, \quad (2.15)$$

where

$$\sigma^{(2)} = \begin{pmatrix} 0 & -i \\ i & 0 \end{pmatrix} \quad (2.16)$$

is the Pauli matrix. We also denote

$$\begin{aligned} F_{\alpha\beta}^\dagger(x_1, x_2) &= -i\sigma_{\alpha\beta}^{(2)}F^\dagger(x_1, x_2) \\ F_{\alpha\beta}(x_1, x_2) &= -i\sigma_{\alpha\beta}^{(2)}F(x_1, x_2) \\ G_{\alpha\beta}(x_1, x_2) &= \delta_{\alpha\beta}G(x_1, x_2) \end{aligned}. \quad (2.17)$$

The Matsubara's function is proportional to the unit matrix, because the interaction does not depend on spin. In this notation we can simplify the equation of motion for the Matsubara's function as

$$\left(\frac{\partial}{\partial\tau_1} - \frac{\nabla_1^2}{2m} - \mu\right)G(x_1, x_2) + \Delta(x_1)F^\dagger(x_1, x_2) = \delta(x_1 - x_2). \quad (2.18)$$

This equation contains unknown functions  $F^\dagger(x_1, x_2)$  and  $\Delta(x_1)$ , which can be written in terms of function  $F(x_1, x_2)$ . To find these functions we need additional equations. We can derive them from Heisenberg equations in a similar way. We have three new equations

$$\left(\frac{\partial}{\partial\tau_1} + \frac{\nabla_1^2}{2m} + \mu\right)F^\dagger(x_1, x_2) + \Delta^*(x_1)G(x_1, x_2) = 0, \quad (2.19)$$

$$-\left(\frac{\partial}{\partial\tau_1} + \frac{\nabla_1^2}{2m} + \mu\right)\bar{G}(x_1, x_2) + \Delta^*(x_1)F^\dagger(x_1, x_2) = \delta(x_1 - x_2), \quad (2.20)$$

$$\left(-\frac{\partial}{\partial\tau_1} + \frac{\nabla_1^2}{2m} + \mu\right)F(x_1, x_2) + \Delta(x_1)\bar{G}(x_1, x_2) = 0. \quad (2.21)$$

Equations (2.18)-(2.21) together with relation  $\Delta(x) = |g|F(x, x)$  and its conjugate form are the closed set of equations.

We can easily write down the above set of equations in the matrix form

$$\begin{pmatrix} \frac{\partial}{\partial\tau_1} - \frac{\nabla_1^2}{2m} - \mu & -\Delta(x_1) \\ \Delta^*(x_1) & -\frac{\partial}{\partial\tau_1} - \frac{\nabla_1^2}{2m} - \mu \end{pmatrix} \begin{pmatrix} G(x_1, x_2) & F(x_1, x_2) \\ -F^\dagger(x_1, x_2) & \bar{G}(x_1, x_2) \end{pmatrix} = \begin{pmatrix} \delta(x_1 - x_2) & 0 \\ 0 & \delta(x_1 - x_2) \end{pmatrix} \quad (2.22)$$



with a symbolic notation

$$(\mathbf{G}_0^{-1} + \mathbf{\Sigma})(x_1)\mathbf{G}(x_1, x_2) = \mathbf{1}\delta(x_1 - x_2). \quad (2.23)$$

This is the Nambu-Gorkov equation in the differential form. The integral form is obtained by multiplying it with  $\mathbf{G}_0$

$$\mathbf{G}(x_3, x_2) = \mathbf{G}_0(x_3, x_2) + \mathbf{G}_0(x_3, \bar{x}_1)\mathbf{\Sigma}(\bar{x}_1)\mathbf{G}(\bar{x}_1, x_2). \quad (2.24)$$

The internal variable is integrated over as denoted by bars.

## 2.3 Dyson equation

The Dyson equation expresses the full Matsubara's function in terms of the bare function and selfenergy

$$G(x_1, x_2) = G_0(x_1, x_2) - G_0(x_1, \bar{x}_3)\Sigma(\bar{x}_3, \bar{x}_4)G(\bar{x}_4, x_2). \quad (2.25)$$

It is possible to rearrange the Nambu-Gorkov equation into the Dyson equation.

Let us write the integral Nambu-Gorkov equation (2.24) in explicit form

$$\begin{pmatrix} G(x_1, x_2) & F(x_1, x_2) \\ -F^\dagger(x_1, x_2) & \bar{G}(x_1, x_2) \end{pmatrix} = \begin{pmatrix} G_0(x_1, x_2) & 0 \\ 0 & \bar{G}_0(x_1, x_2) \end{pmatrix} + \begin{pmatrix} G_0(x_1, \bar{x}_3) & 0 \\ 0 & \bar{G}_0(x_1, \bar{x}_3) \end{pmatrix} \begin{pmatrix} 0 & -\Delta(\bar{x}_3) \\ \Delta^*(\bar{x}_3) & 0 \end{pmatrix} \begin{pmatrix} G(\bar{x}_3, x_2) & F(\bar{x}_3, x_2) \\ -F^\dagger(\bar{x}_3, x_2) & \bar{G}(\bar{x}_3, x_2) \end{pmatrix}.$$

Components in the first column satisfy

$$G(x_1, x_2) = G_0(x_1, x_2) + G_0(x_1, \bar{x}_3)\Delta(\bar{x}_3)F^\dagger(\bar{x}_3, x_2), \quad (2.26)$$

$$-F^\dagger(x_3, x_2) = \bar{G}_0(x_3, \bar{x}_4)\Delta^*(\bar{x}_4)G(\bar{x}_4, x_2). \quad (2.27)$$

Eliminating  $F^\dagger$  we arrive at equation for the full Green's function

$$G(x_1, x_2) = G_0(x_1, x_2) - G_0(x_1, \bar{x}_3)\Delta(\bar{x}_3)\bar{G}_0(\bar{x}_3, \bar{x}_4)\Delta^*(\bar{x}_4)G(\bar{x}_4, x_2). \quad (2.28)$$

Comparing this equation with the Dyson equation we can identify the selfenergy corresponding to the Nambu-Gorkov theory

$$\Sigma(x_3, x_4) = \Delta(x_3)\bar{G}_0(x_3, x_4)\Delta^*(x_4). \quad (2.29)$$

Note that the matrix selfenergy  $\mathbf{\Sigma}$  has only a single space-time argument, while the selfenergy  $\Sigma$  of the Dyson equation is a double-time function of two space arguments. The locality in time and space makes Nambu-Gorkov formulation very convenient, but one should keep in mind that this property is restricted to given model and approximation. For the  $d$ -wave pairing the double-space structure appears also for  $\Delta$ . For the retarded interaction mediated by phonons,  $\Delta$  has double-time structure. Going beyond the lowest order approximation used above, the matrix selfenergy depends on two space-time arguments always.

# 3. Unified theory of normal and superconducting state

## 3.1 Introduction

In the last chapter we have introduced Nambu-Gorkov equations. This technique was developed only for description of a condensate, whereas a normal state is covered by standard perturbative methods and the Dyson equation. But a general theory should cover both states. This is needed in systems, where strong fluctuations influence transition from normal to superconducting state.

We saw in the previous chapter that Green's function technique in theory of superconductivity was based on a decoupling schema and anomalous Green's functions. This gave us relation between the gap parameter and the selfenergy in the Dyson equation. The Nambu-Gorkov selfenergy was constructed with a bare Green function and therefore nonselfconsistently  $\Sigma[G^0]$ . It turns out generally that this nonselfconsistency is the necessary for the gap to develop.

On the normal side of the superconducting phase transition, the classical perturbation theory based on Wick's theorem works. One of its formulations is Schwinger-Dyson schema, which conjugates one-particle Dyson equation and two-particle Bethe-Salpeter equation. The two-particle propagation carried by Bethe-Salpeter equation seemed to be suitable for description of two-particle correlations in the superconductor.

There are plenty of approximations of two-particle propagators. Among these approximation there is a  $T$ -matrix in the ladder approximation. It usually appears in description of normal state of metals and nuclear matter with strong interaction potential. Attempts to apply this Galitskii-Feynman schema for attractive interaction and eventually describe by it the superconducting state were not successful. The theory gives an instability of the normal state at the critical temperature but it fails to give the gap at lower temperatures.

The problem was hidden in the selfconsistent construction of the Galitskii-Feynman  $T$ -matrix. This problem disappears when one replaces the selfconsistent schema with a nonselfconsistent one. This is done by a replacement the full Green function by a bare Green function. This schema was followed in Kadanoff-Martin theory. Unfortunately, this schema cannot describe the normal state, which is consequence of the nonselfconsistency.

On one hand, we have selfconsistent Galitskii-Feynman theory, which is applicable to the normal state, on the other hand we have nonselfconsistent Kadanoff-Martin theory which, gives the gap and the superconducting state. Each theory fails down in the domain of the second one. Therefore there is a question. "How the worse approximation can better describe superconducting phenomena?" This problem is called Prange paradox [10].

The problem of selfconsistent treatment is hidden in the two-particle propagation. As any other approximative selfconsistent schema the Galitskii-Feynman approximation has an overcounting of some terms in expansion because of the use of full Green's function to build the selfenergy. This overcounting is minor in the normal state. Below transition temperature the condensate will enhance this

overcounting, however.

If the overcounting is excluded, there is no enhancement. Such a schema was proposed by supervisor of author [10]. The overcounting in physical terms of repeated collisions was forbidden by Soven schema, which was originally developed for multiple scattering of electrons in substitutional alloys [11]. The Galitskii-Feynman  $T$ -matrix with multiple scattering corrections can describe both states of matter. One can recover Nambu-Gorkov selfenergy (2.29) in appropriate limit also.

In the next sections we will introduce Galitskii-Feynman and Kadanoff-Martin theory, followed by multiple scattering corrections to  $T$ -matrix based on Galitskii-Feynman. We will also formulate alternative theory with corrections to Kadanoff-Martin theory. Finally we will discuss the Nambu-Gorkov limit.

In this chapter we will use equilibrium Green's function technique. In the next chapter the nonequilibrium version of the theory will be obtained by using the Langreth-Wilkins rules.

## 3.2 Galitskii-Feynman $T$ -matrix approximation

First we introduce the Galitskii-Feynman approximation, which is commonly used in the normal state of metal. Because we are in equilibrium, it is more convenient to switch by the Fourier transformation to  $k$ -space and to frequencies.

We treat the system of electrons with the Hamiltonian

$$\hat{H} = \sum_{\mathbf{k}} \epsilon(\mathbf{k})(a_{\uparrow\mathbf{k}}^\dagger a_{\uparrow\mathbf{k}} + a_{\downarrow\mathbf{k}}^\dagger a_{\downarrow\mathbf{k}}) + \frac{1}{\Omega} \sum_{\mathbf{k}\mathbf{p}\mathbf{q}} V_{\mathbf{q}}(\mathbf{p}, \mathbf{k}) a_{\downarrow\mathbf{q}-\mathbf{k}}^\dagger a_{\uparrow\mathbf{k}}^\dagger a_{\uparrow\mathbf{p}} a_{\downarrow\mathbf{q}-\mathbf{p}}. \quad (3.1)$$

This Hamiltonian omits interaction between equal spin (triplet interaction) we focus only on singlet interaction. The kinetic energy has zero at the Fermi energy  $\epsilon(\mathbf{k}) = k^2/2m - E_F$ . Variables  $\mathbf{p}$  and  $\mathbf{k}$  are relative momenta before and after interaction. The total momentum of the interacting pairs of particles is denoted as  $\mathbf{q}$ . The creation  $a_{\uparrow\mathbf{k}}^\dagger$  and the annihilation operators are normalized to a sample (or quantization) volume  $\Omega$ , e.g.  $\psi^\dagger(\mathbf{r}) = (1/\sqrt{\Omega}) \sum_{\mathbf{k}} a_{\uparrow\mathbf{k}}^\dagger e^{-i\mathbf{k}\cdot\mathbf{r}}$ .

The standard Dyson equation has a form

$$G_{\uparrow}(\omega, \mathbf{k}) = G_{\uparrow}^0(\omega, \mathbf{k}) + G_{\uparrow}^0(\omega, \mathbf{k}) \Sigma_{\uparrow}(\omega, \mathbf{k}) G_{\uparrow}(\omega, \mathbf{k}), \quad (3.2)$$

where  $G_{\uparrow}(\omega, \mathbf{k})$  is the full Matsubara's function and the bare function reads

$$G_{\uparrow}^0(\omega, \mathbf{k}) = \frac{1}{i\omega - \epsilon(\mathbf{k})}. \quad (3.3)$$

The Dyson equation resp. selfenergy  $\Sigma$  describes averaged effects of all electrons on the motion of a selected electron with momentum  $\mathbf{k}$  spin  $\uparrow$  and Matsubara's frequency  $\omega$ . The Galitskii-Feynman selfenergy is constructed from the two-particle  $T$  matrix

$$\Sigma_{\uparrow}^{GF}(\omega; \mathbf{k}) = \frac{k_B T}{\Omega} \sum_{z\mathbf{q}} T_{\mathbf{q}\uparrow}^{GF}(z; \mathbf{k}, \mathbf{k}) \cdot G_{\downarrow}(z - \omega; \mathbf{q} - \mathbf{k}). \quad (3.4)$$

This still does not say anything about approximation which we use. The specification of approximation is within the  $T$ -matrix.

The Galitskii-Feynman selfenergy uses the ladder approximation of  $T$ -matrix

$$T_{\mathbf{q}\uparrow}^{GF}(z, \mathbf{p}, \mathbf{k}) = V_{\mathbf{q}\uparrow}(\mathbf{p}, \mathbf{k}) + \frac{1}{\Omega} \sum_{z\mathbf{k}'} V_{\mathbf{q}\uparrow}(\mathbf{p}, \mathbf{k}') \mathcal{G}_{\mathbf{q}\uparrow}^{GF}(z, \mathbf{k}') T_{\mathbf{q}\uparrow}^{GF}(z, \mathbf{k}', \mathbf{k}), \quad (3.5)$$

where

$$\mathcal{G}_{\mathbf{q}\uparrow}^{GF}(z, \mathbf{p}) = k_B T \sum_{\omega} G_{\uparrow}(\omega, \mathbf{p}) G_{\downarrow}(z - \omega, \mathbf{q} - \mathbf{p}) \quad (3.6)$$

describes the propagation of two particles or two holes during the collision. We use the convention of signs from [2]. One can note that we have no equations for Matsubara's function of electrons with opposite spins. This complementary equation is recovered by simple replacement of spins by opposite one in all expressions. The set of equations is closed.

Of course like others perturbative approaches the Galitskii-Feynman schema has also some shortcomings. Because of summation of only specific class of diagrams the Galitskii-Feynman approximation contains non-physical processes. Repeated scattering out and scattering in processes are hidden in the schema.

The repeated scattering out processes appear due to products of the selfenergy in the Dyson equation. We can expand the Dyson equation:

$$G_{\uparrow}(\omega, \mathbf{k}) = G_{\uparrow}^0(\omega, \mathbf{k}) + \dots + G_{\uparrow}^0(\omega, \mathbf{k}) \Sigma_{\uparrow}(\omega, \mathbf{k}) G_{\uparrow}^0(\omega, \mathbf{k}) \Sigma_{\uparrow}(\omega, \mathbf{k}) \dots G_{\uparrow}^0(\omega, \mathbf{k}) + \dots \quad (3.7)$$

In the second order we have two sums

$$G_{\uparrow}^0 \Sigma_{\uparrow} G_{\uparrow}^0 \Sigma_{\uparrow} G_{\uparrow}^0 = \frac{k_B^2 T^2}{\Omega^2} G_{\uparrow}^0 \sum_{z\mathbf{q}} (T_{\mathbf{q}} G_{\uparrow}) G_{\uparrow}^0 \sum_{z'\mathbf{q}'} (T_{\mathbf{q}'} G_{\uparrow}) G_{\uparrow}^0. \quad (3.8)$$

The non-physical repeated scattering out collisions  $\mathbf{q} = \mathbf{q}'$  should be excluded.

Repeated scattering in processes are hidden in the selfconsistent construction of the selfenergy. The selfenergy is a functional of the dressed Matsubara's functions  $\Sigma_{\uparrow}^{GF}[G_{\downarrow}, G_{\uparrow}]$ . In this way the collision processes described by selfenergy  $\Sigma_{\uparrow}^{GF}[G_{\downarrow}, G_{\uparrow}]$  also contributes to its internal Matsubara's function  $G_{\downarrow}$ . Therefore these processes supply particles into its own initial state.

$$\Sigma_{\uparrow}^{GF}[G_{\downarrow}, G_{\uparrow}] = \frac{k_B T}{\Omega} \sum_{z, \mathbf{q}} \left( T_{\mathbf{q}} \left[ G_{\uparrow}^0 + G_{\uparrow}^0 \frac{k_B T}{\Omega} \sum_{z', \mathbf{q}'} (T_{\mathbf{q}'} G_{\downarrow}) G_{\uparrow}^0 + \dots, G_{\downarrow} \right] G_{\downarrow} \right). \quad (3.9)$$

Again we have a double sum in the selfenergy  $\mathbf{q} = \mathbf{q}'$  which should be excluded.

It should be noted that in normal metal every channel  $\mathbf{q}$  in the summation (3.4) has the weight of an inverse of the volume and vanishes in the thermodynamical limit. Therefore the error due to repeated collisions is negligible. It is the reason why the Galitskii-Feynman approximation widely used in normal phase is successful. In a superconductor, however, the repeated collisions in the pairing channel are enhanced due to macroscopic occupation of the pairing channel. These repeated collisions block the formation of the gap.

### 3.3 Kadanoff-Martin $T$ -matrix approximation

One possibility how to eliminate the repeated collisions is to prohibit a whole class of diagrams in schema of Galitskii and Feynman. This is equivalent to the use of bare Matsubara's function instead the full one in two-particle propagation.

We will thus modify the equations (3.4) for construction of selfenergy

$$\Sigma_{\uparrow}^{KM}(\omega; \mathbf{k}) = \frac{k_B T}{\Omega} \sum_{z\mathbf{q}} T_{\mathbf{q}\uparrow}^{KM}(z; \mathbf{k}, \mathbf{k}) \cdot G_{\downarrow}^0(z - \omega; \mathbf{q} - \mathbf{k}). \quad (3.10)$$

We are closing  $T$ -matrix by bare Matsubara's function here.

The second equation which has to be changed is equation for  $T$ -matrix (3.5) in way

$$T_{\mathbf{q}\uparrow}^{KM}(z, \mathbf{p}, \mathbf{k}) = V_{\mathbf{q}\uparrow}(\mathbf{p}, \mathbf{k}) + \frac{1}{\Omega} \sum_{z\mathbf{k}'} V_{\mathbf{q}\uparrow}(\mathbf{p}, \mathbf{k}') \mathcal{G}_{\mathbf{q}\uparrow}^{KM}(z, \mathbf{k}') T_{\mathbf{q}\uparrow}^{GF}(z, \mathbf{k}', \mathbf{k}), \quad (3.11)$$

where two-particle propagator (3.6) is constructed from one bare Matsubara's function, which closed the loop in (3.12)

$$\mathcal{G}_{\mathbf{q}\uparrow}^{KM}(z, \mathbf{p}) = k_B T \sum_{\omega} G_{\uparrow}(\omega, \mathbf{p}) G_{\downarrow}^0(z - \omega, \mathbf{q} - \mathbf{p}). \quad (3.12)$$

This modification leads to an approximation, which covers gap in superconducting state. One can recover Nambu-Gorkov selfenergy from equation (3.10). We suppose that pairing occurs in states not only with different spin, but also with different momenta, which is in our notation channel  $\mathbf{q} = 0$  and zero energy. Others channels create surroundings and we neglect them for the moment. We have

$$\Sigma_{\uparrow}^{NG}(\omega; \mathbf{k}) = \frac{k_B T}{\Omega} T_{0\uparrow}^{KM}(0; \mathbf{k}, \mathbf{k}) \cdot G_{\downarrow}^0(0 - \omega; -\mathbf{k}). \quad (3.13)$$

Important assumption is supposed,  $T$ -matrix is separable in pairing channel

$$\frac{k_B T}{\Omega} T_{0\uparrow}^{KM}(0; \mathbf{k}, \mathbf{k}) = \Delta(\mathbf{k}) \Delta^*(\mathbf{k}). \quad (3.14)$$

The weight of  $T$ -matrix in pairing channel is proportional to the volume, so the gap parameter is order of unity in the volume.

Substituted to equation (3.13) one finds

$$\Sigma_{\uparrow}^{NG}(\omega; \mathbf{k}) = \Delta(\mathbf{k}) G_{\downarrow}^0(-\omega; -\mathbf{k}) \Delta^*(\mathbf{k}), \quad (3.15)$$

which resembles Nambu-Gorkov selfenergy (2.29). Nambu-Gorkov selfenergy can describe the gap parameter. From construction above it is obvious that Nambu-Gorkov selfenergy can not be obtained from Galitskii-Feynman schema.

### 3.4 Multiple scattering corrections to the Galitskii-Feynman approximation

In this section we introduce multiple scattering correction to the Galitskii-Feynman approximation. This correction repairs the Galitskii-Feynman schema in the manner, which allows the equations to describe the gap.

Standard Dyson equation remains unchanged

$$G_{\uparrow}(\omega, \mathbf{k}) = G_{\uparrow}^0(\omega, \mathbf{k}) + G_{\uparrow}^0(\omega, \mathbf{k})\Sigma_{\uparrow}(\omega, \mathbf{k})G_{\uparrow}(\omega, \mathbf{k}). \quad (3.16)$$

Dyson equation is an equation for full Matsubara's function  $G[\Sigma]$ , provided one has an equation for selfenergy  $\Sigma[G]$ . The set of equations  $\Sigma[G]$  from the Galitskii-Feynman schema has to be modified. The Soven idea how to remove the repeated collisions can be adopted to Galitskii-Feynman approximation as following.

Separable potential  $V_{\mathbf{q}}$  from (3.1) is split into channels belonging to the total momentum of particles  $\mathbf{q}$ . In the same manner one can split the total selfenergy

$$\Sigma_{\uparrow}(\omega, \mathbf{k}) = \sum_{\mathbf{q}} \Sigma_{\mathbf{q}\uparrow}(\omega, \mathbf{k}). \quad (3.17)$$

This splitting was used, implicitly, also in equations (3.4), (3.10).

We define a subsidiary Matsubara's function, in which the  $\mathbf{q}$  channel is not included

$$G_{\mathbf{q}\uparrow}(\omega, \mathbf{k}) = G_{\uparrow}(\omega, \mathbf{k}) - G_{\uparrow}(\omega, \mathbf{k})\Sigma_{\mathbf{q}\uparrow}(\omega, \mathbf{k})G_{\mathbf{q}\uparrow}(\omega, \mathbf{k}). \quad (3.18)$$

In terms of the bare Matsubara function the reduced Matsubara function reads  $G_{\mathbf{q}\uparrow} = G_{\uparrow}^0 + G_{\uparrow}^0(\Sigma_{\uparrow} - \Sigma_{\mathbf{q}\uparrow})G_{\mathbf{q}\uparrow}$ . From this relation one sees the reduced function as almost full Matsubara's function.

From  $\mathbf{q}$ -reduced Matsubara's function we will construct two-particle  $\mathbf{q}$ -reduced propagator

$$\mathcal{G}_{\mathbf{q}\uparrow}(z, \mathbf{p}) = k_B T \sum_{\omega} G_{\mathbf{q}\uparrow}(\omega, \mathbf{p})G_{\downarrow}(z - \omega, \mathbf{q} - \mathbf{p}). \quad (3.19)$$

Note that the Matsubara's function for the spin  $\downarrow$  is not reduced, because we have excluded only the spin  $\uparrow$  part of selfenergy. The reduced spin component is specified in the subscript of two-particle function.

We can see the difference in the construction of two-particle propagator in Galitskii-Feynman, Kadanoff-Martin and Multiple scattering theory. In the first theory we use two full Matsubara's function, in the second we use bare and full Matsubara's function and in the last case we used  $\mathbf{q}$ -reduced and full functions.

Two-particle propagator is an intermediate component of two interacting particles in ladder approximation of  $T$ -matrix

$$T_{\mathbf{q}\uparrow}(z, \mathbf{p}, \mathbf{k}) = V_{\mathbf{q}\uparrow}(\mathbf{p}, \mathbf{k}) + \frac{1}{\Omega} \sum_{\mathbf{k}'} V_{\mathbf{q}\uparrow}(\mathbf{p}, \mathbf{k}')\mathcal{G}_{\mathbf{q}\uparrow}(z, \mathbf{k}')T_{\mathbf{q}\uparrow}(z, \mathbf{k}', \mathbf{k}). \quad (3.20)$$

Using the  $\mathbf{q}$ -reduced Matsubara function in internal two-particle propagator we have eliminated the repeated scattering in processes.

The  $T$ -matrix covers all orders of the binary interaction. The dressed Matsubara's function reads

$$G_{\uparrow}(\omega, \mathbf{k}) = G_{\mathbf{q}\uparrow}(\omega, \mathbf{k}) + G_{\mathbf{q}\uparrow}(\omega, \mathbf{k})S_{\mathbf{q}\uparrow}(\omega, \mathbf{k})G_{\mathbf{q}\uparrow}(\omega, \mathbf{k}), \quad (3.21)$$

where

$$S_{\mathbf{q}\uparrow}(\omega; \mathbf{k}) = \frac{k_B T}{\Omega} \sum_z T_{\mathbf{q}\uparrow}(z; \mathbf{k}, \mathbf{k})G_{\downarrow}(z - \omega; \mathbf{q} - \mathbf{k}), \quad (3.22)$$

is the reducible selfenergy for the internal channel  $\mathbf{q}$ . The reducible selfenergy  $S$  has to be distinguished from the irreducible selfenergy  $\Sigma$ . This construction is free of successive scattering out collisions.

The relation between reducible selfenergy  $S$  and irreducible selfenergy  $\Sigma$  follows from relations (3.19) and (3.30)

$$\Sigma_{\mathbf{q}\uparrow}(\omega; \mathbf{k}) = \frac{S_{\mathbf{q}\uparrow}(\omega; \mathbf{k})}{1 + G_{\mathbf{q}\uparrow}(\omega; \mathbf{k})S_{\mathbf{q}\uparrow}(\omega; \mathbf{k})}. \quad (3.23)$$

The above set of equations eliminates the repeated collisions, which appear in the original Galitskii-Feynman schema. We can see that this method is fully selfconsistent. This means that selfenergy is a functional of full Matsubara's function  $\Sigma[G, G_{\mathbf{q}}[G]]$ . Together with the Dyson equation  $G[\Sigma]$  the selfenergy  $\Sigma[G, G_{\mathbf{q}}[G]]$  constitute the closed set of equation.

Historically, the Soven idea of effective medium was developed for one-particle scattering on impurities. The reformulation of the original Soven condition is made in the appendix A. This allow us to bring this idea from alloys, where scattering is between electron and impurity, to a the problem of scattering of two electrons. We derive the set of equations (A.24)-(A.29), which parallel (3.17)-(3.30). There are two differences. Instead of channel, which relate to impurity side in alloys, the channel  $\mathbf{q}$  means the total momentum of a electron pair. The second difference is the use of two-particle  $T$ -matrix instead of one-particle  $T$ -matrix, suitable for scattering on impurity. For more details see appendix A.

### 3.5 Limit of Nambu-Gorkov selfenergy

One can recover Nambu-Gorkov selfenergy from multiple scattering theory in the limit of one pairing channel  $\Sigma_{\uparrow 0}$ . In this limit we neglect all other channels setting  $\Sigma_{\uparrow \mathbf{q} \neq 0} = 0$ , therefore

$$\Sigma_{\uparrow}(\omega, \mathbf{k}) = \Sigma_{0\uparrow}(\omega, \mathbf{k}), \quad (3.24)$$

and the reduced Matsubara function is the same as the bare Matsubara function

$$\begin{aligned} G_{0\uparrow}(\omega, \mathbf{k}) &= G_{\uparrow}(\omega, \mathbf{k}) - G_{\uparrow}(\omega, \mathbf{k})\Sigma_{0\uparrow}(\omega, \mathbf{k})G_{0\uparrow}(\omega, \mathbf{k}), \\ &= G_{\uparrow}(\omega, \mathbf{k}) - G_{\uparrow}(\omega, \mathbf{k})\Sigma_{\uparrow}(\omega, \mathbf{k})G_{0\uparrow}(\omega, \mathbf{k}), \\ &= G_{\uparrow}^0(\omega, \mathbf{k}). \end{aligned} \quad (3.25)$$

Equation (3.23) can be written in form

$$\Sigma_{0\uparrow}(\omega; \mathbf{k}) + \Sigma_{0\uparrow}(\omega; \mathbf{k})G_{0\uparrow}(\omega; \mathbf{k})S_{0\uparrow}(\omega; \mathbf{k}) = S_{0\uparrow}(\omega; \mathbf{k}), \quad (3.26)$$

or using (3.25) as

$$\Sigma_{\uparrow}(\omega; \mathbf{k}) + \Sigma_{\uparrow}(\omega; \mathbf{k})G_{\uparrow}^0(\omega; \mathbf{k})S_{\uparrow}(\omega; \mathbf{k}) = S_{\uparrow}(\omega; \mathbf{k}). \quad (3.27)$$

The resulting reducible selfenergy can be put in (3.21)

$$\begin{aligned} G_{\uparrow}(\omega, \mathbf{k}) &= G_{0\uparrow}(\omega, \mathbf{k}) + G_{0\uparrow}(\omega, \mathbf{k})S_{0\uparrow}(\omega, \mathbf{k})G_{0\uparrow}(\omega, \mathbf{k}), \\ &= G_{\uparrow}^0(\omega, \mathbf{k}) + G_{\uparrow}^0(\omega, \mathbf{k})S_{\uparrow}(\omega, \mathbf{k})G_{\uparrow}^0(\omega, \mathbf{k}), \\ &= G_{\uparrow}^0(\omega, \mathbf{k}) + G_{\uparrow}^0(\omega, \mathbf{k})\Sigma_{\uparrow}(\omega; \mathbf{k})G_{\uparrow}^0(\omega, \mathbf{k}) \\ &\quad + G_{\uparrow}^0(\omega, \mathbf{k})\Sigma_{\uparrow}(\omega; \mathbf{k})G_{\uparrow}^0(\omega; \mathbf{k})S_{\uparrow}(\omega; \mathbf{k})G_{\uparrow}^0(\omega, \mathbf{k}). \end{aligned} \quad (3.28)$$

We can group the last two terms

$$G_{\uparrow}(\omega, \mathbf{k}) = G_{\uparrow}^0(\omega, \mathbf{k}) + G_{\uparrow}^0(\omega, \mathbf{k})\Sigma_{\uparrow}(\omega; \mathbf{k})(G_{\uparrow}^0(\omega, \mathbf{k}) + G_{\uparrow}^0(\omega; \mathbf{k})S_{\uparrow}(\omega; \mathbf{k})G_{\uparrow}^0(\omega, \mathbf{k})). \quad (3.29)$$

Let us use equation for  $T$ -matrix (3.30), where, in condensate, the dominant term is  $T_{0\uparrow}(0; \mathbf{k}, \mathbf{k}) \gg T_{0\uparrow}(z \neq 0; \mathbf{k}, \mathbf{k})$ ,

$$\begin{aligned} S_{\uparrow}(\omega; \mathbf{k}) &= \frac{k_B T}{\Omega} T_{0\uparrow}(0; \mathbf{k}, \mathbf{k}) G_{\downarrow}(-\omega; -\mathbf{k}), \\ &= \Delta(\mathbf{k}) G_{\downarrow}(-\omega; -\mathbf{k}) \Delta^*(\mathbf{k}), \end{aligned} \quad (3.30)$$

In the second line we have used the separability of  $T$ -matrix. Substituting into (3.31) we obtain

$$G_{\uparrow}(\omega, \mathbf{k}) = G_{\uparrow}^0(\omega, \mathbf{k}) + G_{\uparrow}^0(\omega, \mathbf{k})\Sigma_{\uparrow}(\omega; \mathbf{k}) (G_{\uparrow}^0(\omega, \mathbf{k}) + G_{\uparrow}^0(\omega; \mathbf{k})\Delta(\mathbf{k})G_{\downarrow}(-\omega; -\mathbf{k})\Delta^*(\mathbf{k})G_{\uparrow}^0(\omega, \mathbf{k})). \quad (3.31)$$

Let us do a nontrivial step with the help of the statement in form of equation (13) in [12]. According to this statement we can write a part of the last term in (3.31) in formation

$$\Delta(\mathbf{k})G_{\downarrow}(-\omega; -\mathbf{k})\Delta^*(\mathbf{k})G_{\uparrow}^0(\omega, \mathbf{k}) = \Delta(\mathbf{k})G_{\downarrow}^0(-\omega; -\mathbf{k})\Delta^*(\mathbf{k})G_{\uparrow}(\omega, \mathbf{k}). \quad (3.32)$$

We put this expression back to equation (3.31)

$$G_{\uparrow}(\omega, \mathbf{k}) = G_{\uparrow}^0(\omega, \mathbf{k}) + G_{\uparrow}^0(\omega, \mathbf{k})\Sigma_{\uparrow}(\omega; \mathbf{k}) (G_{\uparrow}^0(\omega, \mathbf{k}) + G_{\uparrow}^0(\omega; \mathbf{k})\Delta(\mathbf{k})G_{\downarrow}^0(-\omega; -\mathbf{k})\Delta^*(\mathbf{k})G_{\uparrow}(\omega, \mathbf{k})). \quad (3.33)$$

According to the Dyson equation the term in bracket is the full Matsubara function

$$G_{\uparrow}(\omega, \mathbf{k}) = G_{\uparrow}^0(\omega, \mathbf{k}) + G_{\uparrow}^0(\omega; \mathbf{k})\Delta(\mathbf{k})G_{\downarrow}^0(-\omega; -\mathbf{k})\Delta^*(\mathbf{k})G_{\uparrow}(\omega, \mathbf{k}). \quad (3.34)$$

We can identify that the selfenergy in the one pairing channel limit is the same as in equation (3.15)

$$\Sigma_{\uparrow}(\omega; \mathbf{k}) = \Sigma_{\uparrow}^{NG}(\omega; \mathbf{k}) = \Delta(\mathbf{k})G_{\downarrow}^0(-\omega; -\mathbf{k})\Delta^*(\mathbf{k}), \quad (3.35)$$

Briefly, the Nambu-Gorkov equation is recovered as a single-channel approximation of the Multiple scattering theory.

## 3.6 Corrections to Kadanoff-Martin approximation

In this section we repair Kadanoff-Martin theory in the manner similar to multiple scattering corrections in Galitskii-Feynman approximation.

The Dyson equation and selfenergy are unchanged

$$G_{\uparrow}(\omega, \mathbf{k}) = G_{\uparrow}^0(\omega, \mathbf{k}) + G_{\uparrow}^0(\omega, \mathbf{k})\Sigma_{\uparrow}(\omega, \mathbf{k})G_{\uparrow}(\omega, \mathbf{k}), \quad (3.36)$$



$$\Sigma_{\uparrow}(\omega, \mathbf{k}) = \sum_{\mathbf{q}} \Sigma_{\mathbf{q}\uparrow}(\omega, \mathbf{k}). \quad (3.37)$$

The equation, which relates reduced and full Matsubara's functions is also unchanged

$$G_{\mathbf{q}\uparrow}(\omega, \mathbf{k}) = G_{\uparrow}(\omega, \mathbf{k}) - G_{\uparrow}(\omega, \mathbf{k})\Sigma_{\mathbf{q}\uparrow}(\omega, \mathbf{k})G_{\mathbf{q}\uparrow}(\omega, \mathbf{k}). \quad (3.38)$$

The differences are in the construction of two-particle propagator. We mutually exchange positions of both Matsubara's function in (3.19)

$$\mathcal{G}_{\mathbf{q}\uparrow}(z, \mathbf{p}) = k_B T \sum_{\omega} G_{\uparrow}(\omega, \mathbf{p}) G_{\mathbf{q}\downarrow}(z - \omega, \mathbf{q} - \mathbf{p}), \quad (3.39)$$

and put the propagator into the  $T$ -matrix equation in the ladder approximation

$$T_{\mathbf{q}\uparrow}(z, \mathbf{p}, \mathbf{k}) = V_{\mathbf{q}\uparrow}(\mathbf{p}, \mathbf{k}) + \frac{1}{\Omega} \sum_{\mathbf{k}'} V_{\mathbf{q}\uparrow}(\mathbf{p}, \mathbf{k}') \mathcal{G}_{\mathbf{q}\uparrow}(z, \mathbf{k}') T_{\mathbf{q}\uparrow}(z, \mathbf{k}', \mathbf{k}). \quad (3.40)$$

From the construction of the  $T$ -matrix follows that we need to close the equation with reduced Matsubara's function

$$\Sigma_{\mathbf{q}\uparrow}(\omega; \mathbf{k}) = \frac{k_B T}{\Omega} \sum_z T_{\mathbf{q}\uparrow}(z; \mathbf{k}, \mathbf{k}) \cdot G_{\mathbf{q}\downarrow}(z - \omega; \mathbf{q} - \mathbf{k}), \quad (3.41)$$

because all Matsubara's function in the loop or open line should be in the same approximation.

The selfenergy remains irreducible as in Kadanoff-Martin theory. There is an essential difference, however. We use the reduced function to close the loop in the Schwinger-Dyson equation (3.41), whereas we have used the full Matsubara function above in equation (3.30).

As in previous subsection, one can recover the Nambu-Gorkov selfenergy in the one pairing channel limit with the help of separability of the  $T$ -matrix. Within this limit the Multiple scattering theory and also the corrected Kadanoff-Martin theory reduce to Nambu-Gorkov theory and become equivalent. The normal state properties are hidden in channels  $\mathbf{q} \neq 0$ , which are outside of condensate.

### 3.7 Selfconsistent $T$ -matrix theory of superconductivity

In all methods, discussed above, we had some particular level of selfconsistency. The problem of selfconsistency in the theory of superconductivity was revised in [13]. In this article a restricted selfconsistent theory, based on a method from section 3.6, is developed for general retarded interaction. There is also a statement that this theory is equivalent to the theory based on theory from section 3.4. Both theories can be brought to the form of the second one, if individual channels are identified via four-momentum, i.e., the momentum and the frequency. Such labeling is necessary for a general retarded interaction mediated by phonons.

Selective elimination of individual Fourier components violates the double-time structure of the  $T$ -matrix making a general four-time function out of it. This does not harm for the retarded interaction, where the  $T$ -matrix is the four-time

function anyway. For the instantaneous interaction assumed here, we want to keep the double-time structure which has much simpler correlation functions. To this end we ban small corrections eliminating all Fourier components in the same time, as it is outlined above. The Multiple scattering theory and the improved Kadanoff-Martin theories are not strictly identical in this case, but differ only by minor contributions.

Why we are not interested in the general retarded interaction? In the next chapter we develop a nonequilibrium version of the theory in section 3.4 by application of Langreth-Wilkins rules. For retarded potential this causes problems, because we bring a new frequency variable, which should be included. The analytic continuation would give us six analytic parts since we have three time functions on general contour. This makes the putative nonequilibrium version prohibitively complicated.

# 4. Theory of nonequilibrium superconductivity

## 4.1 Introduction

The unified theory of superconducting and normal state developed in the last chapter is needed in systems with strong fluctuations close to transitions between normal and superconducting state. A family of such systems includes high temperature superconductors with their pseudogap phase, ultracold Fermi gases near the BEC-BCS crossover, and also low dimensional systems, such as nano-superconductors.

The last example is a well known system, where many features were observed by spectroscopic measurements [14]. In the tunneling spectroscopy the measured system is generally out of equilibrium. For this reason the general nonequilibrium theory should be applied.

There are classical textbooks about nonequilibrium in superconductors. These theories are based on Nambu-Gorkov equations so they are able to include only properties of the condensate. Analytic continuation of Nambu-Gorkov equations is done by Keldysh or Kadanoff-Baym formalism. The effects of retarded interaction on the condensate can be also studied. By a quasiclassical approximation one can derive time dependent Ginzburg-Landau theory and thereby explain phenomena like motion of Abrikosov vortices.

We are interested in regimes not studied till recent development in ultracold gases – in regimes, where the normal and superconducting phase compete. To allow a fair competition, a physical theory has to treat both phases on the same level. In this chapter we develop nonequilibrium version of the theory introduced in section 3.4.

## 4.2 Imaginary time formalism

The theory of superconductivity with multiple scattering corrections was formulated for equilibrium in section 3.4. We want to extend the theory to nonequilibrium systems by using the Langreth-Wilkins rules (1.30)-(1.33). To this end the set of equations (3.16)-(3.30) has to be brought to the time domain by the Fourier transformation on imaginary segment. The Dyson equation reads

$$G_{\uparrow}(t_1, t_2, \mathbf{k}) = G_{\uparrow}^0(t_1, t_2, \mathbf{k}) + G_{\uparrow}^0(t_1, \bar{t}_3, \mathbf{k})\Sigma_{\uparrow}(\bar{t}_3, \bar{t}_4, \mathbf{k})G_{\uparrow}(\bar{t}_4, t_2), \quad (4.1)$$

where selfenergy is a sum over channels

$$\Sigma_{\uparrow}(t_1, t_2, \mathbf{k}) = \sum_{\mathbf{q}} \Sigma_{\mathbf{q}\uparrow}(t_1, t_2, \mathbf{k}). \quad (4.2)$$

The bar denotes integration over imaginary segment (or Kadanoff-Baym complex time path).

The reduced Green function depends on the full Green function as

$$G_{\mathbf{q}\uparrow}(t_1, t_2, \mathbf{k}) = G_{\uparrow}(t_1, t_2, \mathbf{k}) - G_{\uparrow}(t_1, \bar{t}_3, \mathbf{k})\Sigma_{\mathbf{q}\uparrow}(\bar{t}_3, \bar{t}_4, \mathbf{k})G_{\mathbf{q}\uparrow}(\bar{t}_4, t_2, \mathbf{k}). \quad (4.3)$$

Alternatively one can use the averaged  $T$ -matrix form

$$G_{\uparrow}(t_1, t_2, \mathbf{k}) = G_{\mathbf{q}\uparrow}(t_1, t_2, \mathbf{k}) + G_{\mathbf{q}\uparrow}(t_1, \bar{t}_3, \mathbf{k})S_{\mathbf{q}\uparrow}(\bar{t}_3, \bar{t}_4, \mathbf{k})G_{\mathbf{q}\uparrow}(\bar{t}_4, t_2, \mathbf{k}). \quad (4.4)$$

The two-particle propagator does not contains any integration

$$\mathcal{G}_{\mathbf{q}\uparrow}(t_1, t_2; \mathbf{k}) = iG_{\mathbf{q}\uparrow}(t_1, t_2; \mathbf{k})G_{\downarrow}(t_1, t_2; \mathbf{q} - \mathbf{k}). \quad (4.5)$$

Note the complex unit which appears since we have turned the time to the real axis,  $\tau \rightarrow it$ . The two-particle propagator enters the  $T$ -matrix ladder

$$T_{\mathbf{q}\uparrow}(t_1, t_2, \mathbf{p}, \mathbf{k}) = V_{\mathbf{q}\uparrow}(\mathbf{p}, \mathbf{k})\delta(t_1 - t_2) + \frac{1}{\Omega} \sum_{\mathbf{k}'} V_{\mathbf{q}\uparrow}(\mathbf{p}, \mathbf{k}')\mathcal{G}_{\mathbf{q}\uparrow}(t_1, \bar{t}_4, \mathbf{k}')T_{\mathbf{q}\uparrow}(\bar{t}_4, t_2, \mathbf{k}', \mathbf{k}). \quad (4.6)$$

The Dirac delta function represents ‘time’ dependence of instantaneous interaction.

The last equation is the averaged  $T$ -matrix

$$S_{\mathbf{q}\uparrow}(t_1, t_2; \mathbf{k}) = \frac{-i}{\Omega} T_{\mathbf{q}\uparrow}(t_1, t_2; \mathbf{k}, \mathbf{k})G_{\downarrow}(t_2, t_1; \mathbf{q} - \mathbf{k}), \quad (4.7)$$

where Green’s function in a loop has opposite order of times. We recall alternative expressions for selfenergy, which can be derived from the equations above

$$\Sigma_{\mathbf{q}\uparrow}(t_1, t_2, \mathbf{k}) = S_{\mathbf{q}\uparrow}(t_1, t_2, \mathbf{k}) - \Sigma_{\mathbf{q}\uparrow}(t_1, \bar{t}_3, \mathbf{k})G_{\mathbf{q}\uparrow}(\bar{t}_3, \bar{t}_4, \mathbf{k})S_{\mathbf{q}\uparrow}(\bar{t}_4, t_2, \mathbf{k}), \quad (4.8)$$

$$S_{\mathbf{q}\uparrow}(t_1, t_2, \mathbf{k}) = \Sigma_{\mathbf{q}\uparrow}(t_1, t_2, \mathbf{k}) + \Sigma_{\mathbf{q}\uparrow}(t_1, \bar{t}_3, \mathbf{k})G_{\uparrow}(\bar{t}_3, \bar{t}_4, \mathbf{k})\Sigma_{\mathbf{q}\uparrow}(\bar{t}_4, t_2, \mathbf{k}). \quad (4.9)$$

We will use expression (4.9) instead of (4.4).

## 4.3 Nonequilibrium Green functions

Now we employ the machinery of nonequilibrium Green’s functions to convert the above set to equations on the real time axis valid under nonequilibrium conditions.

### 4.3.1 GKB equation

The Dyson equation (4.1) has a short notation  $G = G^0 + G^0 \times \Sigma \times G$ . According to the Langreth-Wilkins rule (1.33), The equation for the retarded Green function thus is

$$G^R = G^{0R} + G^{0R} \cdot \Sigma^R \cdot G^R. \quad (4.10)$$

Equation for the advanced Green function one obtains by a simple interchange of retarded and advanced functions.

The analytic continuation of  $G$  is thus given by relation (1.39). Therefore for correlation function we use the relation (1.39) which yields

$$G^< = G^R \cdot \Sigma^< \cdot G^A + (1 + G^R \cdot \Sigma^R) \cdot G^{0<} \cdot (1 + \Sigma^A \cdot G^A). \quad (4.11)$$

It has two terms. The first term simulates particles outgoing from scattering. It should be mentioned that it also describes non-dissipative response of particles to the background motion.

The second term includes  $G^{0<}$  which is related either to the initial or boundary condition. It can be neglected if all particles in the system have undergone many collisions in the past. The generalized Kadanoff-Baym equation then simplifies as

$$G^{<} = G^R \cdot \Sigma^{<} \cdot G^A. \quad (4.12)$$

Starting from the Dyson equation in imaginary time domain we derived a set of equations for retarded, advanced, particle and hole correlations functions:

$$\begin{aligned} G^R &= G^{0R} + G^R \cdot \Sigma^R \cdot G^{0R} \\ G^A &= G^{0A} + G^A \cdot \Sigma^A \cdot G^{0A} \\ G^{<} &= G^R \cdot \Sigma^{<} \cdot G^A \\ G^{>} &= G^R \cdot \Sigma^{>} \cdot G^A \end{aligned} \quad (4.13)$$

Here dots denote integrations on the real time axis. Note that we have obtained four times more functions and four times more equations of motions as compared to the equilibrium theory. Our set of equations in equilibrium has 7 equations for spin  $\downarrow$  and 7 equations for spin  $\uparrow$ , therefore in the nonequilibrium theory we will have 28 equations for spin  $\downarrow$  and 28 equations for spin  $\uparrow$ . The number of equations can be reduced by symmetry in special cases.

## 4.4 Reduced Green's function

The equation for reduced Green's function  $G_{\mathbf{q}} = G - G \times \Sigma_{\mathbf{q}} \times G_{\mathbf{q}}$  has the structure similar to the Dyson equation. Its analytical continuation thus reads

$$\begin{aligned} G_{\mathbf{q}}^R &= G^R - G^R \cdot \Sigma_{\mathbf{q}}^R \cdot G_{\mathbf{q}}^R \\ G_{\mathbf{q}}^A &= G^A - G^A \cdot \Sigma_{\mathbf{q}}^A \cdot G_{\mathbf{q}}^A \\ G_{\mathbf{q}}^{<} &= (1 - G_{\mathbf{q}}^R \cdot \Sigma_{\mathbf{q}}^R) \cdot G^{<} \cdot (1 - \Sigma_{\mathbf{q}}^A \cdot G_{\mathbf{q}}^A) - G_{\mathbf{q}}^R \cdot \Sigma_{\mathbf{q}}^{<} \cdot G_{\mathbf{q}}^A \\ G_{\mathbf{q}}^{>} &= (1 - G_{\mathbf{q}}^R \cdot \Sigma_{\mathbf{q}}^R) \cdot G^{>} \cdot (1 - \Sigma_{\mathbf{q}}^A \cdot G_{\mathbf{q}}^A) - G_{\mathbf{q}}^R \cdot \Sigma_{\mathbf{q}}^{>} \cdot G_{\mathbf{q}}^A \end{aligned} \quad (4.14)$$

Now both terms of the correlation function has to be kept. The first term is the dominant giving  $G_{\mathbf{q}}^{<}[G^{<}]$ . The approximation  $G_{\mathbf{q}}^{<} \approx G^{<}$  simplifies the Multiple scattering theory to the Galitskii-Feynman approximation. It can be used in the normal state, but not in the superconducting state.

The second term is a correction which subtracts particles emitted by the channel  $\mathbf{q}$ . This subtraction is necessary when the correlation function  $G_{\mathbf{q}}^{<}$  is used to describe particles entering the channel  $\mathbf{q}$ . Briefly, particles leaving the scattering process  $\mathbf{q}$  cannot be used as initial states of the same process.

### 4.4.1 Selfenergy

The  $\mathbf{q}$  channel of the selfenergy relates to the reducible selfenergy (4.4) as  $\Sigma_{\mathbf{q}} = S_{\mathbf{q}} - S_{\mathbf{q}} \times G_{\mathbf{q}} \times \Sigma_{\mathbf{q}}$ . Again we need the analytic continuation of the fraction which

reads

$$\begin{aligned}
\Sigma_{\mathbf{q}}^R &= S_{\mathbf{q}}^R - S_{\mathbf{q}}^R \cdot G_{\mathbf{q}}^R \cdot \Sigma_{\mathbf{q}}^R \\
\Sigma_{\mathbf{q}}^A &= S_{\mathbf{q}}^A - S_{\mathbf{q}}^A \cdot G_{\mathbf{q}}^A \cdot \Sigma_{\mathbf{q}}^A \\
\Sigma_{\mathbf{q}}^< &= \frac{1}{(1 + S_{\mathbf{q}}^R \cdot G_{\mathbf{q}}^R)} \cdot S_{\mathbf{q}}^< \cdot \frac{1}{(1 + G_{\mathbf{q}}^A \cdot S_{\mathbf{q}}^A)} - \Sigma_{\mathbf{q}}^R \cdot G_{\mathbf{q}}^< \cdot \Sigma_{\mathbf{q}}^A \\
\Sigma_{\mathbf{q}}^> &= \frac{1}{(1 + S_{\mathbf{q}}^R \cdot G_{\mathbf{q}}^R)} \cdot S_{\mathbf{q}}^> \cdot \frac{1}{(1 + G_{\mathbf{q}}^A \cdot S_{\mathbf{q}}^A)} - \Sigma_{\mathbf{q}}^R \cdot G_{\mathbf{q}}^> \cdot \Sigma_{\mathbf{q}}^A
\end{aligned} \tag{4.15}$$

Analytic continuation of decomposition of the selfenergy into channels is straightforward because expression (4.2) does not contain any time integral

$$\begin{aligned}
\Sigma^< &= \sum_{\mathbf{q}} \Sigma_{\mathbf{q}}^< \\
\Sigma^> &= \sum_{\mathbf{q}} \Sigma_{\mathbf{q}}^> \\
\Sigma^R &= \sum_{\mathbf{q}} \Sigma_{\mathbf{q}}^R \\
\Sigma^A &= \sum_{\mathbf{q}} \Sigma_{\mathbf{q}}^A
\end{aligned} \tag{4.16}$$

## 4.5 Two-particle propagator

Two-particle propagator is a bosonic function. Bosonic function has the definition of correlation function with opposite sign due to the bosonic statistic

$$\mathcal{G}_{\mathbf{q}\uparrow}^<(t_1, t_2) = i\mathcal{G}_{\mathbf{q}\uparrow}(t_1, t_2)|_{t_1 < ct_2}, \tag{4.17}$$

and

$$\mathcal{G}_{\mathbf{q}\uparrow}^>(t_1, t_2) = i\mathcal{G}_{\mathbf{q}\uparrow}(t_1, t_2)|_{t_1 < ct_2}. \tag{4.18}$$

Let us apply the definition

$$\begin{aligned}
\mathcal{G}_{\mathbf{q}\uparrow}^<(t_1, t_2) &= i\mathcal{G}_{\mathbf{q}\uparrow}(t_1, t_2)|_{t_1 < ct_2} \\
&= (-iG_{\mathbf{q}\uparrow}(t_1, t_2)|_{t_1 < ct_2})(-iG_{\downarrow}(t_1, t_2)|_{t_1 < ct_2}).
\end{aligned} \tag{4.19}$$

In the first line we used the equation (4.5) and in second line we prepared the expression for definition of the fermionic correlation function (1.22)

$$\mathcal{G}_{\mathbf{q}}^<(t_1, t_2) = G_{\mathbf{q}}^<(t_1, t_2)G^<(t_1, t_2). \tag{4.20}$$

Similarly, we can derive hole function

$$\mathcal{G}_{\mathbf{q}}^>(t_1, t_2) = G_{\mathbf{q}}^>(t_1, t_2)G^>(t_1, t_2). \tag{4.21}$$

Bosonic retarded and advanced functions are defined as

$$\begin{aligned}
\mathcal{G}_{\mathbf{q}}^R(t_1, t_2) &= -i\theta(t_1 - t_2)(\mathcal{G}_{\mathbf{q}}^>(t_1, t_2) - \mathcal{G}_{\mathbf{q}}^<(t_1, t_2)), \\
\mathcal{G}_{\mathbf{q}}^A(t_1, t_2) &= +i\theta(t_2 - t_1)(\mathcal{G}_{\mathbf{q}}^>(t_1, t_2) - \mathcal{G}_{\mathbf{q}}^<(t_1, t_2)),
\end{aligned} \tag{4.22}$$

with the minus sign between correlation function. With the help of the identity

$$\begin{aligned}
C^R(t_1, t_2) &= -i\theta(t_1 - t_2) (A^>B^> - A^<B^<) \\
&= -i\theta(t_1 - t_2) ((A^> + A^<)B^> - A^<(B^> + B^<)) \\
&= A^R(t_1, t_2)B^>(t_1, t_2) - A^<(t_1, t_2)B^R(t_1, t_2),
\end{aligned} \tag{4.23}$$

we can write (4.20) and (4.21) in short notation

$$\begin{aligned}
\mathcal{G}_{\mathbf{q}}^R &= G_{\mathbf{q}}^R G^> - G_{\mathbf{q}}^< G^R \\
\mathcal{G}_{\mathbf{q}}^A &= G_{\mathbf{q}}^A G^> - G_{\mathbf{q}}^< G^A
\end{aligned} \tag{4.24}$$

There is no time integration in the two-particle propagator.

### 4.5.1 T-matrix

With the bosonic two-particle propagator derived in previous section one can build the  $T$ -matrix. The  $T$ -matrix has two time structure and satisfies the ladder equation  $T_{\mathbf{q}} = V_{\mathbf{q}} + \frac{1}{\Omega} \sum_{\mathbf{k}'} V_{\mathbf{q}} \times \mathcal{G}_{\mathbf{q}} \times T_{\mathbf{q}}$ .

The Langreth-Wilkins rules for bosonic functions are formally identical to those we have derived for fermionic functions. The analytic continuation of the ladder equation thus is

$$\begin{aligned}
T_{\mathbf{q}}^R &= V_{\mathbf{q}}^R + V_{\mathbf{q}}^R \cdot \mathcal{G}^R \cdot T_{\mathbf{q}}^R \\
T_{\mathbf{q}}^A &= V_{\mathbf{q}}^A + V_{\mathbf{q}}^A \cdot \mathcal{G}^A \cdot T_{\mathbf{q}}^A \\
T_{\mathbf{q}}^< &= T_{\mathbf{q}}^R \cdot \mathcal{G}^< \cdot T_{\mathbf{q}}^A \\
T_{\mathbf{q}}^> &= T_{\mathbf{q}}^R \cdot \mathcal{G}^> \cdot T_{\mathbf{q}}^A
\end{aligned} \tag{4.25}$$

Note that there is no term of type  $(1 + \mathcal{G}^R T_{\mathbf{q}}^R) \cdot (V_{\mathbf{q}} \delta(t_1 - t_2))^< \cdot (1 + T_{\mathbf{q}}^A \mathcal{G}^A)$ , because correlation function of nonretarded potential  $(V_{\mathbf{q}} \delta(t_1 - t_2))^<$  is zero automatically due to delta function in time.

### 4.5.2 Averaged T-matrix

Finally we construct the reducible selfenergy as an averaged  $T$ -matrix. In this relation there is no genuine time integral, therefore we can immediately write in short notation

$$\begin{aligned}
S_{\mathbf{q}}^< &= \frac{1}{\Omega} T_{\mathbf{q}}^< G^> \\
S_{\mathbf{q}}^> &= \frac{1}{\Omega} T_{\mathbf{q}}^> G^<
\end{aligned} \tag{4.26}$$

The  $T$ -matrix has identical order of time arguments as the reducible selfenergy, while the Green function has the opposite one. It is reflected by the structure of sign  $>$  or  $<$ .

The retarded function is constructed by definition

$$\begin{aligned}
S_{\mathbf{q}}^R(t_1, t_2) &= -i\theta(t_1 - t_2) (S_{\mathbf{q}}^>(t_1, t_2) + S_{\mathbf{q}}^<(t_1, t_2)) \\
&= -i\theta(t_1 - t_2) \frac{1}{\Omega} (T_{\mathbf{q}}^>(t_1, t_2) G^<(t_2, t_1) + T_{\mathbf{q}}^<(t_1, t_2) G^>(t_2, t_1)).
\end{aligned} \tag{4.27}$$

Adding and subtracting the term  $T_{\mathbf{q}}^>(t_1, t_2)G^>(t_2, t_1)$  we obtain

$$S_{\mathbf{q}}^R(t_1, t_2) = -i\theta(t_1 - t_2)\frac{1}{\Omega}(T_{\mathbf{q}}^>(t_1, t_2)G^<(t_2, t_1) + T_{\mathbf{q}}^>(t_1, t_2)G^>(t_2, t_1) - T_{\mathbf{q}}^>(t_1, t_2)G^>(t_2, t_1) + T_{\mathbf{q}}^<(t_1, t_2)G^>(t_2, t_1)). \quad (4.28)$$

Finally, using the definitions  $i\theta(t_1 - t_2)(G^>(t_2, t_1) + G^<(t_2, t_1)) = G^A(t_2, t_1)$  for fermionic function and  $-i\theta(t_1 - t_2)(T_{\mathbf{q}}^>(t_2, t_1) - T_{\mathbf{q}}^<(t_2, t_1)) = T_{\mathbf{q}}^A(t_2, t_1)$  for bosonic function we end up with

$$S_{\mathbf{q}}^R(t_1, t_2) = \frac{1}{\Omega}(T_{\mathbf{q}}^R(t_1, t_2)G^<(t_2, t_1) - T_{\mathbf{q}}^<(t_1, t_2)G^A(t_2, t_1)). \quad (4.29)$$

In short notation

$$\begin{aligned} S_{\mathbf{q}}^R &= \frac{1}{\Omega}(T_{\mathbf{q}}^R G^< - T_{\mathbf{q}}^< G^A) \\ S_{\mathbf{q}}^A &= \frac{1}{\Omega}(T_{\mathbf{q}}^A G^< - T_{\mathbf{q}}^< G^R) \end{aligned} \quad (4.30)$$

The relation for the advanced function can be obtained in analogous way.



# 5. Spectroscopy of ultrasmall metallic grains

## 5.1 Introduction

One of the possible systems, where the present unified theory of superconductivity could be verified are ultrasmall metallic grains. It is measured by tunneling spectroscopy, which drives the system out of the equilibrium. To describe this experiment under general conditions, we derive the appropriate nonequilibrium version of the unified theory presented in chapter 4.

Our aim is to identify how the unified theory differs from the BCS theory. The BCS theory works with an effective Hamiltonian which does not conserve the number of particles in the system. Whereas the unified theory is build from the particle conserving Hamiltonian. The differences might be substantial in nano-particles and we want to discuss under what conditions they should be visible.

By decreasing the size of the grain from bulk limit to ultrasmall grain limit the system became influenced by strong fluctuations. The ultrasmall metallic grain represents a system with strong size effects as even-odd effect. In general, ultrasmall metallic grains require a theory based on canonical system, but such approach is extremely complicated. Most of the studies are thus done with the help of the BCS theory in spite of its grandcanonical origin. For very small model systems there are studies with the BCS wave function projected to the fixed number of particles. Such theory is desirable for grains where fluctuations in the number of particles are strongly suppressed by high electrostatic charging energies, the so-called Coulomb blockade.

The unified theory is based on the grandcanonical system. It seems to be impossible to measure predictions of such theory because of Coulomb blockade, which is the standard part of spectroscopic measurements. In order to observe the differences between the BCS theory and the unified theory, the Coulomb blockade should be suppressed.

We will explain the Coulomb blockade and a possible way to minimalize it. This will allow us to neglect a charging energy contribution in a Hamiltonian and to simplify our model. The model will thus cover only interactions which do not relate to electrostatics.

## 5.2 History of spectroscopy of discrete energy levels

A quantum mechanical picture of particles confined in a small region is well known. Such a system shows discrete or quantized energy with increasing spacing between energy levels by decreasing volume of the system.

Spectroscopic measurement were earlier developed in areas as nuclear or atomic physics, where the discrete structure is natural. This measurement brought a lot of informations about the correlations between particles in atoms and nuclei.

Spectroscopy of single electron levels in metals or semiconductors was unable due to volume size, until the mesoscopic or nanoscopic samples were manufactured. The problem was hidden in resolution of a discrete structure, because energetic scales in systems were small against thermal energies.

The first devices, quantum dots, were fabricated in the early 1990s. Semiconductor dots are small regions (radius of order tens of nm) where the electrons are trapped in three dimensions by potential walls. In that small region one can resolve the spectrum at dilution refrigerator in the 10-100 mK range.

The measurement method was called single-electron-tunneling spectroscopy. The experiment resembles a transistor. The central island – the dot in this case – is connected to the leads. Means for connections are electrostatically defined tunnel barriers. The whole set is called single-electron-transistor, shortly SET. This devices started a new regime of probing of the condensed matter.

It is beneficial to study SET systems. Under certain conditions one can observe in a current-voltage characteristic a step structure. Therefore the conductance shows well-defined resonances. The resonances can be associated with a tunneling through discrete channels of the dot. It turns out that quantum dots exhibited similar behavior as atoms. For example we can apply the Hund's rule as in atoms or there are some stable configurations with magic numbers.

The idea of SET measurement was also brought to the area of metals. The first measurement was done by Ralph, Black and Tinkham (RBT) in the middle of 1990s. The central island in the single-electron-transistor was made from an ultrasmall metallic grain. The radius was about  $r=5$  nm and mean level distance  $d=90$  meV. The grain was jointed to the leads via oxide tunnel barriers.

The nanoscale opened up a new limit in the study of electron correlations because it allows us to resolve the single electron spectrum in the ultrasmall grain, moreover with high precision. During the last several years, single-electron-tunneling spectroscopy of ultrasmall metallic grains was used to probe superconducting pairing correlations, nonequilibrium excitations, spin-orbit interactions in normal grains, and also ferromagnetic correlations.

There are many differences between quantum dots and ultrasmall metallic grains. Metals have much higher densities of states and samples thus need to be much smaller. In result, the metallic dots have larger charging energies and thereby fluctuations of an average number of particles are suppressed. Moreover, the variability of metallic materials allow us to study such effects as superconductivity and ferromagnetism. In metallic grains the tunnel barriers are less affected by applied bias, therefore nonequilibrium effects can be more easily studied. By applying a magnetic field one can also probe the spin and spin-orbit effects [14].

### 5.3 SET experiment

We will describe the SET experiment with the help of figure 5.1 taken over from [14] with modified notation of voltages to match our presentation. A metallic grain placed as a central island is connected via high resistance tunnel junctions, with the capacitances  $C_R$  and  $C_L$ . The grain is also coupled capacitively to a gate, with the capacitance  $C_g$ . When we apply a bias voltage between the leads a tunnel current  $I$  flows between the leads through the grain. The current is

caused by incoherent sequential tunneling through the tunnel junctions and can be varied by the gate voltage  $V_g$ .

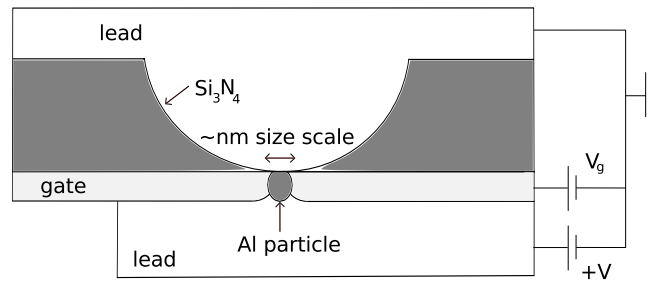


Figure 5.1: Schematic cross section of the ultrasmall SETs studied by RBT

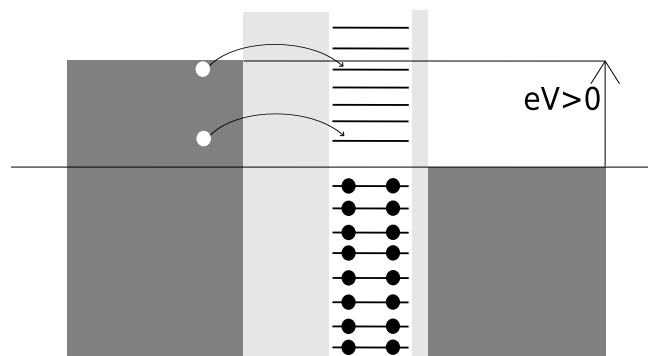


Figure 5.2: Measurement of excitation grain spectra, process which serves as bottleneck is represented by arrows. This process corresponds to one of shadow regions in figure 5.5. A chemical potential in equilibrium is depicted as a long horizontal line.

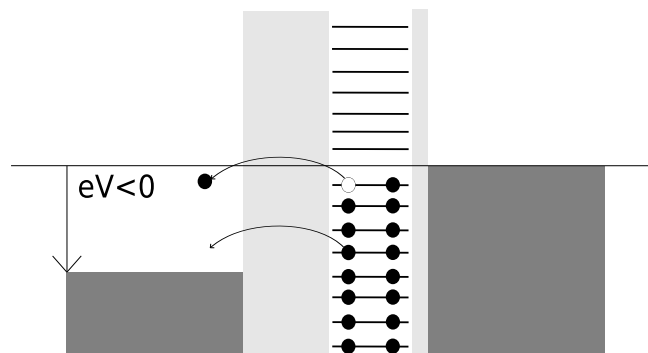


Figure 5.3: Measurement of spectrum of filled states on the grain, process which serves as bottleneck is represented by arrows. This process corresponds to one of the shadow regions in figure 5.5. A chemical potential in equilibrium is depicted as a long horizontal line.

The leads are connected by highly non-symmetric barriers with the thicker one serving as bottleneck. The state of grain can be assumed as nearly equilibrium with temperature and chemical potential of the lead connected by the thinner barrier. The physical processes which determine the current are depicted in

figures 5.2 and 5.3. As one can see, flipping the sign of the bias voltage, one measures either the empty electronic states in the grain shown in figure 5.2 or the occupied states shown in figure 5.3.

## 5.4 Coulomb blockade

The important feature of the nanoscopic grains size is that the grain charging energy  $E_C = \frac{e^2}{2C}$  (where  $C = C_L + C_R + C_g$ ) is much larger than for the mesoscopic size of semiconductor dots. The scale of  $E_C$  determines the energy cost of charging the  $N$ -electrons grain by one electron. For ultrasmall grains such energy exceeds other energies related to the tunneling. Fluctuations in the number of electrons are suppressed.

There are typically two scales in the SET experiments characterized by the scale of energy. The first scale is when  $V$  is varied on a large scale about tens of mV. The  $I - V$  curve has a typical shape. In a low voltage  $|V|$  there is a zero current (Coulomb blockade regime) or a flat step. Once some threshold is reached, the current will increase with a finite slope.

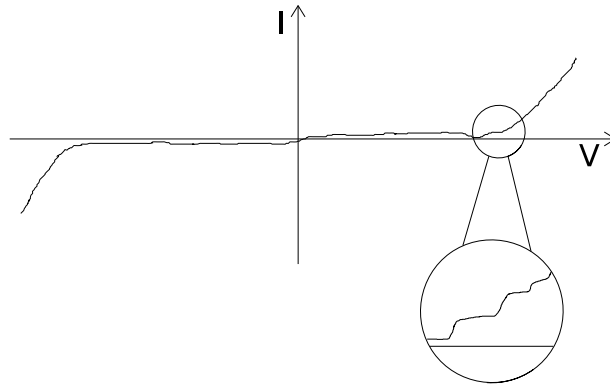


Figure 5.4: Two scales of SET experiment. The flat step corresponds to the Coulomb blockade regime, on which end there is a step like structure on smaller scales.

The value of the Coulomb blockade regime depends on the gate voltage. The maximal value of the flat step is  $E_C$ , the minimal is zero. The minima occur in so-called degeneracy points, where energies of the states with average number of particles differing by one become equal. As  $V_g$  is increased, the wide flat steps and also degeneracy points periodically repeat with a period  $e/C_g$  see figure 5.5. The Coulomb blockade thus serves as a tool for varying the average number of particles.

Our aim is the opposite situation and we want to study systems in an equilibrium. This is reached by tuning the gate voltage to a vicinity of the degeneracy points which are depicted as shadow regions in figure 5.5. If one wants to study the nonequilibrium effects, one tunes the  $V_g$  to the maximal flat step.

The second smaller scales are located near the threshold of the Coulomb blockade regime (the edge of flat step). The variation of the voltage is typically in the order of  $mV$ . In this area the  $I - V$  curve has a step like substructure. Such small steps in the  $I - V$  curve are expected to appear whenever the voltage

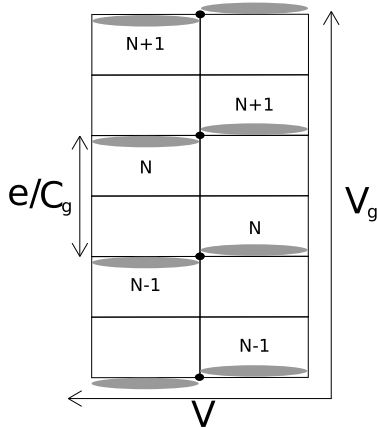


Figure 5.5: Regions of SET measurements in  $V - V_g$  plane where an almost isolated dot is measured (shadow regions), the degeneracy points (black circles) repeat with a period  $e/C_g$ . Numbers have the meaning of the average number of electrons on the dot.

drop across one of the tunnel junctions equals to the threshold energy. The rate for tunneling across that junction into or out of one of the grain's discrete energy eigenstates becomes nonzero. This opens up another channel for the current across that junction and the current thus increases.

The differential conductance ( $dI/dV$ ) will contain a series of fine resonances. Discrete eigenstates of the conduction electron energy spectrum became resolvable due to the mean distance between eigenlevels  $d$ . The scale  $d$  is usually at least one order lower than the scale  $E_C$ . We assume also  $T \ll d$  because of the suppression of thermal fluctuations. Under conditions, shadow regions in figure 5.5, the distance between these peaks directly reflects the energy differences between the eigenenergies of the  $N$ -electron grain. Such conductance curves thus directly yield the grain fixed- $N$  excitation spectrum.

In spite of its importance we are not interested in the Coulomb blockade in our model. Although we are led to this neglect by a request of simplicity, the model with the neglected Coulomb blockade is not necessarily non-realistic.

To suppress the Coulomb blockade in experiments one can increase the value of  $C_g$  by using a suitable ferroelectric dielectrics between the dot and the gate. For example materials like  $\text{SrRuO}_3/\text{SrTiO}_3$  have a relative permittivity 3700 [15] which allows us to reduce the Coulomb blockade  $e/C_g$  nearly thousand times. The necessary consequence will be an uncertainty in the average of the number of particles. Because we will use the Green function technique which is related to the grand canonical system this property is desirable.

The gate is also used for tuning an electrostatic potential on the grain and its average number of electrons  $N$ . The gate voltage enters our formulation exclusively via values the single electronic levels. Accordingly, we will not discuss the gate any more.

# 6. Superconductivity in metallic grains

## 6.1 Hamiltonian

In this chapter we present the unified theory, developed in chapters 3 and 4, for the description of ultrasmall metallic grains introduced in chapter 5. We need to modify the identification of the channel by the total momentum of the pair  $\mathbf{q}$  because in nanoscale the momentum of particle is not a good quantum number.

The main feature of the nanoscale is the discrete energy spectrum. A spacing between levels increases when the volume of the system is decreasing. The discrete energy spectrum is natural in atoms and in nuclei. The ultrasmall metallic grains also show these features.

Moreover, there are systems, where the symmetry of the system leads to a degeneracy of energy levels. Good quantum numbers for electronic states in ultrasmall spheres are similar to the numbers of naturally spheric atoms. We will use the orbital number, the angular momentum number (called the magnetic number) and the spin number for denotation of the electronics state.

The analogy between the momentum in bulk system and the angular momentum in ultrasmall grains will be our starting point. Instead of the total momentum of a pair of electron  $\mathbf{q}$ , here the identification of the channel is via the total angular momentum of the pair  $\mathbf{M}$ .

Since we want to describe the system within the SET experiment we need to develop a general theory of the whole system. The Hamiltonian has five parts. An isolated grain is described by  $\hat{H}_g$ , and isolated left and right leads by  $\hat{H}_l$  and  $\hat{H}_r$ , respectively. The leads are connected to the grain by tunneling Hamiltonians  $\hat{U}_l$  and  $\hat{U}_r$ . In this chapter we will call the ultrasmall metallic grain shortly a grain.

### 6.1.1 Non-interacting electrons in the grain

We assume that the grain is an ideal sphere, therefore the orbital momentum  $L$  commutes with the grain Hamiltonian,  $\hat{L}\hat{H} - \hat{H}\hat{L} = 0$ . Each one-particle eigenstate-states thus has the orbital number of

$$l = 0, 1, 2, \dots \quad (6.1)$$

with orbital number  $L_l$  and the magnetic number

$$m = -L_l, -L_l + 1, \dots - 2, -1, 0, 1, 2, \dots L_l - 1, L_l. \quad (6.2)$$

The eigenstate-energy is independent of the magnetic number and (Pauli) spin

$$\epsilon_{l,m,\sigma} = \epsilon_l. \quad (6.3)$$

The energy  $\epsilon_l$  is related to the chemical potential  $\mu$ .

It is possible to split the levels by a magnetic field  $B$  so that  $\epsilon_{l,m,\sigma} = \epsilon_l + Bm\mu_l + B\sigma\mu_B$ , where  $\mu_B$  is the Bohr magneton and  $\mu_l$  is the magnetic moment

of the  $p$ -state ( $m = 1$ ). We will not assume the magnetic field, however. The Hamiltonian of non-interacting electrons in the grain thus reads

$$\hat{H}^0 = \sum_{l,m,\sigma} \epsilon_l a_{\sigma,l,m}^\dagger a_{\sigma,l,m}. \quad (6.4)$$

We will assume only few levels near the Fermi energy. This restriction will serve as a cutoff.

### 6.1.2 Pairing interaction

The pairing interaction is restricted to the grain. It was described on two levels: the BCS model and the Richardson (or also reduced) model. We will develop our theory for a model which includes more interaction elements than the model of Richardson but less than the BCS model. In numerical implementations, however, we will restrict our discussion to the Richardson model.

The BCS model includes interaction of any two electrons with opposite spin

$$\hat{V}^{\text{BCS}} = \sum_{l,m,k,n,l',m',k',n'} \tilde{\lambda} a_{\downarrow,k,n}^\dagger a_{\uparrow,l,m}^\dagger a_{\uparrow,l',m'} a_{\downarrow,k',n'}. \quad (6.5)$$

The tilde reminds that the sum has to respect conservation of sum angular momentum of the interacting pair, i.e.,  $m + n = m' + n'$ .

The model of Richardson restricts interaction exclusively between two electrons linked by the time-reversal symmetry

$$\hat{V}^{\text{Rich}} = \sum_{l,m,l',m'} \lambda a_{\downarrow,l,-m}^\dagger a_{\uparrow,l,m}^\dagger a_{\uparrow,l',m'} a_{\downarrow,l',-m'}. \quad (6.6)$$

Since the time reversed states form the condensate of the Cooper pairs, this model is sufficient to describe the condensation. In the same time it has no interaction among electrons out of the condensate.

Our model

$$\hat{V} = \hat{V}^{\text{Rich}} + \hat{V}^{\text{ext}} \quad (6.7)$$

extends the Richardson model assuming additional interactions between two electrons from the same shell

$$\hat{V}^{\text{ext}} = \sum_{l,m,l',m',M \neq 0} \lambda' a_{\uparrow,l,M-m}^\dagger a_{\downarrow,l,m}^\dagger a_{\downarrow,l',m'} a_{\uparrow,l',M-m'}. \quad (6.8)$$

Setting  $\lambda' = 0$  our model reduces to the Richardson model. In practical applications the sum over the pair magnetic number  $M$  can be catted at small values. The Richardson model cuts interaction at  $M = 0$ . The simplest form of our extended model cuts the interaction on the level  $M = \pm 1$ .

The Hamiltonian of non-interacting electrons in the grain together with the interaction constitutes the grain Hamiltonian

$$\hat{H}_g = \hat{H}^0 + \hat{V}. \quad (6.9)$$

Comparing the interaction Hamiltonian (6.5) with the Hamiltonian (3.1) from the section 3.4 we see that the interaction constant  $\lambda_M$  is related to the BCS interaction and the volume of sample,  $\lambda_M = \frac{\mathcal{V}_M}{\Omega_{Vol}}$ . We should stress also that in bulk system the energy is a function of the momentum  $\epsilon(\mathbf{k})$ . In ultrasmall grains, however, for the same angular momentum  $m$  the energy can have several values because the energy depends only on the orbital number  $l$ .

### 6.1.3 Leads

The left and right leads have Hamiltonians

$$\begin{aligned}\hat{H}_l &= \sum_{\alpha,\sigma} \epsilon_\alpha^l a_{\sigma,\alpha}^\dagger a_{\sigma,\alpha} \\ \hat{H}_r &= \sum_{\beta,\sigma} \epsilon_\beta^r a_{\sigma,\beta}^\dagger a_{\sigma,\beta}\end{aligned}\quad (6.10)$$

Values of  $\epsilon_\alpha^{l,r}$  include eventual bias voltage on the structure.

The connecting terms read

$$\hat{U}_l = \sum_{\alpha,l,m,\sigma} u_\alpha^l a_{\sigma,\alpha}^\dagger a_{\sigma,l,m} \quad (6.11)$$

$$\hat{\tilde{U}}_l = \sum_{\alpha,l,m,\sigma} \tilde{u}_\alpha^l a_{\sigma,l,m}^\dagger a_{\sigma\alpha}, \quad (6.12)$$

$$\hat{U}_r = \sum_{\beta,l,m,\sigma} u_\beta^r a_{\sigma,\beta}^\dagger a_{\sigma,l,m} \quad (6.13)$$

$$\hat{\tilde{U}}_r = \sum_{\beta,l,m,\sigma} \tilde{u}_\beta^r a_{\sigma,l,m}^\dagger a_{\sigma\beta}. \quad (6.14)$$

In implementations it is sufficient to assume only real elements  $u_\alpha^{l,r}$ . We keep the bare over the conjugated terms as an eyeguide which helps to trace the origin of hopping terms in the equation of motion.

## 6.2 Elimination of leads

In this section we will show how to eliminate leads and project to subspace of the grain. The current is a one-particle observable, therefore we need the one-particle Green function

$$G(1,2) = -i \langle \mathbf{T}_C a_1 a_2^\dagger \rangle, \quad (6.15)$$

where the numbers are cumulative indices which cover the time on the complex path and the necessary state indices. In the left lead  $1 \equiv (t_1, \alpha_1, \sigma_1)$ , in the right lead  $1 \equiv (t_1, \beta_1, \sigma_1)$  and in the grain  $1 \equiv (t_1, l_1, m_1, \sigma_1)$ .

Taking the time derivative of the one-particle Green's function (6.15) one finds

$$i\partial_{t_1} G = \hat{\mathbf{1}} - i \langle \mathbf{T}_C [a_1, \hat{H}] a_2^\dagger \rangle, \quad (6.16)$$

where the first term is a product of delta functions, which is non-zero only if both space indices are identical, e.g.  $\hat{\mathbf{1}} = \delta(t_1 - t_2) \delta_{l_1 l_2} \delta_{m_1 m_2} \delta_{\sigma_1 \sigma_2}$  for both indices from the grain. It results from the time-step due to the time ordering operator, and the second term results from the Heisenberg equation.

Let us assume that both arguments of the Green's function are from the grain. We denote this restriction by indices  $G = G_{\text{dd}}$  for  $1 \equiv (t_1, l_1, m_1, \sigma_1)$  and  $2 \equiv (t_2, l_2, m_2, \sigma_2)$ . Similarly,  $G = G_{\text{dr}}$  for  $1 \equiv (t_1, l_1, m_1, \sigma_1)$  and  $2 \equiv (t_2, \beta_2, \sigma_2)$  and so on.



The commutators with one-particle parts of the Hamiltonian are readily evaluated giving

$$(i\partial_t - \epsilon_{l_1}) G_{\text{dd}} = \hat{\mathbf{1}} + \bar{u}^l G_{\text{ld}} + \bar{u}^r G_{\text{rd}} - i \left\langle \mathbf{T}_C \left[ a_1, \hat{V} \right] a_2^\dagger \right\rangle. \quad (6.17)$$

Elements  $G_{\text{ld}}$  and  $G_{\text{rd}}$  connecting the grain with leads are easily evaluated from equation (6.16),

$$(i\partial_t - \epsilon_{\alpha_1}^l) G_{\text{ld}} = u^l G_{\text{dd}}. \quad (6.18)$$

We define the Green's function of the (disconnected) left lead

$$(i\partial_t - \epsilon_{\alpha_1}^l) G_{\text{ll}}^0 = \hat{\mathbf{1}} \quad (6.19)$$

which formally solves equations (6.18) as

$$G_{\text{ld}}(t_1, t_2) = \int G_{\text{ll}}^0(t_1, \bar{t}) u^l G_{\text{dd}}(\bar{t}, t_2) d\bar{t}. \quad (6.20)$$

In the next we do not write the time integrals explicitly so that equation (6.20) reads

$$G_{\text{ld}} = G_{\text{ll}}^0 u^l G_{\text{dd}}. \quad (6.21)$$

Similarly we arrive at

$$G_{\text{rd}} = G_{\text{rr}}^0 u^r G_{\text{dd}}. \quad (6.22)$$

Substituting equations (6.21, 6.22) into equation (6.17), we obtain

$$(i\partial_t - \epsilon_{l_1} - \bar{u}^l G_{\text{ll}}^0 u^l - \bar{u}^r G_{\text{rr}}^0 u^r) G_{\text{dd}} = \hat{\mathbf{1}} - i \left\langle \mathbf{T}_C \left[ a_1, \hat{V} \right] a_2^\dagger \right\rangle. \quad (6.23)$$

Finally we introduce the Green's function of non-interacting electrons on a connected grain

$$(i\partial_t - \epsilon_{l_1} - \bar{u}^l G_{\text{ll}}^0 u^l - \bar{u}^r G_{\text{rr}}^0 u^r) G_{\text{dd}}^{\text{free}} = \hat{\mathbf{1}} \quad (6.24)$$

in terms of which equation (6.23) reads

$$G_{\text{dd}} = G_{\text{dd}}^{\text{free}} - i G_{\text{dd}}^{\text{free}} \left\langle \mathbf{T}_C \left[ a_1, \hat{V} \right] a_2^\dagger \right\rangle. \quad (6.25)$$

From now on all algebra will be on the subspace of the grain. For simplicity we will not write subscripts dd. To have the standard notation for the expansion in the interaction, the free function will be renamed as

$$G^0 \equiv G_{\text{dd}}^{\text{free}}. \quad (6.26)$$

In applications we will assume that  $G^0$  is diagonal in the orbital and magnetic number and in the spin. For simplicity we will approximate the lead functions by time-dependent functions

$$(\bar{u}^l G_{\text{ll}}^0 u^l)(1, 2) \approx \hat{\mathbf{1}} h_l(t_1, t_2), \quad (6.27)$$

$$(\bar{u}^r G_{\text{rr}}^0 u^r)(1, 2) \approx \hat{\mathbf{1}} h_r(t_1, t_2). \quad (6.28)$$

It is not true in general. The leads cannot have a full spheric symmetry so that the lead functions  $\bar{u}^l G_{\text{ll}}^0 u^l$  and  $\bar{u}^r G_{\text{rr}}^0 u^r$  have in general off-diagonal elements. This corresponds to processes in which an electron of given orbital and magnetic number tunnels out and coherently returns with a different momentum.

## 6.3 Perturbative expansion

The interaction term in equation (6.23) we express in terms of the selfenergy

$$-i \left\langle \mathbf{T}_C [a_1, V] a_2^\dagger \right\rangle = \Sigma(1, \bar{3})G(\bar{3}, 2). \quad (6.29)$$

The electron Green's function thus satisfies the Dyson equation

$$G = G^0 + G^0 \times \Sigma \times G. \quad (6.30)$$

The Green function and all functions entering it are diagonal in the spin index. We will use convention that  $G_\uparrow \equiv G$  and  $G_\downarrow \equiv \tilde{G}$ . Similarly,  $\Sigma_\uparrow \equiv \Sigma$  and  $\Sigma_\downarrow \equiv \tilde{\Sigma}$ .

For the present model and approximations the Green's function is diagonal in orbital and magnetic number

$$G_{l,l'}(t_1, t_2; m, m') = G_l(t_1, t_2; m)\delta_{mm'}\delta_{ll'}. \quad (6.31)$$

The same is true for the selfenergy. The Dyson equation thus simplifies as

$$G_l = G_l^0 + G_l^0 \times \Sigma_l \times G_l. \quad (6.32)$$

## 6.4 Selfenergy

The selfenergy is a sum over the total magnetic numbers of interacting pair

$$\Sigma = \sum_M \Sigma_M. \quad (6.33)$$

For the Richardson model it has only a single element,  $\Sigma = \Sigma_{M=0}$ , but for our model there are additional contributions.

### 6.4.1 Multiple scattering theory

Let us evaluate the part of selfenergy  $\Sigma_M$ . When we evaluate process giving  $\Sigma_M$  (briefly process  $\Sigma_M$ ), this contribution is explicit and cannot be included in the averaged effective medium, because the process cannot selfconsistently affect itself. As an effective medium for the process  $\Sigma_M$  we thus introduce the reduced Green function, which does not include the selected part of the selfenergy

$$G_M = G^0 + G^0 \times \left( \sum_{N \neq M} \Sigma_N \right) \times G_M. \quad (6.34)$$

This can be also expressed as

$$G_M = G - G \times \Sigma_M \times G_M. \quad (6.35)$$

Interaction inside the grain will be approximated with the  $T$ -matrix in the ladder approximation. This is given by the following set of equations. The  $T$ -matrix  $T_M$  describes an interaction of a pair of electrons with the orbital momentum  $M$ .

$$T_M(t_1, t_2) = \lambda_M \delta(t_1 - t_2) + \lambda_M \mathcal{G}_M(t_1, \bar{t}_3) T_M(\bar{t}_3, t_2), \quad (6.36)$$

where the bar denotes integration. In this case the integration runs along the complex time path.

Since we evaluate the  $\Sigma_M$  process, we construct the  $T$ -matrix from the reduced Green function

$$\mathcal{G}_M(t, t') = i \sum_{lm} \tilde{G}_l(t_1, t_2; M - m) G_{M,l}(t_1, t_2; m). \quad (6.37)$$

The  $T$ -matrix represents interaction of the selected pair to the infinite order. The full Green function thus reads

$$G_l = G_{M,l} + G_{M,l} \times S_{M,l} \times G_{M,l}, \quad (6.38)$$

where

$$S_{M,l}(t_1, t_2; m) = -iT_M(t_1, t_2) \tilde{G}_l(t_2, t_1; M - m) \quad (6.39)$$

is the  $T$ -matrix averaged over the distribution of interaction partner.

Comparing equations (6.35, 6.38) we find  $\Sigma_M$

$$\Sigma_{M,l} = \frac{S_{M,l}}{1 + G_{M,l} \times S_{M,l}}. \quad (6.40)$$

Equations are closed. Assume some starting set of the selfenergy parts  $\Sigma_M$  and  $\tilde{\Sigma}_M$ . From equation (6.33) we get  $\Sigma$  and  $\tilde{\Sigma}$ . From the Dyson equation (6.32) we obtain Green's functions  $G$  and  $\tilde{G}$ . Now we select  $M$ . From equation (6.35) we evaluate  $G_M$ . From equation (6.37) we obtain  $\mathcal{G}_M$  and from equation (6.36) the  $T$ -matrix  $T_M$ . Using equation (6.39) we construct  $S_M$  from which we obtain via (6.40) the new value of the selfenergy part  $\Sigma_M$ . Values of  $\Sigma_M$  should be upgraded for both spins and all orbital and magnetic numbers.

## 6.4.2 Galitskii-Feynman theory

It could be interesting to compare the multiple scattering  $T$ -matrix with the corresponding  $T$ -matrix approximation derived within Feynman expansion by Galitskii. One can convert the above theory into Galitskii theory neglecting a difference between the full and reduced propagator,

$$G_M \approx G \quad (6.41)$$

and neglecting a difference between the averaged  $T$ -matrix and the selfenergy

$$\Sigma_{M,l} \approx S_{M,l}. \quad (6.42)$$

For an infinite system the Galitskii theory is known to fail to describe the superconducting gap in the energy spectrum. It would be interesting to see how this theory behaves for the metallic nano-sphere.

## 6.4.3 Kadanoff-Martin theory

The theory used to study the superconductivity has been derived by Kadanoff and Martin using the variational method. Its resulting formulas can be obtained from the above set approximating the reduced Green's function by the bare one

$$G_M \approx G^0. \quad (6.43)$$

With this strong neglect one can ignore minor corrections and to replace the multiple scattering definition of the selfenergy using simply

$$\Sigma_{M,l} = S_{M,l}. \quad (6.44)$$

As it was shown by Morawetz [12], the dominant pairing channel is not affected by this approximation.

## 6.5 Various approximations

Solving the multiple scattering theory by numerical tools is a hard problem. Clearly, one has to approach the solution by iterations. It is important to start the iteration from a good starting point. To this end we write down a series of three increasingly more complex approximations. The simpler one provides a starting point for the more complex.

### 6.5.1 BCS approximation

The simplest approximation is the BCS theory. Let us approximate the  $T$ -matrix by a constant in the pairing orbital momentum,

$$\begin{aligned} T_0 &= i\bar{\Delta}\Delta, \\ T_M &= 0 \quad \text{for} \quad M \neq 0. \end{aligned} \quad (6.45)$$

In this approximation the averaged  $T$ -matrix equation (6.39) reads

$$S_{0,l}(t_1, t_2; m) = \bar{\Delta}\tilde{G}_l(t_2, t_1; -m)\Delta. \quad (6.46)$$

Since  $T_{\pm 1} = 0$  we find  $S_{\pm 1} = 0$  and also  $\Sigma_{\pm 1} = 0$ . Therefore from equation (6.34) follows

$$G_0 = G^0 + G^0 \times \left( \sum_{N \neq 0} \Sigma_N \right) \times G_0 = G^0. \quad (6.47)$$

Briefly, in this approximation the reduced Green function equals to the free Green function.

Now we substitute relations (6.46) and (6.47) into the full Green function (6.38)

$$\begin{aligned} G_l &= G_{0,l} + G_{0,l} \times S_{0,l} \times G_{0,l} \\ &= G_l^0 + G_l^0 \times S_{0,l} \times G_l^0 \\ &= G_l^0 + G_l^0 \times \bar{\Delta} \times \tilde{G}_l \times \Delta \times G_l^0. \end{aligned} \quad (6.48)$$

The Green function for the reversed spin satisfies an analogous equation

$$\tilde{G}_l = \tilde{G}_l^0 + \tilde{G}_l^0 \times \Delta \times G_l \times \bar{\Delta} \times \tilde{G}_l^0. \quad (6.49)$$

By substitution of equation (6.49) into (6.48) one finds

$$G_l = G_l^0 + G_l^0 \times \bar{\Delta} \times \left( \tilde{G}_l^0 + \tilde{G}_l^0 \times \Delta \times G_l \times \bar{\Delta} \times \tilde{G}_l^0 \right) \times \Delta \times G_l^0 \quad (6.50)$$

$$= G_l^0 + G_l^0 \times \bar{\Delta} \times \tilde{G}_l^0 \times \Delta \times \left( G_l^0 + G_l \times \bar{\Delta} \times \tilde{G}_l^0 \times \Delta \times G_l^0 \right). \quad (6.51)$$

Expressing the Dyson equation (6.32) in equivalent form

$$G_l = G_l^0 + G_l \times \Sigma_l \times G_l^0 \quad (6.52)$$

and substituting  $G_l$  from (6.52) into equation (6.32) we obtain the same structure

$$G_l = G_l^0 + G_l^0 \times \Sigma_l \times (G_l^0 + G_l \times \Sigma_l \times G_l^0). \quad (6.53)$$

Comparing (6.53) with (6.51) one finds that

$$\Sigma_l = \bar{\Delta} \times \tilde{G}_l^0 \times \Delta. \quad (6.54)$$

Since  $\Sigma_l = \Sigma_{0,l}$ , one can check that the selfenergy (6.54) also satisfies relation to the averaged  $T$ -matrix (6.40)

$$\begin{aligned} \Sigma_{0,l} + \Sigma_{0,l} \times G_l \times \Sigma_{0,l} &= \bar{\Delta} \times \tilde{G}_{0,l} \times \Delta + \bar{\Delta} \times \tilde{G}_{0,l} \times \Delta \times G_l \times \bar{\Delta} \times \tilde{G}_{0,l} \Delta \\ &= \bar{\Delta} \left( \tilde{G}_{0,l} + \tilde{G}_{0,l} \times \Delta \times G_l \times \bar{\Delta} \times \tilde{G}_{0,l} \right) \times \Delta \\ &= \bar{\Delta} \times \tilde{G}_l \times \Delta \\ &= S_{0,l}. \end{aligned} \quad (6.55)$$

In the rearrangement we have used equations (6.49) and (6.46).

The Dyson equation (6.32) with the selfenergy (6.54)

$$G_l = G_l^0 + G_l^0 \times \bar{\Delta} \times \tilde{G}_l^0 \times \Delta \times G_l. \quad (6.56)$$

is identical to the Nambu-Gorkov equation. The approximation of the  $T$ -matrix (6.45) is thus identical to the BCS approximation.

To establish the value of  $\Delta$ , we use equation (6.36) for  $T_0 = i\bar{\Delta}\Delta$  at  $t_1 \neq t_2$ ,

$$i\bar{\Delta}\Delta = \lambda \mathcal{G}^0(t, \bar{t}) i\bar{\Delta}\Delta. \quad (6.57)$$

Using equation (6.47) in (6.37) one finds that

$$\mathcal{G}_0(t_1, t_2) = i \sum_{lm} \tilde{G}_l(t_1, t_2) G_l^0(t_1, t_2), \quad (6.58)$$

therefore the gap equation (6.57) includes a convolution of the full and bare Green function, as it is found in the Nambu-Gorkov theory.

Note that the selfenergy is independent of the magnetic number  $m$  and therefore the Green's function is independent of  $m$ . This is a consequence of the fact that the BCS approximation neglects any effect of the interaction potential  $V^{\text{ext}}$ , because it does not contribute to the pairing. Briefly, the BCS approximation does not distinguish the Richardson model from the BCS model and our intermediate model.

## 6.5.2 Equations for Richardson model

For the Richardson model one can write down an approximation which should be still easily solvable and keeps more features than the BCS approximation.

The energy  $\epsilon_{\sigma,l,m} = \epsilon_{\sigma,l}$  does not depend on the magnetic number  $m$ . According to our approximation, lead functions also do not depend on  $m$ . Now we show that for the Richardson model, i.e. with  $\lambda' = 0$  in our model, the selfenergy also does not depend on  $m$ .

Since the free Green function does not depend on  $m$ , i.e.,  $G_l^0(m) \equiv G_l^0$ , we can start from assumption that the full  $G$  is independent of  $m$ . We can then evaluate the sums over  $m$  in equation (6.37)

$$\mathcal{G}_0(t_1, t_2) = i \sum_l (2L_l + 1) \tilde{G}_l(t_1, t_2) G_{0,l}(t_1, t_2). \quad (6.59)$$

For the Richardson model the only non-zero  $T$ -matrix is

$$T_0 = \lambda_0 + \lambda_0 \mathcal{G}_0 T_0. \quad (6.60)$$

We have suppressed the time arguments which are identical to equation (6.36). The corresponding averaged  $T$ -matrix reads

$$S_{0,l}(t_1, t_2; m) = -iT_0(t_1, t_2) \tilde{G}_l(t_2, t_1; -m). \quad (6.61)$$

The Green function is independent of  $m$ , therefore the right hand side is independent of  $m$ . The averaged  $T$ -matrix is then the same function for all magnetic numbers

$$S_{0,l}(t_1, t_2) = -iT_0(t_1, t_2) \tilde{G}_l(t_2, t_1). \quad (6.62)$$

Since the Green function is independent of  $m$ , from equation (6.40) we find that the selfenergy is also independent of  $m$ . It does depend on the orbital number  $l$ , however, as given by

$$\Sigma_{0,l} = \frac{S_{0,l}}{1 + G_{0,l} \times S_{0,l}}. \quad (6.63)$$

For the Richardson model the set of equations is particularly simple. For  $N$  values of  $l$  it includes  $N$ -times  $\Sigma_{0,l}$ ,  $G_l$  and  $S_{0,l}$ , and one  $\mathcal{G}_0$  and  $T_0$ . These are  $3N + 2$  functions, but this number will grow out of the equilibrium. Since  $\Sigma = \Sigma_0$ , the reduced Green function  $G_0$  equals to the known free Green function  $G^0$ , which is expressed by relation  $G_0 = G^0$ . Unlike in the BCS approximation, the  $T$ -matrix is a function of two times, i.e., of the time difference in the equilibrium or under a steady current. This time difference will result into energy dependence of the  $T$ -matrix. Likely the solution has a dominant constant part like the BCS approximation and some correction due to the energy dependence.

### 6.5.3 Approximation of our model

With  $M \neq 0$  parts of the selfenergy, the Green function depends on the magnetic number  $m$ . Let us inspect why.

The averaged  $T$ -matrix is given by equation (6.39). Let us assume that  $\tilde{G}_l(M - m) = \tilde{G}_l$ . We show that it cannot be satisfied. Indeed, for  $|M - m| \leq l$  the selfenergy is independent from  $m$ , but for  $|M - m| > l$  it is zero. With  $M = \pm 1$  one thus always finds that  $S_{1,l}(-l) = 0$  and  $S_{-1,l}(l) = 0$ . From it follows that  $G_l(\mp l) \neq G_l(0)$ . From equation (6.39) thus follows that  $S_{1,l}(1 - l) \neq S_{1,l}(0)$  and  $S_{-1,l}(1 - l) \neq S_{-1,l}(0)$ . Recursively one finds all  $G_l(m)$ 's are different.

Perhaps, it is possible to use (and eventually test) the approximation in which the difference at extreme magnetic numbers is neglected,  $S_{\pm 1,l}(m) \approx S_{\pm 1,l}$ , with

$$S_{\pm 1,l}(t_1, t_2) = -iT_{\pm 1}(t_1, t_2)\tilde{G}_l(t_2, t_1). \quad (6.64)$$

In this approximation the selfenergy is again independent of  $m$  and thus  $G$ 's are independent of  $m$ .

It should be noticed that in this approximation  $\mathcal{G}$  depends on the pair magnetic number  $M$

$$\mathcal{G}_M(t_1, t_2) = i \sum_l (2L_l + 1 - 2|M|)\tilde{G}_l(t_1, t_2)G_{M,l}(t_1, t_2). \quad (6.65)$$

In general  $M$  reaches values from  $-2L_l$  to  $2L_l$ , therefore each orbital number has different maximal  $|M|$ . In result, for largest  $M$  only highest energy levels contribute. Since we assume only the lowest values of  $M$ , this limitation is not important.

Since  $T_{-1} = T_1$  and thus  $S_{-1} = S_1$ , and  $\tilde{G} = G$ , we are left with following independent functions.  $N$ -times  $G_{0,l}$ ,  $G_{1,l}$ ,  $G_l$ ,  $S_{0,l}$ ,  $S_{1,l}$ ,  $\Sigma_{0,l}$  and  $\Sigma_{1,l}$ , and one-times  $\mathcal{G}_0$ ,  $\mathcal{G}_1$ ,  $T_0$  and  $T_1$ . These are  $7N + 4$  functions. Again, this number will grow up out of the equilibrium.

## 6.6 Nonequilibrium Green's functions

Now we convert equations on the complex time path to equations on the real time axis. All functions in the previous sections are causal on the path. All equations from now on will be on the real time axis.

### 6.6.1 Two parallel lines

Using results from chapter 4 we can directly express the averaged  $T$ -matrix (6.39)

$$S_{M,l}^<(t_1, t_2; m) = T_M^<(t_1, t_2)\tilde{G}_l^>(t_2, t_1; M - m) \quad (6.66)$$

and  $\mathcal{G}$  from equation (6.37)

$$\mathcal{G}^{M<}(t_1, t_2) = \sum_{lm} \tilde{G}_l^<(t_1, t_2; M - m)G_{M,l}^<(t_1, t_2; m). \quad (6.67)$$

### 6.6.2 Selfenergy

Analytic continuation of the selfenergy gives

$$\Sigma^< = \sum_M \Sigma_M^<, \quad (6.68)$$

and

$$\Sigma^R = \sum_M \Sigma_M^R. \quad (6.69)$$

We do not write elements  $\Sigma^>$ , which are easily obtained by the interchange  $>\longleftrightarrow<$ . It is also trivial to rewrite the retarded function into the advanced one.

### 6.6.3 Matrix products

Applying the Langreth-Wilkins rules we get from equation (6.24) with  $G_{\text{dd}}^{\text{free}} \equiv G^0$

$$(i\partial_t - \epsilon_l - h_l^R - h_r^R) G_l^{0<} - (h_l^< + h_r^<) G_l^{0A} = 0, \quad (6.70)$$

therefore

$$G_l^{0<} = G_l^{0R} \cdot (h_l^< + h_r^<) \cdot G_l^{0A}. \quad (6.71)$$

Here the retarded function satisfies

$$(i\partial_t - \epsilon_l - h_l^R - h_r^R) G_l^{0R} = \hat{\mathbf{1}} \quad (6.72)$$

and the equation for the advanced function is similar.

From the Dyson equation we obtain the generalized Kadanoff-Baym equation

$$G^< = G^R \cdot \Sigma^< \cdot G^A + (1 + G^R \cdot \Sigma^R) G^{0<} (1 + \Sigma^A \cdot G^A). \quad (6.73)$$

Substituting from equation (6.72) and using the retarded (and advanced) Dyson equation

$$G^R = G^{0R} + G^{0R} \cdot \Sigma^R \cdot G^R \quad (6.74)$$

one finds

$$G^< = G^R \cdot (\Sigma^< + h_l^< + h_r^<) \cdot G^A. \quad (6.75)$$

Functions  $h_l^<$ ,  $h_r^<$  are boundary conditions.

For the reduced Green function (6.35) we find

$$G_M^R = G^R - G^R \cdot \Sigma_M^R \cdot G_M^R \quad (6.76)$$

and

$$G_M^< = (1 + G_M^R \cdot \Sigma_M^R) \cdot G^< \cdot (1 + \Sigma_M^A \cdot G_M^A) - G_M^R \cdot \Sigma_M^< \cdot G_M^A. \quad (6.77)$$

The relation between averaged  $T$ -matrix and the selfenergy (6.40) gives

$$\Sigma_{M,l}^R(m) = \frac{S_{M,l}^R(m)}{1 + G_{M,l}^R(m) \cdot S_{M,l}^R(m)} \quad (6.78)$$

and

$$\begin{aligned} \Sigma_{M,l}^<(m) &= \frac{1}{1 + S_{M,l}^R(m) \cdot G_{M,l}^R(m)} \cdot S_{M,l}^<(m) \cdot \frac{1}{1 + G_{M,l}^A(m) \cdot S_{M,l}^A(m)} \\ &\quad + \Sigma_{M,l}^R(m) \cdot G_{M,l}^<(m) \cdot \Sigma_{M,l}^A(m). \end{aligned} \quad (6.79)$$

The  $T$ -matrix (6.36) yields

$$T_M^R = \lambda_M + \lambda_M \mathcal{G}_M^R \cdot T_M^R \quad (6.80)$$

and

$$T_M^< = T_M^R \cdot \mathcal{G}_M^< \cdot T_M^A. \quad (6.81)$$

It remains to derive retarded functions of  $\mathcal{G}$  and  $S$ . Relation

$$G_M^R(t_1, t_2) = -i\theta(t_1 - t_2) \sum_{lm} \left( \tilde{G}_l^>(M - m) G_{M,l}^>(m) - \tilde{G}_l^<(M - m) G_{M,l}^<(m) \right). \quad (6.82)$$



we rearrange as

$$\mathcal{G}_M^R(t_1, t_2) = \sum_{lm} \left( \tilde{G}_l^R(t_1, t_2; M-m) G_{M,l}^>(t_1, t_2, m) - \tilde{G}_l^<(t_1, t_2; M-m) G_{M,l}^R(t_1, t_2; m) \right). \quad (6.83)$$

Similarly we express  $S$  as

$$S_{M,l}^R(t_1, t_2; m) = T_M^R(t_1, t_2) \tilde{G}_l^<(t_1, t_2; M-m) - T_M^<(t, t') \tilde{G}_l^A(t_1, t_2; M-m). \quad (6.84)$$

The set of equations is complete.

## 6.7 Stationary regime

In the stationary regime all double-time functions depend only on the time difference,  $A(t_1, t_2) = A(t_1 - t_2)$ . It is thus advantageous to transform them into frequency representation

$$A(\omega) = \int d(t_1 - t_2) e^{i\omega(t_1 - t_2)} A(t_1 - t_2) \quad (6.85)$$

in which majority of equations become trivial algebraic relations.

Without solving any equations we can evaluate the free Green function (6.72)

$$G_l^{0R}(\omega) = \frac{1}{\omega - \epsilon_l - h_l^R(\omega) - h_r^R(\omega)}. \quad (6.86)$$

Contact functions  $h_l^R(\omega)$  and  $h_r^R(\omega)$  can be modeled by simple analytic functions. The simplest choice is a broad Lorentzian function

$$h_{l,r}^R(\omega) = \frac{\beta_{l,r}}{\omega - \epsilon_{l,r} + i\gamma_{l,r}} \quad (6.87)$$

with real parameters  $\beta$  and  $\gamma$  such that contact functions are smaller than distance between energy levels,  $|h_{l,r}^R(\omega)| \ll \epsilon_{l+1} - \epsilon_l$ . A reasonable energy spectrum of  $h$  is broader than the interval of energies in the grain, which will be achieved by large  $\gamma$ s.

The correlation functions of contact functions have local equilibrium values,  $h^< = f_{\text{FD}}(-2) \text{Im} h^R$ , therefore

$$h_{l,r}^<(\omega) = \frac{1}{e^{\frac{\omega - \mu_{l,r}}{T_{l,r}}} + 1} \frac{2\beta_{l,r}\gamma_{l,r}}{(\omega - \epsilon_{l,r})^2 + \gamma_{l,r}^2}. \quad (6.88)$$

Chemical potentials  $\mu_{l,r}$  and temperatures  $T_{l,r}$  are in general different. One can use identical temperatures but chemical potentials differ by a bias voltage  $U$ ,  $\mu_l - \mu_r = U$ . For  $\mu_l = \mu_r$  and  $T_l = T_r$  the system is at equilibrium.

## 6.8 Iteration loop

We will write down all equations in the order they appear in the iteration. Let us assume that we know some starting value of the selfenergy, i.e., we know the set of functions  $\Sigma_{M,l}^R(\omega; m)$  and  $\Sigma_{M,l}^<(\omega; m)$ . Trivially they yield the total selfenergy

$$\Sigma_l^R(\omega; m) = \sum_M \Sigma_{M,l}^R(\omega; m), \quad (6.89)$$

and

$$\Sigma_l^<(\omega; m) = \sum_M \Sigma_{M,l}^<(\omega; m). \quad (6.90)$$

### 6.8.1 Electronic functions in energy domain

From  $\Sigma^R$  we evaluate the full Green function

$$G_l^R(\omega; m) = \frac{1}{\omega - \epsilon_l - h_l^R(\omega) - h_r^R(\omega) - \Sigma_l^R(\omega; m)}. \quad (6.91)$$

We have used the free function (6.86) in the Dyson equation (6.74). The reduced Green function reads

$$G_{M,l}^R(\omega; m) = \frac{1}{\omega - \epsilon_l - h_l^R(\omega) - h_r^R(\omega) - \Sigma_l^R(\omega) + \Sigma_{M,l}^R(\omega; m)}. \quad (6.92)$$

We have used the full function (6.91) in equation (6.76). From  $\Sigma^<$  we evaluate the full correlation function (6.75)

$$G_l^<(\omega; m) = |G_l^R(\omega; m)|^2 (\Sigma_l^<(\omega; m) + h_l^<(\omega) + h_r^<(\omega)). \quad (6.93)$$

We have used that  $G_l^A(\omega; m)$  is complex conjugate to  $G_l^R(\omega; m)$ . The reduced correlation function (6.77) reads

$$\begin{aligned} G_{M,l}^<(\omega; m) &= |1 + G_{M,l}^R(\omega; m)\Sigma_{M,l}^R(\omega; m)|^2 G_l^<(\omega; m) \\ &- |G_{M,l}^R(\omega; m)|^2 \Sigma_l^<(\omega; m). \end{aligned} \quad (6.94)$$

If the leads are strongly non-symmetric, say the left one serves as a bottleneck, the lead functions are unequal,  $|h_l^R(\omega)| \ll |h_r^R(\omega)|$ . In the region of occupied states one also finds  $h_l^<(\omega) \ll h_r^<(\omega)$ , therefore from equation (6.93) one finds that the distribution in the grain will be very close to equilibrium in the right lead. In the implementation we will use this locally equilibrium limit. Equation (6.93) can be used to evaluate eventual nonequilibrium corrections.

### 6.8.2 Electronic functions in time domain

The most efficient method to evaluate  $\mathcal{G}$  from relation (6.67) is the fast Fourier transformation. To this end we convert  $G_l$  and  $G_{M,l}$  into time representation

$$G_l^<(t; m) = \int \frac{d\omega}{2\pi} e^{-i\omega t} G_l^<(\omega; m), \quad (6.95)$$

$$G_l^R(t; m) = \int \frac{d\omega}{2\pi} e^{-i\omega t} G_l^R(\omega; m), \quad (6.96)$$

$$G_{M,l}^<(t; m) = \int \frac{d\omega}{2\pi} e^{-i\omega t} G_{M,l}^<(\omega; m), \quad (6.97)$$

$$G_{M,l}^R(t; m) = \int \frac{d\omega}{2\pi} e^{-i\omega t} G_{M,l}^R(\omega; m). \quad (6.98)$$

Four additional functions do not need any numerical effort but it is advantageous to save the advanced functions in separate fields, because reading of vectors

in the reversed order makes vector products and thus the Fourier transformation very slow. The advanced Green's function in time representation is

$$G_l^A(t_1 - t_2; m) = G_l^A(t_1, t_2; m) = \bar{G}_l^R(t_1, t_2; m) = \bar{G}_l^R(t_1 - t_2; m), \quad (6.99)$$

where the bar denotes the complex conjugation. To derive this expression we have used that  $G_l^A(\omega; m) = \bar{G}_l^R(\omega; m)$  so that  $\bar{G}_l^A(-t; m) = \int \frac{d\omega}{2\pi} e^{-i\omega t} G_l^R(\omega; m) = G_l^R(t; m)$ . Similarly

$$G_{M,l}^A(t_1 - t_2; m) = G_{M,l}^A(t_1, t_2; m) = \bar{G}_{M,l}^R(t_1, t_2; m) = \bar{G}_{M,l}^R(t_1 - t_2; m). \quad (6.100)$$

The hole functions are

$$G_l^>(t; m) = iG_l^R(t; m) - G_l^<(t; m) \quad \text{for } t \geq 0, \quad (6.101)$$

$$G_l^>(t; m) = -iG_l^A(t; m) - G_l^<(t; m) \quad \text{for } t < 0, \quad (6.102)$$

$$G_{M,l}^>(t; m) = iG_{M,l}^R(t; m) - G_{M,l}^<(t; m) \quad \text{for } t \geq 0, \quad (6.103)$$

$$G_{M,l}^>(t; m) = -iG_{M,l}^A(t; m) - G_{M,l}^<(t; m) \quad \text{for } t < 0. \quad (6.104)$$

Now Green's functions are ready and we can proceed to bosonic functions.

### 6.8.3 Bosonic functions

First we have to construct the function  $\mathcal{G}$ . From equation (6.67) we get  $\mathcal{G}^<$  in time representation

$$\mathcal{G}_M^<(t; m) = \sum_{lm} G_l^<(t; M - m) G_{M,l}^<(t; m). \quad (6.105)$$

We have used that both spin components have the same values of functions,  $\tilde{G}_l^<(t; M - m) = G_l^<(t; M - m)$ .

Similarly, from equation (6.83) we find the retarded  $\mathcal{G}$

$$\mathcal{G}_M^R(t) = \sum_{lm} \left( G_l^R(t; M - m) G_{M,l}^>(t; m) - G_l^<(t; M - m) G_{M,l}^R(t; m) \right). \quad (6.106)$$

Using Fourier transformations these functions are converted to the frequency representation

$$\mathcal{G}_M^<(\omega) = \int dt e^{i\omega t} \mathcal{G}_M^<(t), \quad (6.107)$$

$$\mathcal{G}_M^R(\omega) = \int dt e^{i\omega t} \mathcal{G}_M^R(t). \quad (6.108)$$

From  $\mathcal{G}$  we evaluate the retarded  $T$ -matrix (6.80)

$$T_M^R(\omega) = \frac{\lambda_M}{1 - \lambda_M \mathcal{G}_M^R(\omega)} \quad (6.109)$$

and the correlation part of the  $T$ -matrix

$$T_M^<(\omega) = |T_M^R(\omega)|^2 \mathcal{G}_M^<(\omega). \quad (6.110)$$

The bosonic functions are complete and we can proceed to the selfenergy.

### 6.8.4 Selfenergy

The major step to obtain a new selfenergy is to evaluate the averaged  $T$ -matrix

$$S_{M,l}^<(t; m) = T_M^<(t; m)G_l^>(-t; M - m) \quad (6.111)$$

and

$$S_{M,l}^R(t; m) = T_M^R(t; m)G_l^<(-t; M - m) - T^<(t; m)G_l^A(-t; M - m). \quad (6.112)$$

These functions are transformed to the energy representation

$$S_{M,l}^<(\omega; m) = \int_{-\infty}^{\infty} dt e^{i\omega t} S_{M,l}^<(t; m), \quad (6.113)$$

$$S_{M,l}^R(\omega; m) = \int_0^{\infty} dt e^{i\omega t} S_{M,l}^R(t; m). \quad (6.114)$$

Finally, from equation (6.78) we obtain the retarded selfenergy

$$\Sigma_{M,l}^R(\omega; m) = \frac{S_{M,l}^R(\omega; m)}{1 + G_{M,l}^R(\omega; m)S_{M,l}^R(\omega; m)} \quad (6.115)$$

and from equation (6.79) results the correlation part

$$\begin{aligned} \Sigma_{M,l}^<(\omega; m) &= \left| \frac{1}{1 + S_{M,l}^R(\omega; m)G_{M,l}^R(\omega; m)} \right|^2 S_{M,l}^<(\omega; m) \\ &+ |\Sigma_{M,l}^R(\omega; m)|^2 G_{M,l}^<(\omega; m). \end{aligned} \quad (6.116)$$

Now one loop of the iteration procedure is closed and one can return to equation (6.89) and start the next loop.

## 6.9 Simplified set

Before the iteration of the full set of equations, it is advantageous to solve a simplified set so that the iteration will start from some reasonable value of the selfenergy.

The subsidiary functions (6.86), (6.87) and (6.88) are the same as in the full solution.

In the simplified model none of quantities depends on the magnetic number  $m$ . The total selfenergy thus is

$$\Sigma_l^R(\omega) = \sum_M \Sigma_{M,l}^R(\omega) \quad (6.117)$$

and

$$\Sigma_l^<(\omega) = \sum_M \Sigma_{M,l}^<(\omega). \quad (6.118)$$

This allows us to evaluate sums over  $m$  in the two-particle propagators

$$\mathcal{G}_M^<(t) = \sum_l (2L_l + 1 - 2|M|) G_l^<(t) G_{M,l}^<(t) \quad (6.119)$$

and

$$\mathcal{G}_M^R(t) = \sum_l (2L_l + 1 - 2|M|) \left( G_l^R(t) G_{M,l}^>(t) - G_l^<(t) G_{M,l}^R(t) \right). \quad (6.120)$$

Other equations are the same as above.

## 6.10 Richardson model

The pairing happens in  $M = 0$  pair momentum. It is reasonable to evaluate this interaction within the Richardson model. The subsidiary functions (6.86), (6.87) and (6.88) are the same as in the full solution.

In the Richardson model only  $M = 0$  interacts. The total selfenergy thus is

$$\Sigma_l^R(\omega) = \Sigma_{0,l}^R(\omega) \quad (6.121)$$

and

$$\Sigma_l^<(\omega) = \Sigma_{0,l}^<(\omega). \quad (6.122)$$

As we have already shown, for this model the reduced Green function is identical to the free function. This is true for all its analytical parts, e.g.  $G_{0,l}^> = G_l^{0>}$ .

In the two-particle propagator we need only the  $M = 0$  channel,

$$\mathcal{G}_0^<(t) = \sum_l (2L_l + 1) G_l^<(t) G_l^{0<}(t) \quad (6.123)$$

and

$$\mathcal{G}_0^R(t) = \sum_l (2L_l + 1) \left( G_l^R(t) G_l^{0>}(t) - G_l^<(t) G_l^{0R}(t) \right). \quad (6.124)$$

The averaged  $T$ -matrix has a single contribution

$$S_{0,l}^<(t) = T_0^<(t) G_l^>(-t) \quad (6.125)$$

and

$$S_{0,l}^R(t) = T_0^R(t) G_l^<(-t) - T_0^<(t) G_l^A(-t) \quad (6.126)$$

from which we evaluate the selfenergy.

## 6.11 BCS approximation

The BCS approximation is even simpler than the Multiple scattering approximation of the Richardson model. The subsidiary functions (6.86), (6.87) and (6.88) are the same as in the full solution.

The BCS selfenergy (6.54) in the frequency representation reads

$$\Sigma_l^R(\omega) = -\Delta^2 G_l^{0A}(-\omega). \quad (6.127)$$

We assume  $\Delta$  real. The correlation function is

$$\Sigma_l^<(\omega) = -\Delta^2 G_l^{0>}(-\omega). \quad (6.128)$$

The gap is related to the  $T$ -matrix, however, its value is obtained from a simplified BCS condition in which the interaction potential is neglected against the  $T$ -matrix.

It should be noted that in all cases it is necessary to evaluate the chemical potential so that the expected number of particles is the same in all approximations.

# 7. Numerics of magic cluster model

## 7.1 Introduction

In this section we demonstrate the use of nonequilibrium Green functions to compute equilibrium properties of the isolated grain. It is illustrative to do it as alternative approach to the Matsubara formalism which can be also applied in the equilibrium.

First, we introduce the equilibrium relations and the limit of weakly coupled grain. In this approximation we compute the BCS theory and the first order of the Multiple scattering theory and the Kadanoff-Martin theory. This is very BCS-friendly comparison, because all theories are tested on the Richardson model which does not include non-pairing interactions neglected in the BCS theory. Nevertheless, we still observe the differences.

The simple model for numerics has only two energy levels, which are degenerated. We will separate the dominant contribution of the T-matrix, therefore we can conveniently identify the gap.

## 7.2 Isolated grain in equilibrium

Let us assume that the grain is only weakly coupled to leads. This means that we make contacts infinitesimally small

$$h^R(\omega) = -i\eta \quad \text{with} \quad \eta \rightarrow 0. \quad (7.1)$$

We will denote this limit as  $h^R(\omega) = -i0$ . This will simplify the set of equations and we can easily do numerics.

We also assume an equilibrium system. For the equilibrium we have following relations

$$\begin{aligned} f_{FD}(\omega) &= \frac{1}{e^{\frac{\omega}{k_B T}} + 1} \\ f_{FD}(-\omega) &= 1 - f_{FD}(\omega) \\ G^<(\omega) &= -2\text{Im}G^R(\omega)f_{FD}(\omega) \\ G^>(\omega) &= -2\text{Im}G^R(\omega)(1 - f_{FD}(\omega)) \end{aligned} \quad (7.2)$$

We remind that energy is related to the chemical potential  $\epsilon_l - \mu$ . In other words, the origin of energies is set at the chemical potential.

## 7.3 Bardeen formula for current - measurement of equilibrium grain spectra

For almost isolated grain, which is in the local equilibrium with the right lead the current can be approximated within the second order of bottleneck hopping

constant  $u^l$  by Bardeen's formula [17]

$$J = |u^l|^2 \int (f_{FD}(\omega - \mu - V) - f_{FD}(\omega - \mu)) (-2)\text{Im}G_{\text{gg}}^R(\omega) (-2)\text{Im}G_{\text{ll}}^R(\omega - V) \frac{d\omega}{2\pi}. \quad (7.3)$$

The Bardeen formula equals to a convolution of the grain density of states ( $-2\text{Im}G_{\text{gg}}^R(\omega)$ ) with the density of states within the left lead ( $-2\text{Im}G_{\text{ll}}^R(\omega)$ ). The weight of the convolution is proportional to a difference  $f_{FD}(\omega - \mu - V) - f_{FD}(\omega - \mu)$ .

The Bardeen formula assumes the weak coupling to the leads. Moreover, the left barrier serve as bottleneck for the tunneling process ( $u^r \gg u^l$ ) allowing to thermalize the grain with the right lead. The chemical potential is thus the same in the grain as in the right lead  $\mu^r = \mu$ . The left lead chemical potential equals to  $\mu + V$ .

The Bardeen formula reduces for a constant density of states  $-2\text{Im}G_{\text{tr}}^R = C$  and for small temperature  $T$  to

$$J = C|u^l|^2 \int_{\mu}^{\mu+V} (-2)\text{Im}G_{\text{gg}}^R(\omega) \frac{d\omega}{2\pi}. \quad (7.4)$$

According to this relation one can directly observe the spectrum in the grain by derivative of the current with respect to voltage

$$\frac{\partial J}{\partial V} = \frac{C|u^l|^2}{2\pi} (-2)\text{Im}G_{\text{gg}}^R(\mu + V). \quad (7.5)$$

All information about the spectrum is hidden in the retarded Green function and thus  $G_{\text{gg}}^R(\omega)$  it will be the target of the next sections.



## 7.4 Two-particle propagator

In the appendix we derived the reduced two-particle propagator. The algebra is very simple, but too long. We thus write here the result

$$\begin{aligned}
\mathcal{G}_0^R(\Omega) = \sum_l (2L_l + 1) & \left\{ \right. \\
& - \frac{1}{\Omega - \Omega_0 - \left( \sqrt{\Delta^2 + \left( \epsilon_l - \frac{\Omega_0}{2} \right)^2} + \left( \epsilon_l - \frac{\Omega_0}{2} \right) \right) + i0} \\
& \frac{\left( \sqrt{\Delta^2 + \left( \epsilon_l - \frac{\Omega_0}{2} \right)^2} + \left( \epsilon_l - \frac{\Omega_0}{2} \right) \right)}{2\sqrt{\Delta^2 + \left( \epsilon_l - \frac{\Omega_0}{2} \right)^2}} \\
& \left( -1 + f_{FD} \left( \left( \epsilon_l - \frac{\Omega_0}{2} \right) + \frac{\Omega_0}{2} \right) - f_{FD} \left( +\sqrt{\Delta^2 + \left( \epsilon_l - \frac{\Omega_0}{2} \right)^2} + \frac{\Omega_0}{2} \right) \right) \\
& + \frac{1}{\Omega - \Omega_0 - \left( -\sqrt{\Delta^2 + \left( \epsilon_l - \frac{\Omega_0}{2} \right)^2} + \left( \epsilon_l - \frac{\Omega_0}{2} \right) \right) + i0} \\
& \frac{\left( -\sqrt{\Delta^2 + \left( \epsilon_l - \frac{\Omega_0}{2} \right)^2} + \left( \epsilon_l - \frac{\Omega_0}{2} \right) \right)}{2\sqrt{\Delta^2 + \left( \epsilon_l - \frac{\Omega_0}{2} \right)^2}} \\
& \left. \left( -1 + f_{FD} \left( \left( \epsilon_l - \frac{\Omega_0}{2} \right) + \frac{\Omega_0}{2} \right) - f_{FD} \left( -\sqrt{\Delta^2 + \left( \epsilon_l - \frac{\Omega_0}{2} \right)^2} + \frac{\Omega_0}{2} \right) \right) \right\}. \tag{7.6}
\end{aligned}$$

derived from the BSC approximation of the selfenergy  $\Sigma_l^R(\omega) = -\Delta^2 G_l^{0A}(\Omega_0 - \omega)$  with the general position of the dominant pole.

## 7.5 BCS theory

The BCS selfenergy (6.54) in the frequency representation reads

$$\Sigma_l^R(\omega) = -\Delta^2 G_{0,l}^A(-\omega). \tag{7.7}$$

The BCS condition for gap in isolated grain at equilibrium reads

$$1 = \lambda_0 \mathcal{G}_0^R(0) \tag{7.8}$$

or explicitly

$$1 = \lambda_0 \sum_l \frac{2L_l + 1}{2\sqrt{\epsilon_l^2 + \Delta^2}} \tanh \left( \frac{\sqrt{\epsilon_l^2 + \Delta^2}}{2k_B T} \right), \tag{7.9}$$

where  $(2L_l + 1)$  is a degeneracy of the energy shell with the energy  $\epsilon_l = E_l - \mu$  related to the chemical potential. This is an equation for the gap. It should be easy to solve for  $\Delta$  assuming only few selected levels  $l$ , because function  $(1/x) \tanh x$  is simple and monotonic.

The second unknown quantity is the chemical potential, therefore we need an additional equation which specifies it. For this purposes we adopt an equation for the number of particles familiar from the BCS approach [16]

$$N = \sum_l \frac{2(2L_l + 1)}{2} \left[ \left( 1 - \frac{\epsilon_l}{\sqrt{\epsilon_l^2 + \Delta^2}} \right) f_{FD} \left( -\sqrt{\epsilon_l^2 + \Delta^2} \right) + \left( 1 + \frac{\epsilon_l}{\sqrt{\epsilon_l^2 + \Delta^2}} \right) f_{FD} \left( \sqrt{\epsilon_l^2 + \Delta^2} \right) \right]. \quad (7.10)$$

We have thus closed the set of equations to determine the parameters  $\mu$  and  $\Delta$ . The equations can be solved with standard numerical methods like the Broyden algorithm taken over from [18].

## 7.6 Characterization of the model for numerics

For numerical studies we choose the model of a magic cluster. Magic clusters are ultrasmall metallic grains, where the atoms constitute a cluster with ideal spherical symmetry, where the last energy level is fully filled. We are inspired by the model introduced by Ovchinnikov and Kresin in the series of articles [16],[19],[20] and [21].

Using a simple model of the magic cluster with two levels near Fermi surface, HOS (highest occupied state) with momentum 7 and LUS (lowest unoccupied state) with momentum 4. In the HOS we have  $N_{l_1} = 30$  electron states and in the LUS layer is  $N_{l_2} = 18$  electron states.

We assume that the gate voltage is tuned to maintain in average 30 electrons in the grain. We will use the set of parameters  $E'_1 = 8000\text{meV}$  and  $E'_2 = 8065\text{meV}$  related to the Fermi energy  $E_F = 8000\text{meV}$ . So the energies are  $E_1 = 0\text{meV}$  and  $E_2 = 65\text{meV}$ .

## 7.7 Two-particle propagator with BCS solution

In the BCS theory we derived the set of equations for the parameters  $\mu$  and  $\Delta$ . The BCS condition has the form

$$1 = \lambda_0 \sum_l \frac{2L_l + 1}{2\sqrt{\epsilon_l^2 + \Delta^2}} \tanh \left( \frac{\sqrt{\epsilon_l^2 + \Delta^2}}{2k_B T} \right). \quad (7.11)$$

or shortly

$$1 = \lambda_0 \mathcal{G}_0^R(0). \quad (7.12)$$

This condition implies that T-matrix  $T_0^R(\Omega)$  is divergent in the zero frequency channel

$$T_0^R(0) = \frac{\lambda_0}{1 - \lambda_0 \mathcal{G}_0^R(0)} = \infty. \quad (7.13)$$

For other frequencies the T-matrix has values

$$T_0^R(\Omega) = \frac{\lambda_0}{1 - \lambda_0 \mathcal{G}_0^R(\Omega)}. \quad (7.14)$$

In the denominator we will use the two-particle propagator  $\mathcal{G}_0^R$

$$\begin{aligned} \mathcal{G}_0^R(\Omega) = \sum_l (2L_l + 1) \left\{ \right. \\ - \left( \frac{1}{\Omega - (\epsilon_l + \sqrt{\epsilon_l^2 + \Delta^2}) + i0} \right) \frac{\epsilon_l + \sqrt{\epsilon_l^2 + \Delta^2}}{2\sqrt{\epsilon_l^2 + \Delta^2}} \\ \left( (-1 + f_{FD}(\epsilon_l)) - f_{FD}(\sqrt{\epsilon_l^2 + \Delta^2}) \right) \\ + \left( \frac{1}{\Omega - (\epsilon_l - \sqrt{\epsilon_l^2 + \Delta^2}) + i0} \right) \frac{\epsilon_l - \sqrt{\epsilon_l^2 + \Delta^2}}{2\sqrt{\epsilon_l^2 + \Delta^2}} \\ \left. \left( (-1 + f_{FD}(\epsilon_l)) - f_{FD}(-\sqrt{\epsilon_l^2 + \Delta^2}) \right) \right\}. \end{aligned} \quad (7.15)$$

This analytic form of the two-particle propagator can be used to compute  $T_0^R(\Omega)$  (for the parameters  $\mu$  and  $\Delta$  from the solution of the BCS set). Generally, for our model of two levels the imaginary part of T-matrix has four poles, so can write

$$T_0^R(\Omega) = \frac{A}{\Omega - \Omega_a} + \frac{B}{\Omega - \Omega_b} + \frac{C}{\Omega - \Omega_c} + \frac{D}{\Omega - \Omega_d} + E, \quad (7.16)$$

where  $A, B, C, D, E$  are general coefficients and  $\Omega_a, \Omega_b, \Omega_c, \Omega_d$  are positions of poles. In one of the poles  $\Omega_a = \Omega_0 = 0$  the Bose-Einstein distribution diverges making this pole the dominant one.

## 7.8 Change of origin of energies

In finite systems the pole  $\Omega_0$  is not in the same position as the chemical potential. They are very close, however. We then choose the origin of the energies in  $\Omega_0$ , not in  $\mu$ . The reason for this choice becomes clear from the following equations.

Let us assume first that the energy origin is fixed at the chemical potential  $\mu$  so that  $\Omega_0$  is non-zero. For our clean system, the Nambu-Gorkov theory is equivalent to the Bogoliubov-de Gennes theory represented by coupled equations

$$\begin{pmatrix} \epsilon_l + \frac{\Omega_0}{2} & \Delta e^{2i\chi} \\ \Delta^* e^{-2i\chi} & -(\epsilon_l + \frac{\Omega_0}{2}) \end{pmatrix} \begin{pmatrix} a_1 \\ a_2 \end{pmatrix} = -i\partial_t \begin{pmatrix} a_1 \\ a_2 \end{pmatrix}, \quad (7.17)$$

which can be expressed as

$$\begin{aligned} -e^{-i\chi}(i\partial_t a_1) &= (\epsilon_l + \frac{\Omega_0}{2})a_1 e^{-i\chi} + \Delta a_2 e^{i\chi} \\ -e^{i\chi}(i\partial_t a_2) &= -(\epsilon_l + \frac{\Omega_0}{2})a_2 e^{i\chi} + \Delta^* a_1 e^{-i\chi}. \end{aligned} \quad (7.18)$$

This set can be simplified by substitution  $\tilde{a}_1 = a_1 e^{-i\chi}$  and  $\tilde{a}_2 = a_2 e^{i\chi}$  as

$$\begin{aligned} (i\partial_t \tilde{a}_1) &= (\epsilon_l + \frac{\Omega_0}{2} - \partial_t \chi) \tilde{a}_1 + \Delta \tilde{a}_2 \\ (i\partial_t \tilde{a}_2) &= -(\epsilon_l + \frac{\Omega_0}{2} - \partial_t \chi) \tilde{a}_2 + \Delta \tilde{a}_1. \end{aligned} \quad (7.19)$$

After the transformation we want to have only energies  $\epsilon_l$ . We than choose the potential  $\chi$  as

$$\chi = \frac{\Omega_0}{2}t. \quad (7.20)$$

Substituting this result to the Nambu-Gorkov selfenergy in time domain

$$\Sigma_l^R(\omega) = -\Delta^*(t_1)G_l^{0A}(t_2 - t_1)\Delta(t_2). \quad (7.21)$$

and transforming from the time domain

$$\Sigma_l^R(\omega) = -\Delta^* e^{-i\Omega_0 t_1} G_l^{0A}(t_2 - t_1) e^{i\Omega_0 t_2} \Delta. \quad (7.22)$$

to frequencies we obtain exactly the same selfenergy (B.4)

$$\Sigma_l^R(\omega) = -\Delta^2 G_l^{0A}(\Omega_0 - \omega). \quad (7.23)$$

The gap parameter should be stationary. This condition can be met by setting the origin of energies at  $\Omega_0$ . The chemical potential is shifted from the origin and we need to change all energies to  $\epsilon_l = E_l - \mu + \delta\mu$ . The term  $2\delta\mu$  is a distance between chemical potential and the pole  $\Omega_0$ . Thus the relations for distributions

$$\begin{aligned} f_{FD}(\omega) &= \frac{1}{e^{\frac{(\omega - \delta\mu)}{k_B T}} + 1}, \\ f_{BE}(\Omega) &= \frac{1}{e^{\frac{(\Omega - 2\delta\mu)}{k_B T}} - 1}. \end{aligned} \quad (7.24)$$

has to be also changed.

## 7.9 The single channel approximation

Now let us return to the beginning and derive corrections to the BCS approximation. This corrections origin from the different position of the chemical potential  $\mu$  and the position of the dominant pole  $\Omega_0$ . The retarded selfenergy in the Multiple scattering theory is constructed as

$$\Sigma_l^R(\omega) = \int_{-\infty}^{\infty} (-T_0^{<}(\Omega)G_{0,l}^A(\Omega - \omega) + T_0^R(\Omega)G_{0,l}^{<}(\Omega - \omega)) \frac{d\Omega}{2\pi}, \quad (7.25)$$

and in the Kadanoff-Martin theory

$$\Sigma_l^R(\omega) = \int_{-\infty}^{\infty} (-T_0^{<}(\Omega)G_l^{0A}(\Omega - \omega) + T_0^R(\Omega)G_l^{0<}(\Omega - \omega)) \frac{d\Omega}{2\pi}. \quad (7.26)$$

In the single channel approximation they are identical because because  $G_l^{0<} = G_{0,l}^{<}$  in this case

The dominant Bose-Einstein contribution is expected in the pole with zero frequency. The divergence of Bose-Einstein type is hidden in quantity  $T_0^{<}(\Omega)$  since in equilibrium holds  $T_0^{<}(\Omega) = -2\text{Im}T_0^R(\Omega)f_{BE}(\Omega)$ . The dominant contribution is thus

$$\int_{-\infty}^{\infty} (2\text{Im}T_0^R(\Omega)f_{BE}(\Omega)G_l^{0A}(\Omega - \omega) + \dots) \frac{d\Omega}{2\pi} \quad (7.27)$$

Now we substitute only contribution from pole  $\Omega_a = \Omega_0 = 0$

$$\int_{-\infty}^{\infty} \left( -A\delta(0)G_l^{0A}(\Omega - \omega) \frac{1}{e^{\frac{\Omega - 2\delta\mu}{k_B T}} - 1} + \dots \right) d\Omega. \quad (7.28)$$

After the integration we have explicit form of the Bose-Einstein distribution near the condensation pole

$$= -AG_l^{0A}(0 - \omega) \frac{1}{e^{\frac{0 - 2\delta\mu}{k_B T}} - 1} + \dots \quad (7.29)$$

We can expand to the first order and we get a final expression

$$\Sigma_l^R(\omega) = -A \frac{k_B T}{-2\delta\mu} G_l^{0A}(-\omega). \quad (7.30)$$

The coefficient  $A$  is related to the derivative of  $\mathcal{G}_0^R(\Omega)$  evaluated in pole  $\Omega_0 = 0$

$$T_0^R(\Omega) = \frac{\lambda_0}{1 - \lambda_0(\mathcal{G}_0^R(0) + \frac{\partial \mathcal{G}_0^R(0)}{\partial \Omega}(\Omega - 0))} = \frac{-1}{\frac{\partial \mathcal{G}_0^R(0)}{\partial \Omega}} \frac{1}{\Omega}. \quad (7.31)$$

Now we are ready to write down the final expression for the dominant part of the selfenergy

$$\Sigma_l^R(\omega) = \frac{-1}{\frac{\partial \mathcal{G}_0^R(0)}{\partial \Omega}} \frac{k_B T}{2\delta\mu} G_l^{0A}(-\omega). \quad (7.32)$$

Comparing it with the Nambu-Gorkov selfenergy  $\Sigma_l^R(\omega) = -\Delta^2 G_l^{0A}(-\omega)$  we find the gap in terms of the two-particle propagator

$$\Delta^2 = \frac{1}{\frac{\partial \mathcal{G}_0^R(0)}{\partial \Omega}} \frac{k_B T}{2\delta\mu}. \quad (7.33)$$

Let us return to the equation for the T-matrix

$$T_0^R(\Omega) = \frac{1}{1 - \lambda_0 \mathcal{G}_0^R(\Omega)}. \quad (7.34)$$

This equation requires  $T_0^R$  as a function of  $\Omega$ . In the vicinity of pole  $\Omega_0$  we can use the general formula

$$\begin{aligned} T_0^R(\Omega) &= \int_{-\infty}^{\infty} \left( \frac{2\text{Im}T_0^R(\Omega')}{\Omega' - \Omega} \right) \frac{d\Omega'}{2\pi} \\ &= \int_{-\infty}^{\infty} \left( \frac{\frac{-1}{\frac{\partial \mathcal{G}_0^R(0)}{\partial \Omega}} \delta(0)}{\Omega' - \Omega} \right) d\Omega' = \frac{\frac{-1}{\frac{\partial \mathcal{G}_0^R(0)}{\partial \Omega}}}{\Omega}. \end{aligned} \quad (7.35)$$

Substituting from (7.33) we get

$$T_0^R(\Omega) = \frac{\frac{-1}{\frac{\partial \mathcal{G}_0^R(0)}{\partial \Omega}}}{\Omega} = \frac{\Delta^2}{k_B T} \frac{-2\delta\mu}{\Omega}. \quad (7.36)$$

We use this result in the equation for the T-matrix

$$T_0^R(-2\delta\mu) = \lambda_0 + \lambda_0 \mathcal{G}_0^R(-2\delta\mu) T_0^R(-2\delta\mu) \quad (7.37)$$

and rearrange the terms in the equation to

$$\frac{1}{\lambda_0} = \frac{k_B T}{\Delta^2} + \mathcal{G}_0^R(-2\delta\mu). \quad (7.38)$$

Finally we substitute for the shift of the chemical potential from the energy origin

$$\frac{1}{\lambda_0} = \frac{k_B T}{\Delta^2} + \mathcal{G}_0^R\left(-\frac{k_B T}{\Delta^2}\right) \quad (7.39)$$

and expand in energy argument

$$\frac{1}{\lambda_0} = \frac{k_B T}{\Delta^2} + \mathcal{G}_0^R(0) + \left(-\frac{k_B T}{\Delta^2}\right) \frac{\partial \mathcal{G}_0^R(0)}{\partial \Omega}. \quad (7.40)$$

The last two terms cancel and we arrive at the standard BCS condition

$$\frac{1}{\lambda_0} = \mathcal{G}_0^R(0). \quad (7.41)$$

We have thus shown that the BCS condition itself is robust with respect to corrections due to the shift of the chemical potential.

There are, however, indirect effects due to shifts of energy levels. Because we do not relate the energy to chemical potential  $\mu$  but to the zero frequency  $\Omega_0 = 0$  the chemical potential is thus  $\mu - \frac{\Omega_0}{2} = \delta\mu < 0$ . So we will relate the energies to  $\epsilon_l = E_l - \mu + \delta\mu$ . We have thus the following set of equations

$$2\delta\mu - \frac{1}{\frac{\partial \mathcal{G}_0^R(0)}{\partial \Omega}} \frac{k_B T}{\Delta^2} = 0 \quad (7.42)$$

$$\frac{1}{\lambda_0} = \mathcal{G}_0^R(0) \quad (7.43)$$

$$N = \sum_l \frac{2(2L_l + 1)}{2} \left[ \left(1 - \frac{\epsilon_l}{\sqrt{\epsilon_l^2 + \Delta^2}}\right) f_{FD}\left(-\sqrt{\epsilon_l^2 + \Delta^2}\right) + \left(1 + \frac{\epsilon_l}{\sqrt{\epsilon_l^2 + \Delta^2}}\right) f_{FD}\left(\sqrt{\epsilon_l^2 + \Delta^2}\right) \right]. \quad (7.44)$$

In the limit of  $\Omega_0 = 0$  the two-particle propagator reduces to

$$\begin{aligned} \mathcal{G}_0^R(\Omega) = \sum_l (2L_l + 1) & \left\{ \right. \\ & - \left( \frac{1}{\Omega - (\epsilon_l + \sqrt{\epsilon_l^2 + \Delta^2}) + i0} \right) \frac{\epsilon_l + \sqrt{\epsilon_l^2 + \Delta^2}}{2\sqrt{\epsilon_l^2 + \Delta^2}} \\ & \left( (-1 + f_{FD}(\epsilon_l)) - f_{FD}(\sqrt{\epsilon_l^2 + \Delta^2}) \right) \\ & + \left( \frac{1}{\Omega - (\epsilon_l - \sqrt{\epsilon_l^2 + \Delta^2}) + i0} \right) \frac{\epsilon_l - \sqrt{\epsilon_l^2 + \Delta^2}}{2\sqrt{\epsilon_l^2 + \Delta^2}} \\ & \left. \left( (-1 + f_{FD}(\epsilon_l)) - f_{FD}(-\sqrt{\epsilon_l^2 + \Delta^2}) \right) \right\}. \end{aligned} \quad (7.45)$$

The difference between the BCS approximation and the present set of equations is in the fact that in the BCS we had a Hamiltonian related to  $\epsilon_l = E_l - \mu$  while with corrections we have  $\epsilon_l = E_l - \mu + \delta\mu$ .

## 7.10 Remark of the neglecting of corrections

If one neglects the correction to the chemical potential  $\delta\mu$  in the two-particle propagator, which is the same as using the zero-order two-particle propagator, the equation (7.39) simplifies to

$$\frac{1}{\lambda_0} = \frac{k_B T}{\Delta^2} + \mathcal{G}_0^R(0). \quad (7.46)$$

This is exactly the equation (A19) for the bulk system derived in [10] which in the present notation reads

$$\frac{1}{\mathcal{V}_0} = \frac{1}{\lambda_0 \Omega_{Vol.}} = \frac{k_B T}{\Omega_{Vol.} \Delta^2} + \frac{1}{\Omega_{Vol.}} \mathcal{G}_0^R(0) \quad (7.47)$$

with  $\Omega_{Vol.}$  being the volume of the sample. This is logical because in the bulk system  $\delta\mu \propto \frac{1}{\Omega_{vol.}} \rightarrow 0$ .

## 7.11 BCS approximation – numerics

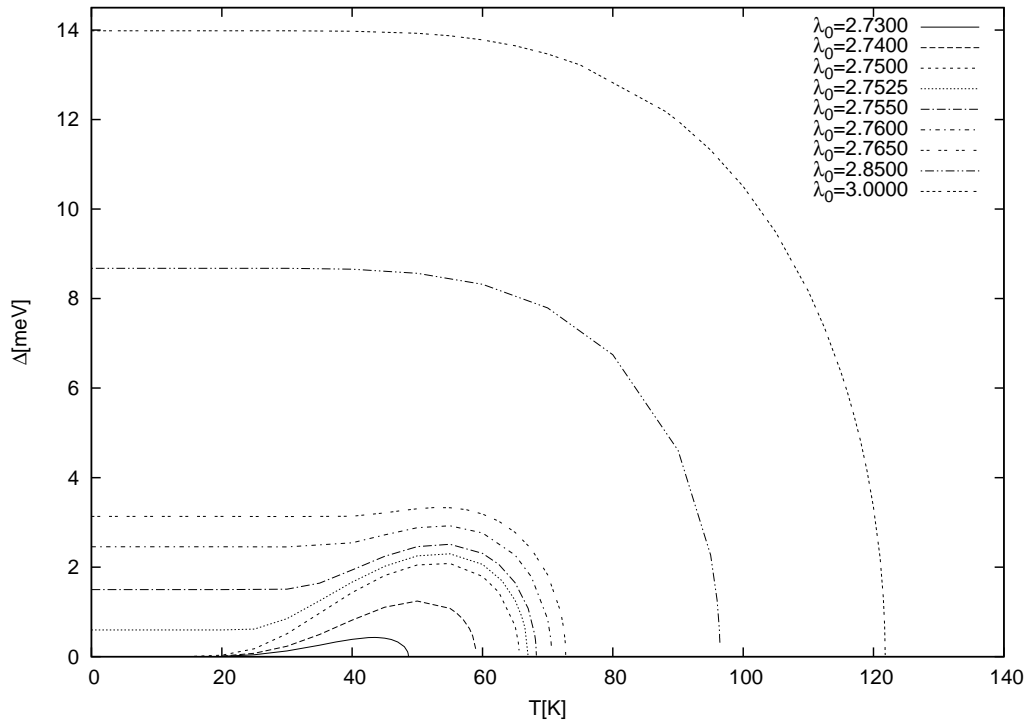


Figure 7.1: The BCS gap  $\Delta$  as a function of temperature  $T$  for different pairing parameters  $\lambda$ .

To obtain the values of the chemical potential  $\mu$  and the gap  $\Delta$  we solve together the BCS condition (7.9) and the  $N$  particle condition (7.10). The resulting temperature dependence of the BCS gap is shown in Fig. 7.1. We can see that for large  $\lambda$ , the temperature dependence is of the BCS-type with the maximal gap at the zero temperature and monotonous decrease towards the critical temperature. The ratio between  $\Delta$  and the transition temperature  $T_c$  approaches in the limit of high  $\lambda$  the value for the bulk system  $\frac{\Delta}{T_c} = 1.76$ , see [9].

While in bulk systems any weak interaction is capable to create a Cooper pair and turn the system superconducting at sufficiently low temperature, in nanograins the coupling parameters has to be larger than  $\lambda \sim 2.72$  for superconductivity to appear. In the same time, unequal degeneracy of two energy levels near the Fermi energy makes it possible that a small thermal population of electrons favors superconductivity leading to the increase of the gap at low temperatures and for very weak coupling interaction can even lead to superconductivity at finite temperatures while the ground state is normal.

## 7.12 The single channel approximation – numerics

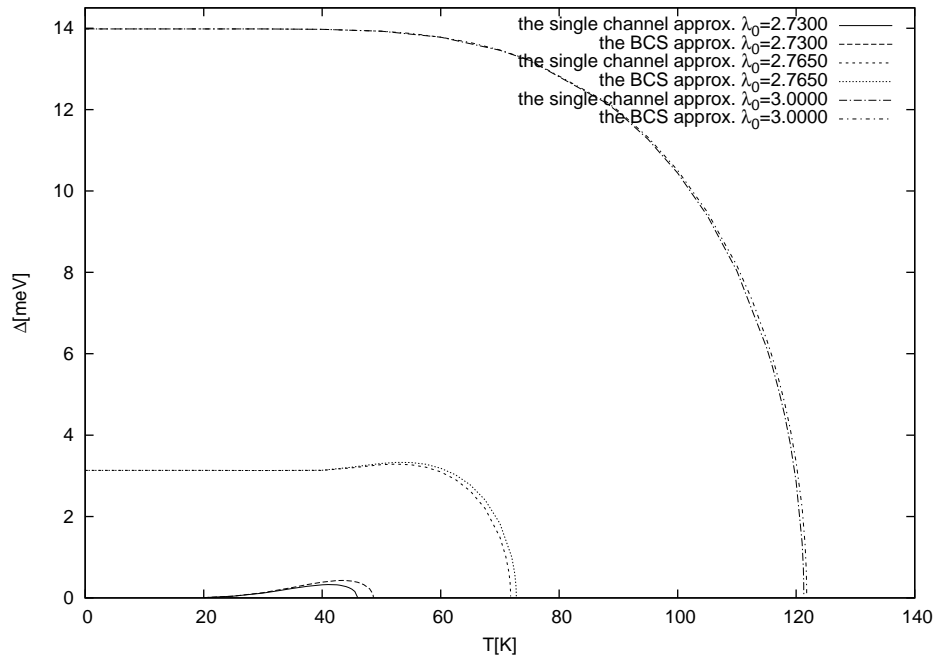


Figure 7.2: The BCS gap  $\Delta$  and its corrections as a function of temperature  $T$  for different parameters  $\lambda$ . The corrections decrease with the increasing interaction constant  $\lambda$ .

The corrected set of equations (7.42), (7.43), (7.44) which we derived above can be solved with the same tools as the BCS set. The results are in figures 7.2 and 7.3. The basic feature is very similar. The corrections are very small showing that the BCS theory is an excellent approximation for the Richardson model. As one can see, there are some minor differences in the critical temperatures. The



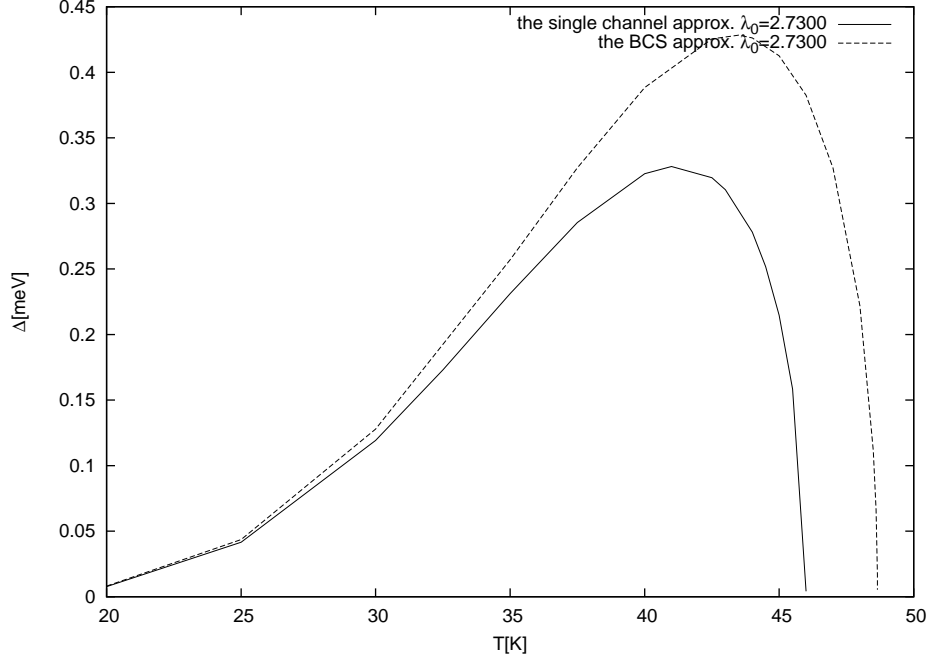


Figure 7.3: The BCS gap  $\Delta$  and its corrections as a function of temperature  $T$  for  $\lambda=2.73$ . The difference between critical temperatures is almost 4K.

shape of the functions are, however, the same as in the BCS theory. The similarity with the BCS theory is a consequence of the one pole-contribution. If we take the contributions from other poles we will obtain a frequency dependent gap parameter and the spectrum will contain new features.

### 7.13 Renormalization of the gap

In this section we discuss possible corrections to the spectrum of energies  $-2\text{Im}G_l^R$  in the grain. They came from iterations of the Kadanoff-Martin or the Multiple scattering theory and should be compared with the single channel approximation.

In the BCS theory the selfenergy is constructed

$$\Sigma_l^R(\omega) = -\Delta^2 G_l^{0A}(-\omega) \quad (7.48)$$

and the chemical potential  $\mu$  equals zero. In the single channel approximation of the Kadanoff-Martin theory the selfenergy is unchanged

$$\Sigma_l^R(\omega) = -\Delta^2 G_l^{0A}(-\omega) \quad (7.49)$$

but the chemical potential is shifted to the value  $\delta\mu$ .

The single channel contribution above is the crudest approximation. We can include other poles of the Kadanoff-Martin T-matrix to the selfenergy

$$\Sigma_l^R(\omega) = \int_{-\infty}^{\infty} (-T_0^<(\Omega)G_l^{0A}(\Omega - \omega) + T_0^R(\Omega)G_l^{0<}(\Omega - \omega)) \frac{d\Omega}{2\pi}, \quad (7.50)$$

using the equilibrium relations  $G_l^{0<} = -2\text{Im}G_l^{0R}f_{FD}$  and  $T_0^{<} = -2\text{Im}T_0^R f_{BE}$ . The selfenergy contains five terms

$$\begin{aligned}\Sigma_l^R(\omega) &= -\Delta^2 G_l^{0A}(-\omega) + \sum_{A=1}^3 \left( \frac{\text{sgn}(\Omega_A)}{\frac{\partial G_0^R(\Omega_A)}{\partial \Omega}} f_{BE}(\Omega_A) G_l^{0A}(\Omega_A - \omega) \right) \\ &\quad + T_0^R(\omega + \epsilon_l) f_{FD}(\epsilon_l),\end{aligned}\tag{7.51}$$

The non-dominant terms can be grouped to the reduced selfenergy  $\Sigma_l^R$

$$= -\Delta^2 G_l^{0A}(-\omega) + \Sigma_l^R(\omega),\tag{7.52}$$

This is the first iteration of the Kadanoff-Martin theory. Note that the bare Green function is used to average the T-matrix.

In the T-matrix theory, introduced in the section 3.6 and which is similar to the Multiple scattering theory, we can include the contributions from the other poles also. Now, however, we build the dominant contribution  $-\Delta^2 G_{0,l}^A$  using the reduced Green function already in the first iteration

$$G_{0,l}^A(-\omega) = \frac{1}{-\omega - \epsilon_l - \Sigma_l^A(-\omega)}.\tag{7.53}$$

This modification results in

$$\begin{aligned}\Sigma_l^R(\omega) &= -\Delta^2 G_{0,l}^A(-\omega) + \sum_{A=1}^3 \left( \frac{\text{sgn}(\Omega_A)}{\frac{\partial G_0^R(\Omega_A)}{\partial \Omega}} f_{BE}(\Omega_A) G_l^{0A}(\Omega_A - \omega) \right) \\ &\quad + T_0^R(\omega + \epsilon_l) f_{FD}(\epsilon_l) \\ &= -\Delta^2 G_{0,l}^A(-\omega) + \Sigma_l^R(\omega),\end{aligned}\tag{7.54}$$

which parallels equation (7.52). Note the bare Green function  $G_l^{0A}$  used for construction of the reduced selfenergy  $\Sigma_l^R$  as before.

The spectrum of energies is a solution of the equation

$$\omega - \epsilon_l = -\Delta^2 G_{0,l}^A(-\omega) + \Sigma_l^R(\omega),\tag{7.55}$$

or could be extract from the full retarded Green function

$$G_l^R(-\omega) = \frac{1}{\omega - \epsilon_l - \Sigma_l^R(\omega)},\tag{7.56}$$

as its imaginary part.

The differences of the full Green functions constructed from the selfenergies (7.49), (7.52) and (7.54) are shown in the figures 7.4 and 7.5. The Green function within the single channel approximation has only two poles. The non-dominant contributions to the selfenergies create new poles of the full Green function.

The most interesting are poles located in the gap. They are proportional to thermal factors and vanish at the zero temperature. Apparently, they correspond to non-BCS mechanisms in the grain since this news poles originate from non-dominant poles of the T-matrix. This poles have smaller weight than the dominant pole from the zero channel and reduce the value of the gap. Weights of few selected poles are in the table:

$\omega$ [meV]	34.00	27.83	26.07	19.29
$\alpha$	0.8	0.067	$7 \cdot 10^{-3}$	$5 \cdot 10^{-7}$
source	main BCS pole	$T^<(\Omega_2)$	Fermi stat.	$T^<(\Omega_3)$

We can see in the figure 7.4 and 7.5 that the Kadanoff-Martin and the Multiple scattering theory contain this interesting poles. In the Multiple scattering theory this new poles are located in symmetric position while in the Kadanoff-Martin theory there is always only one of them. This follows from the fact that in the Multiple scattering theory the renormalization via  $\Sigma'$  enters both lines while in the KM theory one of the lines remains bare.

The weight of the additional poles is important for their eventual observation in experiment. As mentioned, it decreases with the decreasing temperature. This is perhaps why there is no evidence of such poles in the measurements of Ralph, Braun and Tinkham performed deep below the critical temperature. There is still hope, however, that in higher temperatures or near the critical temperature this additional poles might be observable.

Even more exciting possibility is to add a lead designed to inject a pair of electrons into a selected excited state of the T-matrix. This can make its occupation relatively large without essential increase of the thermal energy of other particles. Such process results in a nonequilibrium distribution of bounded pairs and its description requires treatment by the complete nonequilibrium theory developed above in this thesis.

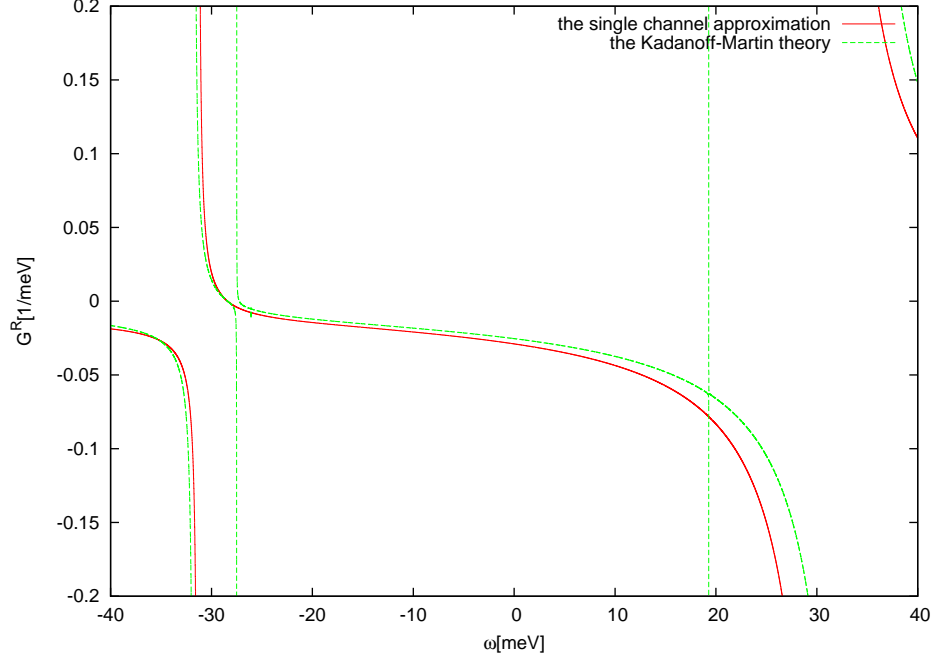


Figure 7.4: Inner structure of the main gap of the single channel approximation and the Kadanoff-Martin theory shown via poles in  $\text{Re}G_2^R$ , where index 2 stands for the upper energy level  $E_2=65$  meV. Set of parameters:  $\lambda=3$  meV,  $T=75$  K,  $\Delta=13.2073$  meV,  $\mu=36.4128$  meV,  $\delta\mu=-0.179262$  meV,  $\Omega_1=-21.12625$  meV,  $\Omega_2=1.16465$  meV,  $\Omega_3=47.6987$  meV. The position of the dominant pole in the Kadanoff-Martin ( $\approx 33.5$  meV) theory is shifted from the position of the pole of the single channel approximation (31.6534 meV). Whereas the single channel approximation decreases slightly the value of the gap ( $\Delta=13.2073$  meV) against the BCS theory ( $\Delta=13.2174$  meV) the Kadanoff-Martin theory increases this value again. The more important feature is the structure of the poles inside the main gap. The pole in the nearest position to zero ( $\approx 19.27$  meV) originates from the highest T-matrix pole  $\Omega_3$  and has the small Bose-Einstein factor. The most noticeable pole ( $\approx -27.5$  meV) within the main gap is related with the T-matrix pole  $\Omega_2$  and has the high Bose-Einstein factor. The last pole in the gap ( $\approx -26.08$  meV) relates to the terms with Fermi-Dirac statistics.

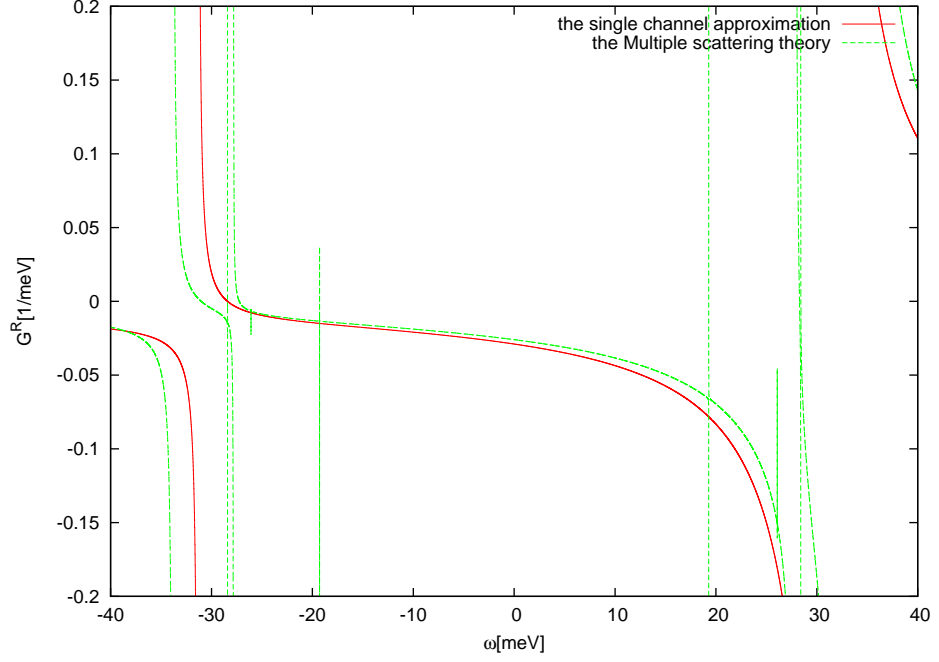


Figure 7.5: Inner structure of the main gap of the single channel approximation and the Multiple scattering theory shown via  $\text{Re}G_2^R$ . All parameters are identical to Fig. 7.4. The position of the dominant pole in the Multiple scattering theory ( $\approx 34$  meV) are shifted from the position of the pole of the single channel approximation (31.6534 meV). As in the KM approximation, the pole in the nearest position to zero ( $\approx \pm 19.29$  meV) originates from the highest T-matrix pole  $\Omega_3$  and has the small Bose-Einstein factor, the most noticeable pole ( $\approx \pm 27.83$  meV) in the gap is related to the T-matrix pole  $\Omega_2$  and has high Bose-Einstein factor, and the pole at  $\approx \pm 26.07$  meV relates to the terms with the Fermi-Dirac statistics. There are two new features. First, as already written, each pole from the KM approximation has its mirror value, note  $\pm$ . Second, there is a new pole ( $\approx \pm 28.42$  meV) which relates to the terms with the Fermi-Dirac statistics. The Multiple scattering theory results in a richer structure giving eight poles in the gap as compared to three of the Kadanoff-Martin theory.

# Conclusion

We have discussed the possibility to observe the corrections beyond the BCS theory in the tunneling spectroscopy of metallic nanospheres. To this end we have employed the machinery of Green functions in which one can express the BCS theory via the Nambu-Gorkov formalism as well as discussed alternative non-BCS theories based on the ladder approximation of the two-particle T-matrix. Our major focus was the T-matrix expansion with multiple scattering corrections.

In the tunneling spectroscopy the system represented by the nanosphere is driven out of the equilibrium and the problem deserves a treatment by nonequilibrium Green functions. The set of nonequilibrium Green functions for the T-matrix with multiple scattering corrections presented in Chap. 4 has not been published before and represents the major achievement of this thesis.

In the discussion of an eventual experimental search for features beyond the BCS theory, we have assumed three BCS friendly simplifications. First, we have shown that using ferroelectric dielectrics for the gate electrode, the Coulomb blockade can be suppressed below observable values. By this we hope to suppress the well known non-BCS features caused by the strict charge conservation enforced by a strong Coulomb blockade. Second, we have assumed highly non-symmetric tunneling contacts which allow us to approximate the state of the nanosphere by the local equilibrium with the chemical potential and the temperature of the strongly connected lead. In this regime, fluctuations of bounded electron pairs which are not assumed in the BCS theory, have a thermal distribution which avoids their large populations eventually created by a tunneling processes. Third, we work with the Richardson Hamiltonian which includes only the pairing interaction. Since the BCS theory neglects all non-pairing interactions, this assumption is likely responsible for remarkably good agreement of the BCS theory and more sophisticated approaches.

The implementation of the developed theory to the tunneling through nanospheres is in Chap. 6. It starts from the formulation of the tunneling Hamiltonian made of the sphere with pairing interaction and two ideal leads. On the level of Green functions we eliminate the leads and formulate all discussed approximations on the subspace of the sphere. To this end it was necessary to modify the multiple scattering corrections proposed originally for the infinite volume to natural eigenstates of the spherical symmetry. Approximations by which the T-matrix approach simplifies to the BCS theory, are introduced step by step. This forms a starting point for their comparison.

A systematic comparison of all successive approximations linking the T-matrix with the BCS theory goes beyond the scope of this thesis. Using the BCS theory as the starting approximation in Chap. 7 we show that the lowest order corrections beyond the BCS theory decreases the critical temperature of the superconducting approximation and the value of gap. This is particularly visible for dots with the weakest interaction strength, where the BCS gap is small and fluctuations are essential. In this regime the achieved corrections are about 10% and might be observable. On the other hand, our results show that the BCS theory is an excellent approximation at least for the Richardson model.

The T-matrix approach also results in small contributions to the density of

states inside the energy gap. Although the weight of the in-gap poles is very small, there is a hope that they might be observable since they appear at the zero background. If observed, this feature signals a clear non-BCS mechanism in the dot. We argue that these non-BCS features can be enhanced in nonequilibrium regime.

# Bibliography

- [1] P. W. Anderson, *J. Phys. Chem. Solids*, **11**, 26-30 (1959)
- [2] A. A. Abrikosov, L. P. Gorkov, I.E. Dzyaloshinski, *Method of Quantum Field Theory in Statistical Physics*, Prentice-Hall Inc., Englewood Cliffs, N. J., 1963.
- [3] A. Altland, B. Simons, *Condensed Matter Field Theory*, Cambridge University Press, Cambridge, 2010.
- [4] L. P. Kadanoff, G. Baym, *Quantum Statistical Physics*, W. A. Benjamin Inc., New York, 1962.
- [5] P. Lipavský, *Použití nerovnovážných Greenových funkcí v teorii nelineárního transportu*, doctoral thesis, Praha, 1896.
- [6] J. Maciejko, *An Introduction to Nonequilibrium Many-Body Theory*, Springer, 2007.
- [7] P. Lipavský, *Teorie transportu v kondenzované látce*, Matfyz Press, Praha, 2007.
- [8] P. Lipavský, K. Morawetz, V. Špička, *Ann. Phys. Fr.* **26**, Number 1, (2001).
- [9] N. B. Kopnin, *Theory of Nonequilibrium Superconductivity*, Clarendon Press, Oxford, 2001.
- [10] P. Lipavský, *Phys. Rev. B* **78**, 214506 (2008).
- [11] P. Soven, *Phys. Rev.* **156**, 809 (1967).
- [12] K. Morawetz, *Phys. Rev.* **82**, 092501 (2010)
- [13] B. Šopík, P. Lipavský, M. Mannel, K. Morawetz, P. Matlock, *Phys. Rev.* **84**, 094529 (2011).
- [14] J. von Delft, D.C. Ralph, *Physics Reports* **345**, 61-173 (2001).
- [15] Yu. A. Boikov, E. Olsson, T. Claeson, *Phys. Rev.* **74**, 024114 (2006)
- [16] Y.N. Ovchinnikov, V.Z. Kresin, *Uspekhi Fizicheskikh Nauk* **178**, 449-458 (2008).
- [17] J. Bardeen, *Phys. Rev. Lett.* **6**, 57 (1998).
- [18] W.H. Press, S.A. Teukolsky, W.T. Vetterling, B.P. Flannery, *Numerical Recipes The Art of Scientific Computing*, Cambridge University Press, 2007.
- [19] Y.N. Ovchinnikov, V.Z. Kresin, *Eur. Phys. J. B* **45**, 5-7 (2005).
- [20] Y.N. Ovchinnikov, V.Z. Kresin, *Eur. Phys. J. B* **47**, 333-336 (2005).
- [21] Y.N. Ovchinnikov, V.Z. Kresin, *Phys. Rev. B* **74**, 024514 (2006).
- [22] B. Velický, S. Kirkpatrick and H. Ehrenreich, *Phys. Rev.* **175**, 747 (1968).



# Appendix

# A. Soven schema

The aim of this Appendix is to reformulate Soven's method so that it can be adopted to the scattering of two particles.

## A.1 Coherent potential model of substitutional disordered alloys

The idea of effective medium in condensed matter was first introduced by Soven [11], who resolved the single-electron electron Green function in a binary alloy. The earlier theory called averaged T-matrix approximation (ATA) was modified to a theory using the coherent potential approximation. We will follow this original paper.

In the scattering theory of binary alloys the T-matrix of scattering on a single impurity atom is

$$t = v + vG_0t, \quad (\text{A.1})$$

where  $v$  is the impurity potential and  $G_0$  is the free-electron Green function. The full Green function  $G$  is given by expansion

$$G = G_0 + \sum_{\alpha} G_0 t_{\alpha} G_0 + \sum_{\alpha, \beta \neq \alpha} G_0 t_{\alpha} G_0 t_{\beta} G_0 + \dots, \quad (\text{A.2})$$

where  $\alpha$  denotes both a site index and the type of atom at the particular site.

The density of states and other observables equal to an ensemble average of the full Green function

$$\langle G \rangle = G_0 + \sum_{\alpha} \langle G_0 t_{\alpha} G_0 \rangle + \sum_{\alpha, \beta \neq \alpha} \langle G_0 t_{\alpha} G_0 t_{\beta} G_0 \rangle + \dots, \quad (\text{A.3})$$

where the angular brackets denote the ensemble average.

The ATA is the replacement of the average of T-matrix products by the products of the average T-matrix

$$\langle G \rangle \cong G_0 + \sum_{\alpha} G_0 \langle t_{\alpha} \rangle G_0 + \sum_{\alpha, \beta \neq \alpha} G_0 \langle t_{\alpha} \rangle G_0 \langle t_{\beta} \rangle G_0 + \dots. \quad (\text{A.4})$$

This approximation is very successful for low concentrations of impurities, but it fails for high concentrations being completely inadequate for binary alloys with comparable content of both components.

The idea of coherent potential, suitable for general binary alloys, is following. We place an unknown potential  $v_0(\mathbf{x}-\mathbf{l})$  at every site  $\mathbf{l}$  and then derive a condition for such potential. The true potential at every site  $\mathbf{l}$  is either  $v_1(\mathbf{x}-\mathbf{l})$  if it is occupied by atom of type 1 or  $v_2(\mathbf{x}-\mathbf{l})$  if by atom of type 2.

Let  $\bar{G}_0$  be the formal Green function for lattice of potentials  $v_0$

$$\bar{G}_0 = G_0 + G_0 \sum_{\mathbf{l}} v_0(\mathbf{x}-\mathbf{l}) \bar{G}_0. \quad (\text{A.5})$$

We want to build a the similar scattering theory as before. Now the atomic T-matrix contains Green function  $\bar{G}_0$  and a potential related to the unknown potential

$$\bar{t}_i = (v_i - v_0) + (v_i - v_0)\bar{G}_0\bar{t}_i, \quad (\text{A.6})$$

where  $i = 1, 2$ . Parallel to equation A.2

$$G = \bar{G}_0 + \sum_{\alpha} \bar{G}_0\bar{t}_{\alpha}\bar{G}_0 + \sum_{\alpha, \beta \neq \alpha} \bar{G}_0\bar{t}_{\alpha}\bar{G}_0\bar{t}_{\beta}\bar{G}_0 + \dots \quad (\text{A.7})$$

The effective potential is arbitrary by definition and our choice of potential was not done so far. The Soven original condition is a requirement that on average there be no further scattering from the perturbing potentials. Soven required

$$\langle \bar{t}_i \rangle = c_1\bar{t}_1 + c_2\bar{t}_2 = 0, \quad (\text{A.8})$$

for each site  $\mathbf{l}$ .  $c_1$  and  $c_2$  are concentrations of constituents.

The ensemble average of the full Green function given by such potential is then

$$\langle G \rangle = \bar{G}_0 + \sum_{\alpha} \sum_{\beta \neq \alpha} \sum_{\gamma \neq \beta} \sum_{\delta \neq \gamma} \langle \bar{G}_0\bar{t}_{\alpha}\bar{G}_0\bar{t}_{\beta}\bar{G}_0\bar{t}_{\gamma}\bar{G}_0\bar{t}_{\delta} \rangle + \dots \quad (\text{A.9})$$

The first correction is of the fourth order in the T-matrices. All formulas above are exact so far. The original Soven approximation is

$$\langle G \rangle \cong \bar{G}_0. \quad (\text{A.10})$$

This approximation should be valid for sufficiently long mean free paths and was tested in the original paper. The coherent potential thus improved the description of substitutional disordered alloys [11].

## A.2 Renotation of Soven's condition

We bring the Soven condition to a different notation. The Soven condition for every site  $\mathbf{l}$  has an explicit form

$$c_1 \frac{v_1(\mathbf{x} - \mathbf{l}) - v_0(\mathbf{x} - \mathbf{l})}{1 - (v_1(\mathbf{x} - \mathbf{l}) - v_0(\mathbf{x} - \mathbf{l}))\bar{G}_0} + c_2 \frac{v_2(\mathbf{x} - \mathbf{l}) - v_0(\mathbf{x} - \mathbf{l})}{1 - (v_2(\mathbf{x} - \mathbf{l}) - v_0(\mathbf{x} - \mathbf{l}))\bar{G}_0} = 0. \quad (\text{A.11})$$

We denote concentrations

$$c_1 = 1 - c, \quad (\text{A.12})$$

$$c_2 = c, \quad (\text{A.13})$$

since they always satisfy  $c_1 + c_2 = 1$ .

The site index  $\mathbf{l}$  is changed to  $\mathbf{q}$ . Further we choose potentials as

$$v_1(\mathbf{x} - \mathbf{q}) = 0, \quad (\text{A.14})$$

$$v_2(\mathbf{x} - \mathbf{q}) = V_{\mathbf{q}}, \quad (\text{A.15})$$

where the difference between values of potentials is  $V_{\mathbf{q}}$ .

The coherent potential is denoted as selfenergy

$$v_0(\mathbf{x} - \mathbf{q}) = \Sigma_{\mathbf{q}}. \quad (\text{A.16})$$

In Soven's notation  $\langle G \rangle \cong \bar{G}_0$  which we denote as  $G = \bar{G}_0$ . The Soven condition thus takes a form

$$(1 - c) \frac{0 - \Sigma_{\mathbf{q}}}{1 - (0 - \Sigma_{\mathbf{q}})G} + c \frac{V_{\mathbf{q}} - \Sigma_{\mathbf{q}}}{1 - (V_{\mathbf{q}} - \Sigma_{\mathbf{q}})G} = 0, \quad (\text{A.17})$$

and similarly equation (A.5)

$$G = G^0 + G^0 \sum_{\mathbf{q}} \Sigma_{\mathbf{q}} G. \quad (\text{A.18})$$

which is a standard Dyson equation

$$G = G^0 + G^0 \Sigma G, \quad (\text{A.19})$$

with the selfenergy

$$\Sigma = \sum_{\mathbf{q}} \Sigma_{\mathbf{q}}, \quad (\text{A.20})$$

The above set of equations (A.17)-(A.20) contains a condition that statical T-matrix is equal to zero in average  $\langle T[\Sigma_{\mathbf{q}}, G] \rangle = 0$  for each site  $\mathbf{q}$ . In the main text we reformulate this condition for dynamical systems.

The Soven condition can be also derived in terms of multiple-scattering theory and single-site approximation. This was done in paper by [22]. This idea of single site approximation is based on averaged medium surrounding each site. In this sense the single site approximation is the same as Soven's original approach and they meet each other in equation (A.17).

### A.3 Reformulation of Soven condition

In this section we reformulate the Soven condition in the form of equations, which are suitable for generalization.

Let us start with a statement that the set of equations from last section:

$$G = G^0 + G^0 \Sigma G, \quad (\text{A.21})$$

$$\Sigma = \sum_{\mathbf{q}} \Sigma_{\mathbf{q}}, \quad (\text{A.22})$$

$$\langle T[\Sigma_{\mathbf{q}}] \rangle = (1 - c) \frac{0 - \Sigma_{\mathbf{q}}}{1 - (0 - \Sigma_{\mathbf{q}})G} + c \frac{V_{\mathbf{q}} - \Sigma_{\mathbf{q}}}{1 - (V_{\mathbf{q}} - \Sigma_{\mathbf{q}})G} = 0, \quad (\text{A.23})$$

is equivalent to the following set of equations:

$$G = G^0 + G^0 \Sigma G, \quad (\text{A.24})$$

$$\Sigma = \sum_{\mathbf{q}} \Sigma_{\mathbf{q}}, \quad (\text{A.25})$$

$$G_{\mathbf{q}} = G - G\Sigma_{\mathbf{q}}G_{\mathbf{q}}, \quad (\text{A.26})$$

$$G = G_{\mathbf{q}} + G_{\mathbf{q}}S_{\mathbf{q}}G_{\mathbf{q}}, \quad (\text{A.27})$$

$$T_{\mathbf{q}} = \frac{V_{\mathbf{q}}}{1 - V_{\mathbf{q}}G_{\mathbf{q}}}, \quad (\text{A.28})$$

$$S_{\mathbf{q}} = cT_{\mathbf{q}}. \quad (\text{A.29})$$

From equations (A.24)-(A.29) we can obtain alternative relations

$$S_{\mathbf{q}} = \Sigma_{\mathbf{q}} + S_{\mathbf{q}}G_{\mathbf{q}}\Sigma_{\mathbf{q}}, \quad (\text{A.30})$$

$$G = G^0 + G^0(\Sigma - \Sigma_{\mathbf{q}})G, \quad (\text{A.31})$$

$$S_{\mathbf{q}} = \Sigma_{\mathbf{q}} + \Sigma_{\mathbf{q}}G\Sigma_{\mathbf{q}}. \quad (\text{A.32})$$

Let us prove that equations above (A.21)-(A.23) are equivalent to equations (A.24)-(A.29). The first two equations are identical in both cases, so for our purpose, it is sufficient to prove only equivalence of (A.23) to (A.26)-(A.29)

Starting with the Soven condition

$$(1 - c)\frac{\Sigma_{\mathbf{q}}}{1 + \Sigma_{\mathbf{q}}G} = c\frac{V_{\mathbf{q}} - \Sigma_{\mathbf{q}}}{1 + (\Sigma_{\mathbf{q}} - V_{\mathbf{q}})G}, \quad (\text{A.33})$$

by multiplication

$$(1 - c)[\Sigma_{\mathbf{q}} + (\Sigma_{\mathbf{q}} - V_{\mathbf{q}})G\Sigma_{\mathbf{q}}] = c[(V_{\mathbf{q}} - \Sigma_{\mathbf{q}}) + \Sigma_{\mathbf{q}}G(V_{\mathbf{q}} - \Sigma_{\mathbf{q}})], \quad (\text{A.34})$$

and rearrangement

$$(1 - c)[\Sigma_{\mathbf{q}} - V_{\mathbf{q}}G\Sigma_{\mathbf{q}} + \Sigma_{\mathbf{q}}G\Sigma_{\mathbf{q}}] = c[V_{\mathbf{q}} - \Sigma_{\mathbf{q}} + \Sigma_{\mathbf{q}}GV_{\mathbf{q}} - \Sigma_{\mathbf{q}}G\Sigma_{\mathbf{q}}], \quad (\text{A.35})$$

we group the terms with the concentration  $c$

$$\Sigma_{\mathbf{q}} - V_{\mathbf{q}}G\Sigma_{\mathbf{q}} + \Sigma_{\mathbf{q}}G\Sigma_{\mathbf{q}} = c[V_{\mathbf{q}} + \Sigma_{\mathbf{q}}GV_{\mathbf{q}} - V_{\mathbf{q}}G\Sigma_{\mathbf{q}}]. \quad (\text{A.36})$$

Following rearrangement is more tricky

$$[1 + (\Sigma_{\mathbf{q}} - V_{\mathbf{q}})G]\Sigma_{\mathbf{q}} + cV_{\mathbf{q}}G\Sigma_{\mathbf{q}} = c(1 + \Sigma_{\mathbf{q}}G)V_{\mathbf{q}}, \quad (\text{A.37})$$

$$(1 + \Sigma_{\mathbf{q}}G)\Sigma_{\mathbf{q}} + (c - 1)V_{\mathbf{q}}G\Sigma_{\mathbf{q}} = (1 + \Sigma_{\mathbf{q}}G)cV_{\mathbf{q}}, \quad (\text{A.38})$$

$$(c - 1)V_{\mathbf{q}}G\Sigma_{\mathbf{q}} = (1 + \Sigma_{\mathbf{q}}G)(cV_{\mathbf{q}} - \Sigma_{\mathbf{q}}), \quad (\text{A.39})$$

$$(c - 1)\frac{V_{\mathbf{q}}G}{1 + \Sigma_{\mathbf{q}}G}\Sigma_{\mathbf{q}} = cV_{\mathbf{q}} - \Sigma_{\mathbf{q}}, \quad (\text{A.40})$$

where all equations are equivalent and contain individual step of algebraic rearrangement. We end up with a form prepared for substitution into some of the equations (A.24)-(A.29)

$$\Sigma_{\mathbf{q}} + (c - 1)\frac{V_{\mathbf{q}}G}{1 + \Sigma_{\mathbf{q}}G}\Sigma_{\mathbf{q}} = cV_{\mathbf{q}}. \quad (\text{A.41})$$

By applying the definition (A.26) for the reduced function  $G_{\mathbf{q}}$

$$\Sigma_{\mathbf{q}} + (c - 1)V_{\mathbf{q}}G_{\mathbf{q}}\Sigma_{\mathbf{q}} = cV_{\mathbf{q}}, \quad (\text{A.42})$$

we are able to manipulate equation

$$(1 - V_{\mathbf{q}}G_{\mathbf{q}})\Sigma_{\mathbf{q}} + cV_{\mathbf{q}}G_{\mathbf{q}}\Sigma_{\mathbf{q}} = cV_{\mathbf{q}} \quad (\text{A.43})$$

to a form suitable for definition of the reduced T-matrix (A.28)

$$\Sigma_{\mathbf{q}} + c\frac{V_{\mathbf{q}}}{1 - V_{\mathbf{q}}G_{\mathbf{q}}}G_{\mathbf{q}}\Sigma_{\mathbf{q}} = c\frac{V_{\mathbf{q}}}{1 - V_{\mathbf{q}}G_{\mathbf{q}}}. \quad (\text{A.44})$$

With the help of equation (A.28)

$$\Sigma_{\mathbf{q}} + cT_{\mathbf{q}}G_{\mathbf{q}}\Sigma_{\mathbf{q}} = cT_{\mathbf{q}}. \quad (\text{A.45})$$

The final step is using the equation (A.29) to obtain the equation (A.30)

$$\Sigma_{\mathbf{q}} + S_{\mathbf{q}}G_{\mathbf{q}}\Sigma_{\mathbf{q}} = S_{\mathbf{q}}. \quad (\text{A.46})$$

Briefly, we have proved that the set of equations (A.26)-(A.29) is equivalent to the Soven condition for the coherent potential (A.23).

## A.4 Soven schema in superconductivity

Let us discuss the properties of equations (A.26)-(A.29). For every site  $\mathbf{q}$  we have a different reduced Green function  $G_{\mathbf{q}}$ . Notice also that  $T_{\mathbf{q}}[G_{\mathbf{q}}]$  is constructed from  $G_{\mathbf{q}}$ , whereas  $\langle T[\Sigma_{\mathbf{q}}, G] \rangle$  is functional of the full Green function  $T[G]$ .

By comparison of equations (A.24)-(A.29) with equations (3.16)-(3.30) we will find the same structure. In both cases they contain irreducible selfenergy  $S$  and the construction of reduced T-matrix from reduced Green function  $T_{\mathbf{q}}[G_{\mathbf{q}}]$ . In this sense equations (3.16)-(3.30) for two particle scattering are a generalization of equations (A.24)-(A.29) for one particle impurity scattering.

## B. Two-particle propagator

In this section we will compute the retarded two-particle propagator in the first iteration of the Kadanoff-Martin theory. We can construct the retarded T-matrix from this propagator. The two-particle propagator is defined as

$$\mathcal{G}_0^R(t) = \sum_l (2L_l + 1) \left( G_l^R(t) G_{0,l}^>(t) - G_l^<(t) G_{0,l}^R(t) \right). \quad (\text{B.1})$$

This is exactly the two particle propagator from the Kadanoff-Martin theory. We assume in the first iteration the selfenergy in the Nambu-Gorkov form

$$\Sigma_l^R(\omega) = -\Delta^2 G_{0,l}^A(-\omega). \quad (\text{B.2})$$

From this selfenergy we will construct the full Green function.

Let us to be more general and suppose the selfenergy in the form, where we have nonzero bosonic frequency  $\Omega_0 \neq 0$

$$\Sigma_l^R(\omega) = -\Delta^2 G_{0,l}^A(\Omega_0 - \omega). \quad (\text{B.3})$$

We can always reduce final expression by setting  $\Omega_0 = 0$ . By knowing the form of the Green functions in the energetic representation we transform them to the time representation and than use it in the equation (B.1). We start with the retarded Green function in the frequency representation

$$G_l^R(\omega) = \frac{1}{\omega - \epsilon_l - \eta_l - \Sigma_l^R} = \frac{1}{\omega - \epsilon_l + i0 - \frac{-\Delta^2}{\Omega_0 - \omega - \epsilon_l - i0}}, \quad (\text{B.4})$$

switch into the time representation by Fourier transformation

$$G_l^R(t) = \int \frac{d(\omega)}{2\pi} \frac{1}{\omega - \epsilon_l + i0 - \frac{-\Delta^2}{\Omega_0 - \omega - \epsilon_l - i0}} e^{-i\omega t}, \quad (\text{B.5})$$

and use the substitution

$$G_l^R(t) = \int \frac{d(\omega' + \frac{\Omega_0}{2})}{2\pi} \frac{1}{\omega' - (\epsilon_l - \frac{\Omega_0}{2}) + i0 + \frac{\Delta^2}{-\omega' - (\epsilon_l - \frac{\Omega_0}{2}) - i0}} e^{-i\omega' t} e^{-i\frac{\Omega_0}{2} t}. \quad (\text{B.6})$$

The substitution is useful for the rearrangement of the expression

$$G_l^R(t) = e^{-i\frac{\Omega_0}{2} t} \int \frac{d(\omega')}{2\pi} \frac{(-\omega' - (\epsilon_l - \frac{\Omega_0}{2}) + i0) e^{-i\omega' t}}{(\omega' - (\epsilon_l - \frac{\Omega_0}{2}) + i0)(-\omega' - (\epsilon_l - \frac{\Omega_0}{2}) - i0) + \Delta^2}, \quad (\text{B.7})$$

to the form which allows the decomposition into the partial fractions

$$G_l^R(t) = e^{-i\frac{\Omega_0}{2} t} \int \frac{d(\omega')}{2\pi} \frac{(\omega' + (\epsilon_l - \frac{\Omega_0}{2}))}{(\omega' + i0)^2 - \Delta^2 - (\epsilon_l - \frac{\Omega_0}{2})^2} e^{-i\omega' t}. \quad (\text{B.8})$$

Applying the decomposition

$$G_l^R(t) = e^{-i\frac{\Omega_0}{2} t} \int \frac{d(\omega')}{2\pi} \frac{(\omega' + (\epsilon_l - \frac{\Omega_0}{2}))}{2\sqrt{\Delta^2 + (\epsilon_l - \frac{\Omega_0}{2})^2}} \left( \frac{1}{\omega' + i0 - \sqrt{\Delta^2 + (\epsilon_l - \frac{\Omega_0}{2})^2}} - \frac{1}{\omega' + i0 + \sqrt{\Delta^2 + (\epsilon_l - \frac{\Omega_0}{2})^2}} \right) e^{-i\omega' t}, \quad (\text{B.9})$$

we can evaluate the integral by the residue theorem

$$G_l^R(t) = -i\theta(t)e^{-i\frac{\Omega_0}{2}t} \left( e^{-i\sqrt{\Delta^2 + (\epsilon_l - \frac{\Omega_0}{2})^2}t} \frac{\left(\sqrt{\Delta^2 + (\epsilon_l - \frac{\Omega_0}{2})^2} + (\epsilon_l - \frac{\Omega_0}{2})\right)}{2\sqrt{\Delta^2 + (\epsilon_l - \frac{\Omega_0}{2})^2}} - e^{i\sqrt{\Delta^2 + (\epsilon_l - \frac{\Omega_0}{2})^2}t} \frac{\left(-\sqrt{\Delta^2 + (\epsilon_l - \frac{\Omega_0}{2})^2} + (\epsilon_l - \frac{\Omega_0}{2})\right)}{2\sqrt{\Delta^2 + (\epsilon_l - \frac{\Omega_0}{2})^2}} \right). \quad (\text{B.10})$$

The correlation function in the equilibrium  $G_l^<(\omega) = -2\text{Im}(G_l^R(\omega))f_{FD}(\omega)$  after Fourier transformation reads

$$G_l^<(t) = \int \frac{d(\omega)}{2\pi} -2\text{Im} \left( \frac{1}{\omega - \epsilon_l + i0 - \frac{-\Delta^2}{\Omega_0 - \omega - \epsilon_l - i0}} e^{-i\omega t} \right) f_{FD}(\omega) e^{-i\omega t}. \quad (\text{B.11})$$

Using exactly the same substitution  $\omega' = \omega + \frac{\Omega_0}{2}$  as before we can directly obtain

$$G_l^<(t) = e^{-i\frac{\Omega_0}{2}t} \int \frac{d(\omega')}{2\pi} \frac{(\omega' + (\epsilon_l - \frac{\Omega_0}{2}))}{\sqrt{\Delta^2 + (\epsilon_l - \frac{\Omega_0}{2})^2}} f_{FD} \left( \omega' + \frac{\Omega_0}{2} \right) e^{-i\omega't} - 2\text{Im} \left( \frac{1}{\omega' + i0 - \sqrt{\Delta^2 + (\epsilon_l - \frac{\Omega_0}{2})^2}} - \frac{1}{\omega' + i0 + \sqrt{\Delta^2 + (\epsilon_l - \frac{\Omega_0}{2})^2}} \right), \quad (\text{B.12})$$

and we end up with the expression

$$G_l^<(t) = e^{-i\frac{\Omega_0}{2}t} \left( e^{-i\sqrt{\Delta^2 + (\epsilon_l - \frac{\Omega_0}{2})^2}t} \frac{\left(\sqrt{\Delta^2 + (\epsilon_l - \frac{\Omega_0}{2})^2} + (\epsilon_l - \frac{\Omega_0}{2})\right)}{2\sqrt{\Delta^2 + (\epsilon_l - \frac{\Omega_0}{2})^2}} f_{FD} \left( \sqrt{\Delta^2 + (\epsilon_l - \frac{\Omega_0}{2})^2} + \frac{\Omega_0}{2} \right) - e^{i\sqrt{\Delta^2 + (\epsilon_l - \frac{\Omega_0}{2})^2}t} \frac{\left(-\sqrt{\Delta^2 + (\epsilon_l - \frac{\Omega_0}{2})^2} + (\epsilon_l - \frac{\Omega_0}{2})\right)}{2\sqrt{\Delta^2 + (\epsilon_l - \frac{\Omega_0}{2})^2}} f_{FD} \left( -\sqrt{\Delta^2 + (\epsilon_l - \frac{\Omega_0}{2})^2} + \frac{\Omega_0}{2} \right) \right). \quad (\text{B.13})$$

Let us derive also the bare correlation Green function in the equilibrium. Switching to the time domain

$$G_l^{0>}(t) = \int \frac{d(\omega)}{2\pi} -2\text{Im} \left( \frac{1}{\omega - \epsilon_l + i0} \right) \left( 1 - f_{FD}(\omega) \right) e^{-i\omega t}, \quad (\text{B.14})$$



and using the residue theorem

$$G_l^{0>}(t) = e^{-i\epsilon_l t}(1 - f_{FD}(\epsilon_l)). \quad (\text{B.15})$$

Finally, the bare retarded Green function in the time representation

$$G_l^{0R}(t) = -i\theta(t)e^{-i\epsilon_l t}. \quad (\text{B.16})$$

We have just derived the all necessary functions for the construction of the two-particle propagator. We can thus put all these functions (B.6), (B.13), (B.15), (B.16) in (B.1) resulting to

$$\begin{aligned} \mathcal{G}_0^R(t) = \sum_l & -i\theta(t)(2L_l + 1)e^{-i(\epsilon_l + \frac{\Omega_0}{2})t} \left\{ \right. \\ & - \left[ e^{-i\sqrt{\Delta^2 + (\epsilon_l - \frac{\Omega_0}{2})^2}t} \frac{\left(\sqrt{\Delta^2 + (\epsilon_l - \frac{\Omega_0}{2})^2} + (\epsilon_l - \frac{\Omega_0}{2})\right)}{2\sqrt{\Delta^2 + (\epsilon_l - \frac{\Omega_0}{2})^2}} \right. \\ & \left. \left( -1 + f_{FD}(\epsilon_l) - f_{FD} \left( +\sqrt{\Delta^2 + \left(\epsilon_l - \frac{\Omega_0}{2}\right)^2} + \frac{\Omega_0}{2} \right) \right) \right] \\ & + \left[ e^{+i\sqrt{\Delta^2 + (\epsilon_l - \frac{\Omega_0}{2})^2}t} \frac{\left(-\sqrt{\Delta^2 + (\epsilon_l - \frac{\Omega_0}{2})^2} + (\epsilon_l - \frac{\Omega_0}{2})\right)}{2\sqrt{\Delta^2 + (\epsilon_l - \frac{\Omega_0}{2})^2}} \right. \\ & \left. \left( -1 + f_{FD}(\epsilon_l) - f_{FD} \left( -\sqrt{\Delta^2 + \left(\epsilon_l - \frac{\Omega_0}{2}\right)^2} + \frac{\Omega_0}{2} \right) \right) \right] \left. \right\}, \end{aligned} \quad (\text{B.17})$$

We used the advantage of the multiplication in the time domain, the transforma-

tion forward and back thus do the convolution. This results to

$$\begin{aligned}
\mathcal{G}_0^R(\Omega) = \sum_l (2L_l + 1) & \left\{ \right. \\
& - \frac{1}{\Omega - \left( \sqrt{\Delta^2 + \left(\epsilon_l - \frac{\Omega_0}{2}\right)^2} + \left(\epsilon_l + \frac{\Omega_0}{2}\right) \right)} \\
& \frac{\left( \sqrt{\Delta^2 + \left(\epsilon_l - \frac{\Omega_0}{2}\right)^2} + \left(\epsilon_l - \frac{\Omega_0}{2}\right) \right)}{2\sqrt{\Delta^2 + \left(\epsilon_l - \frac{\Omega_0}{2}\right)^2}} \\
& \left( -1 + f_{FD}(\epsilon_l) - f_{FD} \left( +\sqrt{\Delta^2 + \left(\epsilon_l - \frac{\Omega_0}{2}\right)^2} + \frac{\Omega_0}{2} \right) \right) \\
& + \frac{1}{\Omega - \left( -\sqrt{\Delta^2 + \left(\epsilon_l - \frac{\Omega_0}{2}\right)^2} + \left(\epsilon_l + \frac{\Omega_0}{2}\right) \right)} \\
& \frac{\left( -\sqrt{\Delta^2 + \left(\epsilon_l - \frac{\Omega_0}{2}\right)^2} + \left(\epsilon_l - \frac{\Omega_0}{2}\right) \right)}{2\sqrt{\Delta^2 + \left(\epsilon_l - \frac{\Omega_0}{2}\right)^2}} \\
& \left. \left( -1 + f_{FD}(\epsilon_l) - f_{FD} \left( -\sqrt{\Delta^2 + \left(\epsilon_l - \frac{\Omega_0}{2}\right)^2} + \frac{\Omega_0}{2} \right) \right) \right\}.
\end{aligned} \tag{B.18}$$

We can bring this propagator to the form where all fermionic energies are related to  $\frac{\Omega_0}{2}$  and bosonic frequency  $\Omega$  is related to  $\Omega_0$

$$\begin{aligned}
\mathcal{G}_0^R(\Omega) = \sum_l (2L_l + 1) \left\{ \right. \\
& - \frac{1}{\Omega - \Omega_0 - \left( \sqrt{\Delta^2 + \left(\epsilon_l - \frac{\Omega_0}{2}\right)^2} + \left(\epsilon_l - \frac{\Omega_0}{2}\right) \right) + i0} \\
& \frac{\left( \sqrt{\Delta^2 + \left(\epsilon_l - \frac{\Omega_0}{2}\right)^2} + \left(\epsilon_l - \frac{\Omega_0}{2}\right) \right)}{2\sqrt{\Delta^2 + \left(\epsilon_l - \frac{\Omega_0}{2}\right)^2}} \\
& \left( -1 + f_{FD} \left( \left(\epsilon_l - \frac{\Omega_0}{2}\right) + \frac{\Omega_0}{2} \right) - f_{FD} \left( \sqrt{\Delta^2 + \left(\epsilon_l - \frac{\Omega_0}{2}\right)^2} + \frac{\Omega_0}{2} \right) \right) \\
& + \frac{1}{\Omega - \Omega_0 - \left( -\sqrt{\Delta^2 + \left(\epsilon_l - \frac{\Omega_0}{2}\right)^2} + \left(\epsilon_l - \frac{\Omega_0}{2}\right) \right) + i0} \\
& \frac{\left( -\sqrt{\Delta^2 + \left(\epsilon_l - \frac{\Omega_0}{2}\right)^2} + \left(\epsilon_l - \frac{\Omega_0}{2}\right) \right)}{2\sqrt{\Delta^2 + \left(\epsilon_l - \frac{\Omega_0}{2}\right)^2}} \\
& \left. \left( -1 + f_{FD} \left( \left(\epsilon_l - \frac{\Omega_0}{2}\right) + \frac{\Omega_0}{2} \right) - f_{FD} \left( -\sqrt{\Delta^2 + \left(\epsilon_l - \frac{\Omega_0}{2}\right)^2} + \frac{\Omega_0}{2} \right) \right) \right\}. \tag{B.19}
\end{aligned}$$

In the limit of  $\Omega_0 = 0$  the two-particle propagator should reduce the two-particle propagator known from the BCS condition. Substituting  $\Omega_0 = 0$

$$\begin{aligned}
\mathcal{G}_0^R(\Omega) = \sum_l (2L_l + 1) \left\{ \right. \\
& - \left( \frac{1}{\Omega - \left(\epsilon_l + \sqrt{\epsilon_l^2 + \Delta^2}\right) + i0} \right) \frac{\epsilon_l + \sqrt{\epsilon_l^2 + \Delta^2}}{2\sqrt{\epsilon_l^2 + \Delta^2}} \\
& \left( (-1 + f_{FD}(\epsilon_l)) - f_{FD}(\sqrt{\epsilon_l^2 + \Delta^2}) \right) \\
& + \left( \frac{1}{\Omega - \left(\epsilon_l - \sqrt{\epsilon_l^2 + \Delta^2}\right) + i0} \right) \frac{\epsilon_l - \sqrt{\epsilon_l^2 + \Delta^2}}{2\sqrt{\epsilon_l^2 + \Delta^2}} \\
& \left. \left( (-1 + f_{FD}(\epsilon_l)) - f_{FD}(-\sqrt{\epsilon_l^2 + \Delta^2}) \right) \right\}. \tag{B.20}
\end{aligned}$$

and putting inside the zero frequency  $\Omega = 0$

$$\begin{aligned}
\mathcal{G}_0^R(0) = \sum_l (2L_l + 1) & \left\{ \right. \\
& - \left( \frac{1}{-(\epsilon_l + \sqrt{\epsilon_l^2 + \Delta^2}) + i0} \right) \frac{\epsilon_l + \sqrt{\epsilon_l^2 + \Delta^2}}{2\sqrt{\epsilon_l^2 + \Delta^2}} \\
& \left( (-1 + f_{FD}(\epsilon_l)) - f_{FD}(\sqrt{\epsilon_l^2 + \Delta^2}) \right) \\
& + \left( \frac{1}{-(\epsilon_l - \sqrt{\epsilon_l^2 + \Delta^2}) + i0} \right) \frac{\epsilon_l - \sqrt{\epsilon_l^2 + \Delta^2}}{2\sqrt{\epsilon_l^2 + \Delta^2}} \\
& \left. \left( (-1 + f_{FD}(\epsilon_l)) - f_{FD}(-\sqrt{\epsilon_l^2 + \Delta^2}) \right) \right\}.
\end{aligned} \tag{B.21}$$

can be the two-particle propagator simplifies to

$$\begin{aligned}
\mathcal{G}_0^R(0) = \sum_l (2L_l + 1) & \left\{ \frac{1}{2\sqrt{\epsilon_l^2 + \Delta^2}} \left( (-1 + f_{FD}(\epsilon_l)) - f_{FD}(\sqrt{\epsilon_l^2 + \Delta^2}) \right) \right. \\
& \left. - \frac{1}{2\sqrt{\epsilon_l^2 + \Delta^2}} \left( (-1 + f_{FD}(\epsilon_l)) - f_{FD}(-\sqrt{\epsilon_l^2 + \Delta^2}) \right) \right\}.
\end{aligned} \tag{B.22}$$

The zero frequency propagator known from the BCS condition

$$\begin{aligned}
\mathcal{G}_0^R(0) = \sum_l (2L_l + 1) & \frac{-1}{2\sqrt{\epsilon_l^2 + \Delta^2}} \left\{ \left( (1 - f_{FD}(\epsilon_l)) + f_{FD}(\sqrt{\epsilon_l^2 + \Delta^2}) \right) \right. \\
& \left. + \left( (-1 + f_{FD}(\epsilon_l)) - f_{FD}(-\sqrt{\epsilon_l^2 + \Delta^2}) \right) \right\},
\end{aligned} \tag{B.23}$$

is thus recovered

$$\begin{aligned}
\mathcal{G}_0^R(0) & = \sum_l (2L_l + 1) \frac{-1}{2\sqrt{\epsilon_l^2 + \Delta^2}} \left( f_{FD} \left( \sqrt{\epsilon_l^2 + \Delta^2} \right) - f_{FD} \left( -\sqrt{\epsilon_l^2 + \Delta^2} \right) \right) \\
& = \sum_l \frac{(2L_l + 1)}{2\sqrt{\epsilon_l^2 + \Delta^2}} \tanh \left( \frac{\sqrt{\epsilon_l^2 + \Delta^2}}{2k_{\text{B}}T} \right).
\end{aligned} \tag{B.24}$$